

UNCLASSIFIED

AD NUMBER
ADB108208
NEW LIMITATION CHANGE
TO Approved for public release, distribution unlimited
FROM Distribution authorized to U.S. Gov't. agencies only; Test and Evaluation; Jan 1986. Other requests shall be referred to Air Force Systems Command, Flight Dynamics Lab., Wright-Patterson AFB, OH 45433.
AUTHORITY
D/A ltr, 1 Nov 1990

THIS PAGE IS UNCLASSIFIED

DISCLAIMER NOTICE

THIS DOCUMENT IS BEST QUALITY PRACTICABLE. THE COPY FURNISHED TO DTIC CONTAINED A SIGNIFICANT NUMBER OF PAGES WHICH DO NOT REPRODUCE LEGIBLY.

AFWAL-TR-86-3034

STRENGTH ANALYSIS OF LAMINATED AND METALLIC PLATES BOLTED TOGETHER BY MANY FASTENERS

R.L. Ramkumar
E.S. Saether
K. Appa

Northrop Corporation, Aircraft Division
One Northrop Avenue
Hawthorne, California 90250

JULY 1986

Final Report for Period June 1984 to December 1985

2

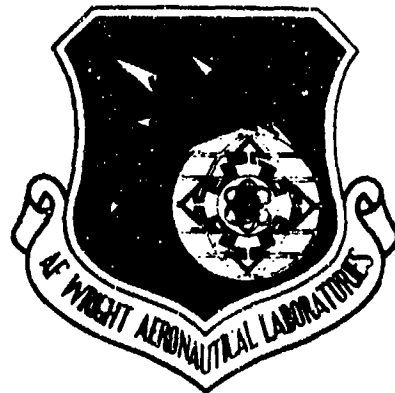
TAE

Distribution limited to U.S. government agencies only,
~~critical technology~~; January 1986. Other requests
for this document must be referred to AFWAL/FIBRA,
WPAFB, OHIO 45433-6553

WARNING - This document contains technical
data whose export is restricted by the Arms
Export Control Act (Title 22, U.S.C.,
Sec 2751 et seq.) or Executive Order 12470.
Violation of these export laws is subject
to severe criminal penalties.

DESTRUCTION NOTICE - Destroy by any
method that will prevent disclosure of
contents or reconstruction of the
document.

FLIGHT DYNAMICS LABORATORY
AIR FORCE WRIGHT AERONAUTICAL LABORATORIES
AIR FORCE SYSTEMS COMMAND
WRIGHT-PATTERSON AIR FORCE BASE, OHIO 45433-6553



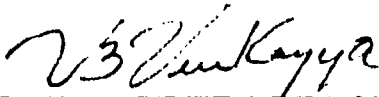
DTIC
ELECTE
JAN 15 1987
S A D

NOTICE

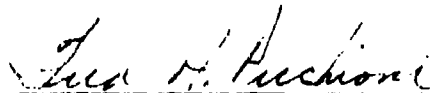
When Government drawings, specifications, or other data are used for any purpose other than in connection with a definitely related Government procurement operation, the United States Government thereby incurs no responsibility nor any obligation whatsoever; and the fact that the government may have formulated, furnished, or in any way supplied the said drawings, specifications, or other data, is not to be regarded by implication or otherwise as in any manner licensing the holder or any other person or corporation, or conveying any rights or permission to manufacture use, or sell any patented invention that may in any way be related thereto.

This report has been reviewed by the Office of Public Affairs (ASD/PA) and is releasable to the National Technical Information Service (NTIS). At NTIS, it will be available to the general public, including foreign nations.

This technical report has been reviewed and is approved for publication.



VIPPERLA B. VENKAYYA
Project Engineer
Design & Analysis Methods Group



FREDERICK A. PICCHIONI, Lt Col, USAF
Chief, Analysis & Optimization Branch

FOR THE COMMANDER



ROGER J. HEGSTROM, Col, USAF
Chief, Structures & Dynamics Div.

"If your address has changed, if you wish to be removed from our mailing list, or if the addressee is no longer employed by your organization please notify AFWAL/FIBRA, W-PAFF, OH 45433-6553 to help us maintain a current mailing list".

Copies of this report should not be returned unless return is required by security considerations, contractual obligations, or notice on a specific document.

The following notice applies to any unclassified (including originally classified and now declassified) technical reports released to "qualified U.S. contractors" under the provisions of DoD Directive 5230.25, Withholding of Unclassified Technical Data From Public Disclosure.

NOTICE TO ACCOMPANY THE DISSEMINATION OF EXPORT-CONTROLLED TECHNICAL DATA

1. Export of information contained herein, which includes, in some circumstances, release to foreign nationals within the United States, without first obtaining approval or license from the Department of State for items controlled by the International Traffic in Arms Regulations (ITAR), or the Department of Commerce for items controlled by the Export Administration Regulations (EAR), may constitute a violation of law.
2. Under 22 U.S.C. 2778 the penalty for unlawful export of items or information controlled under the ITAR is up to two years imprisonment, or a fine of \$100,000, or both. Under 50 U.S.C., Appendix 2410, the penalty for unlawful export of items or information controlled under the EAR is a fine of up to \$1,000,000, or five times the value of the exports, whichever is greater; or for an individual, imprisonment of up to 10 years, or a fine of up to \$250,000, or both.
3. In accordance with your certification that establishes you as a "qualified U.S. Contractor", unauthorized dissemination of this information is prohibited and may result in disqualification as a qualified U.S. contractor, and may be considered in determining your eligibility for future contracts with the Department of Defense.
4. The U.S. Government assumes no liability for direct patent infringement, or contributory patent infringement or misuse of technical data.
5. The U.S. Government does not warrant the adequacy, accuracy, currency, or completeness of the technical data.
6. The U.S. Government assumes no liability for loss, damage, or injury resulting from manufacture or use for any purpose of any product, article, system, or material involving reliance upon any or all technical data furnished in response to the request for technical data.
7. If the technical data furnished by the Government will be used for commercial manufacturing or other profit potential, a license for such use may be necessary. Any payments made in support of the request for data do not include or involve any license rights.
8. A copy of this notice shall be provided with any partial or complete reproduction of these data that are provided to qualified U.S. contractors.

D E S T R U C T I O N N O T I C E

For classified documents, follow the procedures in DoD 5200.22-M, Industrial Security Manual, Section II-19 or DoD 5200.1-R, Information Security Program Regulation, Chapter IX. For unclassified, limited documents, destroy by any method that will prevent disclosure of contents or reconstruction of the document.

ADB108208L

REPORT DOCUMENTATION PAGE

1a. REPORT SECURITY CLASSIFICATION UNCLASSIFIED			1b. RESTRICTIVE MARKINGS TUE										
2a. SECURITY CLASSIFICATION AUTHORITY			3. DISTRIBUTION/AVAILABILITY OF REPORT Distribution limited to U.S. Government Agencies only; critical technology 1/86. Other requests must be referred to AFWAL/FIBRA. WPAFB OH 45433										
2b. DECLASSIFICATION/DOWNGRADING SCHEDULE			5. MONITORING ORGANIZATION REPORT NUMBER(S) AFWAL-TR-86-3034										
4. PERFORMING ORGANIZATION REPORT NUMBER(S) NOR 86-210			7a. NAME OF MONITORING ORGANIZATION Flight Dynamics Laboratory (AFWAL/FIBRA) Air Force Wright Aeronautical Laboratories										
6a. NAME OF PERFORMING ORGANIZATION Northrop Corporation Aircraft Division		6b. OFFICE SYMBOL (If applicable)	7b. ADDRESS (City, State and ZIP Code) Wright-Patterson Air Force Base Dayton, OH 45433-6553										
6c. ADDRESS (City, State and ZIP Code) One Northrop Avenue Hawthorne, CA 90250		8. PROCUREMENT INSTRUMENT IDENTIFICATION NUMBER Contract F33615-82-C-3217											
6d. NAME OF FUNDING/SPONSORING ORGANIZATION		6e. OFFICE SYMBOL (If applicable)	10. SOURCE OF FUNDING NOS.										
6f. ADDRESS (City, State and ZIP Code)		<table border="1"> <thead> <tr> <th>PROGRAM ELEMENT NO.</th> <th>PROJECT NO.</th> <th>TASK NO.</th> <th>WORK UNIT NO.</th> </tr> </thead> <tbody> <tr> <td>62201F</td> <td>2401</td> <td>02</td> <td>55</td> </tr> </tbody> </table>				PROGRAM ELEMENT NO.	PROJECT NO.	TASK NO.	WORK UNIT NO.	62201F	2401	02	55
PROGRAM ELEMENT NO.	PROJECT NO.	TASK NO.	WORK UNIT NO.										
62201F	2401	02	55										
11. TITLE (Include Security Classification) See Reverse													
12. PERSONAL AUTHOR(S) R. L. Ramkumar, E. S. Saether, K. Appa													
13a. TYPE OF REPORT Final		13b. TIME COVERED FROM 6/1/84 TO 12/1/85		14. DATE OF REPORT (Yr., Mo., Day) July 1986									
15. PAGE COUNT 105													
16. SUPPLEMENTARY NOTATION													
17. COSATI CODES			18. SUBJECT TERMS (Continue on reverse if necessary and identify by block number)										
FIELD	GROUP	SUB. GR.	See Reverse										
01	03												
13	05												
19. ABSTRACT (Continue on reverse if necessary and identify by block number) This report presents a strength analysis for laminated and/or metallic plates bolted together by many fasteners. This analysis has been programmed and designated as the SAMCJ (Strength Analysis of Multi-fastened Composite Joints) computer code. SAMCJ incorporates a finite element method using special elements developed in this program to predict fastener load distributions, a stress analysis to compute average stress components at fastener locations, and a failure analysis which predicts joint failure load, failure location and mode of failure. Analytical predictions of failure mode and location show an excellent agreement with experimental data generated in this program. Predictions of joint strengths are fairly accurate and generally conservative. SAMCJ represents the first one-step, test-independent analysis that computes load distribution among many fasteners, and predicts joint failure load, failure mode and failure location. This is a validated analytical that can be used in the design of efficient joints in laminated structural parts. The use of the SAMCJ computer code is fully explained in the design guide being issued concurrently.													
20. DISTRIBUTION/AVAILABILITY OF ABSTRACT UNCLASSIFIED/UNLIMITED <input type="checkbox"/> SAME AS RPT <input checked="" type="checkbox"/> DTIC USERS <input type="checkbox"/>			21. ABSTRACT SECURITY CLASSIFICATION Unclassified										
22a. NAME OF RESPONSIBLE INDIVIDUAL V. B. Venkayya			22b. TELEPHONE NUMBER (Include Area Code) (513) 255-6992		22c. OFFICE SYMBOL AFWAL/FIBRA								

11. Title

Strength Analysis of Laminated and Metallic Plates Bolted Together by Many Fasteners.

18. Subject Terms

(cont)
→ Bolted plates; metals and composites; multiple fasteners; adjacent cut-outs; strength analysis; ~~special finite elements~~; fastener load distribution; failure analysis; average stress failure criteria; test correlation; validation of analysis; various fastener arrangements.

→ Composite structures.

PREFACE

This report was prepared under Contract F33615-82-C-3217, titled "Bolted Joints in Composite Structures: Design Analysis and Verification," and administered by the Air Force Wright Aeronautical Laboratories. The Air Force Project Engineer for the program is Dr. V. B. Venkayya. Capt. M. Sobota and 2nd Lt. D. L. Graves are the co-monitors at the Air Force. The program manager and principal investigator at Northrop is Dr. R. L. Ramkumar.

This report addresses the analytical effort in Task 2 of the referenced program (Program 2401).

The authors extend their appreciation to R. Cordero for her assistance with graphics, and to C. Harris for typing this report.



Accession For	
NTIS GRA&I	<input type="checkbox"/>
DTIC TAB	<input checked="" type="checkbox"/>
Unannounced	<input type="checkbox"/>
Justification	
By _____	
Distribution/	
Availability Codes	
Dist	Avail and/or Special
B-3	4 57

TABLE OF CONTENTS

SECTION		PAGE
1	INTRODUCTION.....	1
2	ANALYTICAL DESCRIPTION.....	5
	2.1 Overview of the Strength Analysis of Bolted Laminates (SAMCJ).....	5
	2.2 Development of Special Finite Elements.....	11
	2.2.1 The Effective Fastener Element.....	12
	2.2.2 Element Stiffness Matrix for a Plate with a Loaded Hole.....	20
	2.2.3 Stiffness Matrices for a Plate with an Unloaded (Open) Hole and for Plain (Unnotched) Elements.....	32
	2.3 Load Distribution Among Fasteners.....	38
	2.4 Stress State at Any Location in a Bolted Plate.....	40
	2.5 Strength and Failure Mode Prediction for a Bolted Plate.....	42
	2.6 Current SAMCJ Limitations.....	45
	2.7 Design Application.....	50
	2.8 Test Requirements.....	50
3	ANALYTICAL PREDICTIONS.....	52
	3.1 Composite-to-Metal Joints with Two Fasteners in Tandem.....	57
	3.2 Composite-to-Metal Joints with Two Fasteners at an Angle to the Load Direction.....	65

TABLE OF CONTENTS (CONCLUDED)

SECTION	PAGE
3.3 Composite-to-Metal Joints with Four Fasteners in a Rectangular Pattern.....	69
3.4 Composite-to-Metal Joints with Three Fasteners in a Triangular Pattern.....	76
3.5 Composite-to-Metal Joints with Six Fasteners and an Adjacent Circular Cut-Out in the Laminate.....	80
3.6 Composite-to-Metal Joints with Five Fasteners in a Row.....	84
4 CONCLUSIONS.....	91
REFERENCES.....	93

LIST OF ILLUSTRATIONS

FIGURE NO.		PAGE
1	Schematic Breakdown of the Strength Analysis of Bolted Joints.....	6
2	Flow Chart of SAMCJ Operations.....	7
3	Application of Load and Displacement Boundary Conditions in the SAMCJ Code.....	9
4	Effect of Joint Configuration (Single Versus Double Shear) on Fastener Deflection.....	13
5	Typical Rigid and Flexible Fasteners.....	14
6	A Single-Lap Configuration with Various End Constraints on the Fastener.....	15
7	Representation of a Single-Lap Configuration by and equivalent Fastener Problem.....	16
8	Boundary and Continuity Conditions for a Typical Single-Lap Joint.....	17
9	Boundary and Continuity Conditions for a Typical Double-Lap Joint.....	18
10	An Example of the Node Layout and Number Scheme in a Single-Lap Shear Joint Configuration.....	19
11	A General Node Arrangement with n Nodes in Plate 1 and m Nodes in Plate 2.....	19
12	Effective Fastener Representation and Stiffness Matrix.....	21
13	A Matrix for the five-Node Element Containing Element Rigid Body Modes.....	26

LIST OF ILLUSTRATIONS (CONTINUED)

FIGURE NO.		PAGE
14	Five-Node Loaded Hole Element with Depicted Nodal Degrees of Freedom.....	29
15	The Seven Natural Load Cases for the Loaded Hole Element.....	30
16	Typical Distribution of Gaussian Quadrature Points in Loaded and Unloaded Hole Elements.....	33
17	Exaggerated Deformation Profile for a Natural Load Case.....	34
18	The Four-Node Open Hole Element with Depicted Nodal Degrees of Freedom.....	35
19	The Five Natural Load Cases for the Unloaded Hole and Plain Elements.....	36
20	Finite Element Model of a Sample Tapered Bolted Joint.....	39
21	The Characteristic Distances Used in the Average Stress Failure Criteria.....	43
22	Locations where Average Stresses are Obtained Under Tension and Compression Loading to Predict Net Section, Bearing, and Shearout Modes of Failure.....	44
23	Comparison of Experimental Data with the Analytical Predictions Using Three Forms of (A) Matrices (Two Rows of Fasteners).....	47
24	Comparison of Experimental Data with the Analytical Predictions Using Three Forms of (A) Matrices (Five Rows of Fasteners).....	48

LIST OF ILLUSTRATIONS (CONTINUED)

FIGURE NO.		PAGE
25	Element Load Recovery for Various a/D and b/D Ratios.....	49
26	Dimensions of the Metal Plates for the Various Composite-to-Metal Multifastener Joints.....	56
27	Finite Element Model for Test Case 201.....	58
28	SAMCJ Input for Test Case 201.....	59
29	SAMCJ Predictions and Test Results for Test Case 201.....	63
30	SAMCJ Predictions and Test Results for Test Case 202.....	64
31	SAMCJ Predictions and Test Results for Test Case 203.....	66
32	SAMCJ Predictions and Test Results for Test Case 206.....	67
33	Two-, Four- and Sixteen- Element Models of the Bolted Plates in Test Case 221.....	68
34	SAMCJ Prediction and Test Results for Test Case 221.....	70
35	Eight-Element Model of Each Bolted Plate in Test Cases 225, 229 and 230.....	72
36	SAMCJ Predictions and Test Results for Test Case 225.....	73
37	SAMCJ Predictions and Test Results for Test Case 229.....	74
38	SAMCJ Predictions and Test Results for Test Case 230.....	75

LIST OF ILLUSTRATIONS (CONCLUDED)

FIGURE NO.		PAGE
39	Four-Element Model of the Bolted Plates in Test Cases 234, 238 and 239.....	77
40	SAMCJ Predictions and Test Results for Test Case 234.....	78
41	SAMCJ Predictions and Test Results for Test Case 238.....	79
42	SAMCJ Predictions and Test Results for Test Case 239.....	81
43	Nine-Element Model of the Bolted Plates in Test Case 243, 246 and 247.....	82
44	SAMCJ Predictions and Test Results for Test Case 243.....	83
45	SAMCJ Predictions and Test Results for Test Case 246.....	85
46	SAMCJ Predictions and Test Results for Test Case 247.....	86
47	Six-Element Model of the Bolted Plates in Test Cases 250 and 251.....	87
48	SAMCJ Predictions and Test Results for Test Case 250.....	89
49	SAMCJ Predictions and Test Results for Test Case 251.....	90

LIST OF TABLES

TABLE		PAGE
1	TASK II TESTS ON MULTIFASTENER JOINTS.....	53

SECTION 1

INTRODUCTION

An analysis was developed in this Northrop/AFWAL program to predict the strength of bolted composite structures. This report presents details of the developed analysis, sample predictions, and a discussion on its validity and its application to structural design.

Prior to the initiation of this program, the strength of a bolted laminate was analytically predicted using approximate analyses and experimental results. The distribution of the applied load among the fasteners was initially obtained, and the most critical fastener location was subsequently analyzed to predict the joint strength. The fastener load distribution analysis was essentially one-dimensional, assuming that all the fasteners in a row (perpendicular to the load direction) carried equal loads. And, the load distribution among the various rows was predicted based on experimentally obtained "joint stiffness" values. The subsequent strength analysis at a fastener location was based on an infinite plate stress analysis and was incapable of accounting for neighboring stress concentrators (like a free edge, a cut-out or a neighboring fastener location).

A strength analysis was developed in this Northrop/AFWAL program to overcome the major deficiencies that existed at its inception. The analysis incorporates special finite elements into a failure analysis procedure that predicts the fastener load distribution, the critical fastener location, the joint strength and its failure mode. Four special finite elements were developed using a fastener analysis and a stress analysis that accounts for finite

laminates planform dimensions (see Reference 1). These elements include a loaded hole element, an unloaded hole element, a plain element, and an effective fastener element. A finite element model of the bolted joint computes the fastener load distribution and averaged stresses at each fastener and cut-out location. The critical fastener or cut-out location, the joint failure load and the corresponding failure mode are predicted based on these computations.

The developed strength analysis has been programmed to be the SAMCJ (Strength Analysis of Multifastener Composite Joints) computer code. SAMCJ requires a definition of the geometry and the material properties of the bolted plates and fasteners as input. The presence of any cut-out is included in the finite element model as an "unloaded hole" element linked to adjacent "loaded hole" and plain elements. The input material properties of the bolted laminates include failure parameters that are required by the average stress failure criteria. These are distances from the fastener or cut-out hole boundaries, at selected locations, over which stresses are averaged and compared to plain laminate strengths, to predict failure (see Reference 1). SAMCJ computes the joint load values for net section, bearing and shear-out modes of failure at each fastener and cut-out location. Information corresponding to the least value provides the joint failure load, the critical fastener or cut-out location, and the failure mode.

In computing the fastener load distribution and the critical average stress values at every fastener/cut-out location, SAMCJ also accounts for fastener flexibility effects. The FDFA fastener analysis, developed earlier in the program (Reference 1), is used to compute the effective fastener stiffness, accounting for bolt torque and load eccentricity (single versus double shear transfer of the applied load). FDFA is employed twice to compute the effective transverse stiffnesses of the fastener, along and perpendicular to the load direction. The effective fastener stiffness matrix connects the bolted plates at the fastener

locations, accounting for all significant joint parameters.

The significant improvements offered by SAMCJ over the state-of-the-art at program inception are:

(1) SAMCJ performs a one-step analysis that computes the fastener load distribution, critical fastener location, joint failure load, and the corresponding failure mode. Hitherto, separate fastener load distribution and failure analyses were performed, requiring a two-step analytical procedure.

(2) SAMCJ only requires the geometric and material properties of the bolted plates and fasteners as input. SAMCJ internally computes the effective transverse fastener stiffness values that account for fastener size, fastener and bolted plate material properties, bolt torque, load eccentricity (single versus double shear load transfer), and the local three dimensional stress state at the fastener location. Hitherto, these effects could only be accounted for via experimentally measured "joint stiffnesses." SAMCJ eliminates the need for these experimental measurements, and is, therefore, the first multifastener bolted joint strength analysis that is devoid of dependence on test results.

(3) SAMCJ performs a two-dimensional load distribution analysis, and predicts the magnitude and orientation of the load at each fastener location via components of the fastener load along and perpendicular to the load direction. Analyses available at program inception only addressed the row-to-row load variation, or the axial components of the fastener loads, resorting to a one-dimensional analysis.

(4) SAMCJ accounts for stress concentration interaction effects that hitherto could not be accounted for. This includes the effects of adjacent free edges, cut-outs and proximate fastener locations.

(5) SAMCJ accounts for tapered bolted plate geometries that are commonplace in practical situations.

There are, however, segments of the SAMCJ computer code that can be improved beyond their present capabilities. These are addressed in the following sections of this report. Nevertheless, the significant achievements of SAMCJ over the state-of-the-art at program inception remain unscathed.

SAMCJ, by virtue of the above qualities, is an excellent design tool. It can be used to evaluate different fastener patterns and to select among these for a specific loading state at a bolted joint location.

SECTION 2

ANALYTICAL DESCRIPTION

This section presents an overview of the strength analysis of bolted laminates (the SAMCJ computer code), a description of the developed special finite elements, and the analytical procedure used in SAMCJ to predict fastener loads, the critical fastener or cut-out location, the corresponding joint strength and the failure mode. The application of the developed analysis in the design of bolted laminates, and the test requirements for this application, are also included.

2.1 Overview of the Strength Analysis of Bolted Laminates (SAMCJ)

The development of a reliable strength analysis is crucial to the design of highly loaded bolted joints in composite structures. As shown in Figure 1, structural loads translate into inplane stress resultants (N_x , N_y and N_{xy}) that transfer from one component to another (skin to substructure, for example) through many fasteners. The SAMCJ (Strength Analysis of Multifastener Composite Joints) computer code was developed to analyze such a load transfer situation, to compute the failure value of the applied load, and to predict the critical fastener location and the joint failure mode.

A flow chart of SAMCJ operations is presented in Figure 2. As input, SAMCJ requires the user to specify how the bolted plates are divided into plain elements and elements with loaded or unloaded holes. The bolted plates are currently assumed by SAMCJ to be subjected to uniaxial tensile or compressive loading, in a single or double shear configuration. The uniaxial restriction on the load

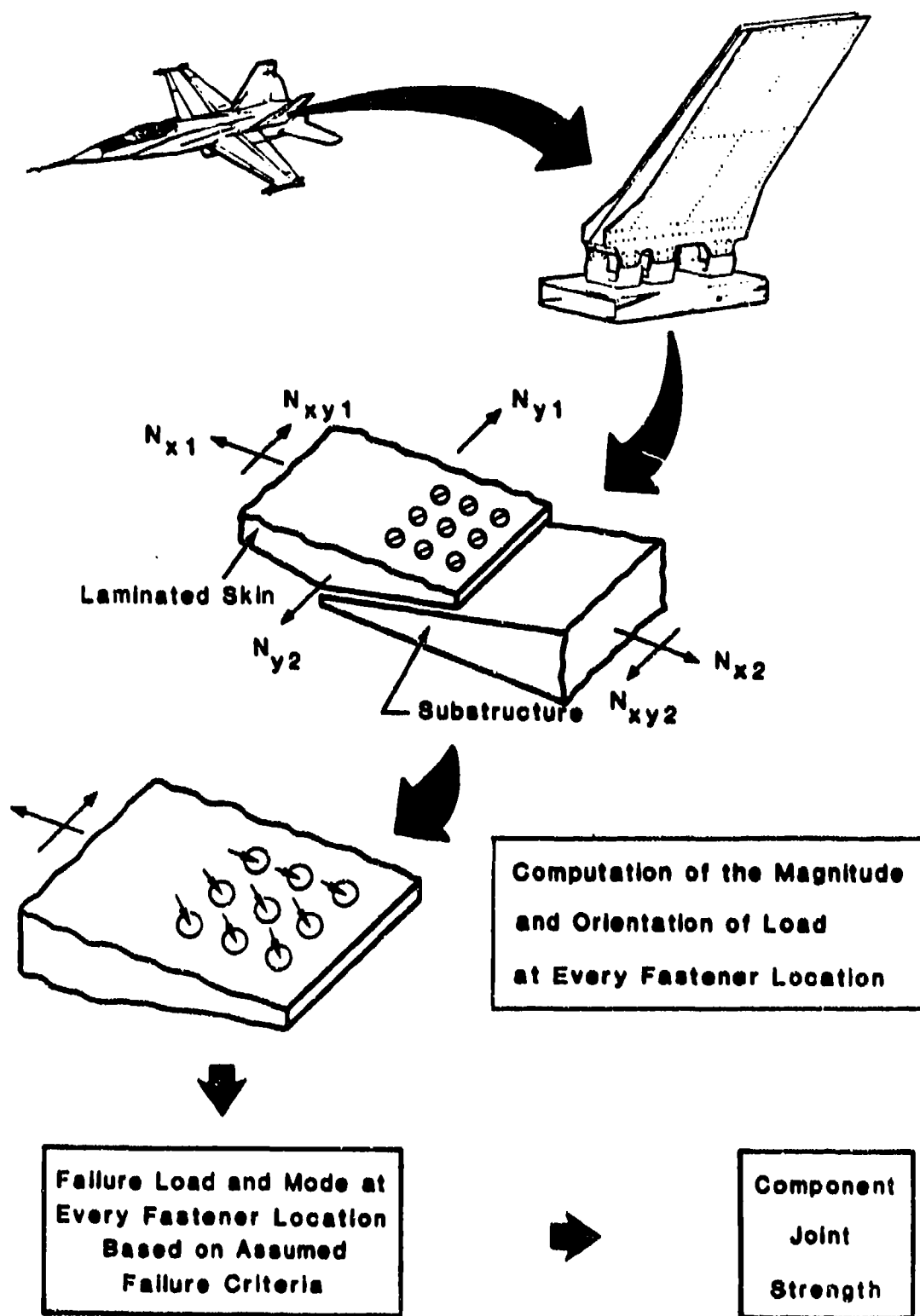


Figure 1. Schematic Breakdown of the Strength Analysis of Bolted Joints.

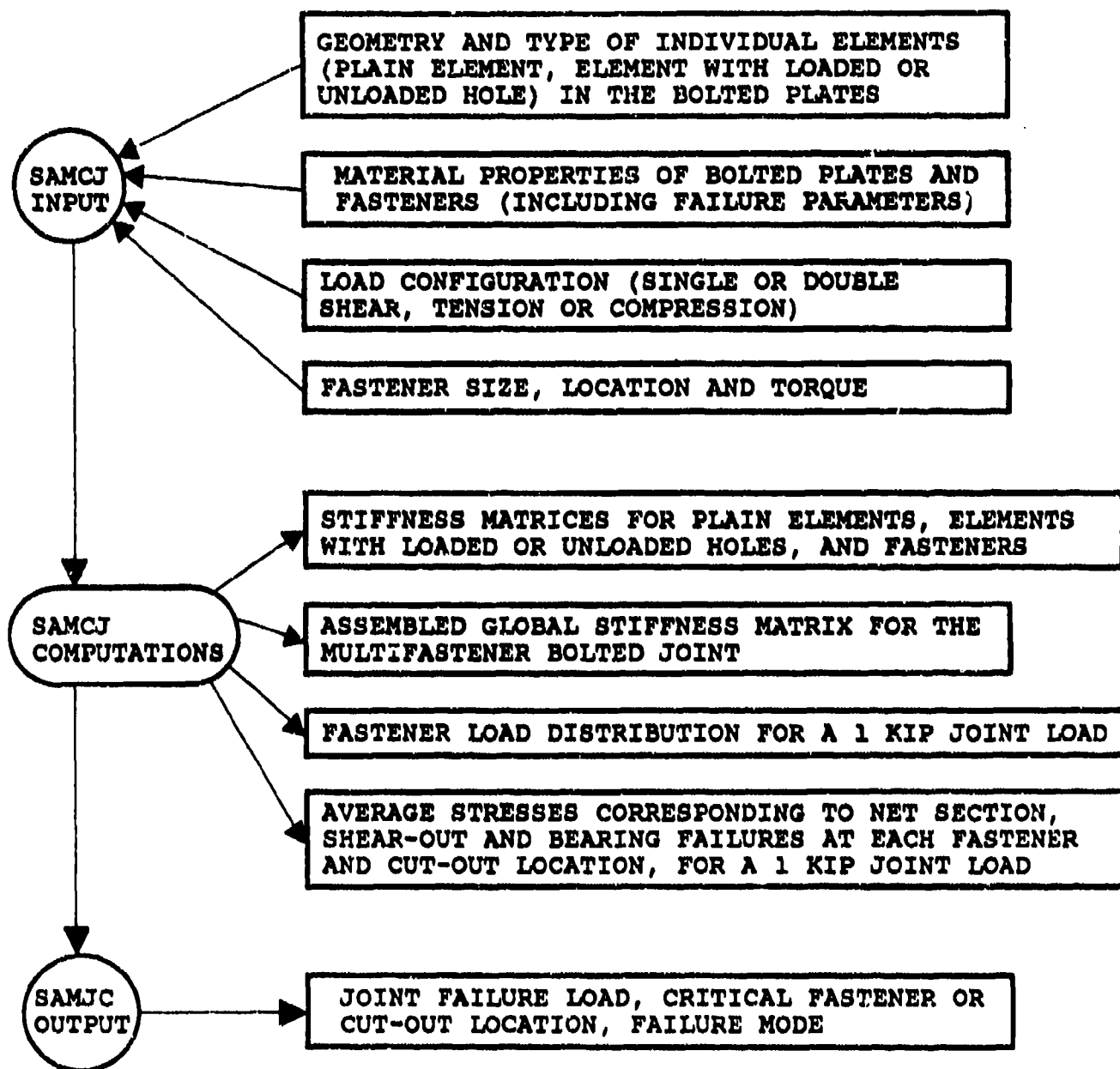


Figure 2. Flow Chart of SAMCJ Operations.

was incorporated into the code because all the test specimens in the experimental part of the program were only subjected to uniaxial loads (see Reference 2). This restriction, however, can be easily removed from the SAMCJ code by modifying it to require the user to specify the general biaxial loading. Additional input requirements for the SAMCJ code include the material properties of the bolted plates and fasteners, and the fastener size, location and torque. The material properties of the bolted laminates include the tensile and compressive failure strains in the fiber direction of the lamina, and the characteristic distances over which stresses are averaged to predict net section, shear-out and bearing failures at the fastener or cut-out location.

With the above input, SAMCJ performs the following computations. It initially generates stiffness matrices for all the elements, namely, plain elements, elements with loaded or unloaded holes, and effective fastener elements. The individual stiffness matrices are subsequently assembled to obtain the global stiffness matrix for the bolted joint. A 1-kip uniaxial tensile or compressive joint load is imposed on the left end of the top plate, in accordance with the input instructions (see Figure 3). The nodes at the right end of the bottom plate are constrained from translating in the load direction, and one of these nodes is also constrained in the transverse direction to preclude rigid body translations, (see Figure 3). The solution to this finite element formulation of the bolted joint provides the axial and transverse components of the load at every fastener location, corresponding to a 1-kip joint load. Also computed are the average net section, shear-out and bearing stresses at every fastener and cut-out location, corresponding to a 1 kip joint load.

SAMCJ provides, as output, the failure value of the uniaxial joint load, the critical fastener or cut-out location, and the joint failure mode. These are obtained as follows. The tensile, compressive and shear strengths of the plain laminates are computed based on the input tensile and compressive failure strains

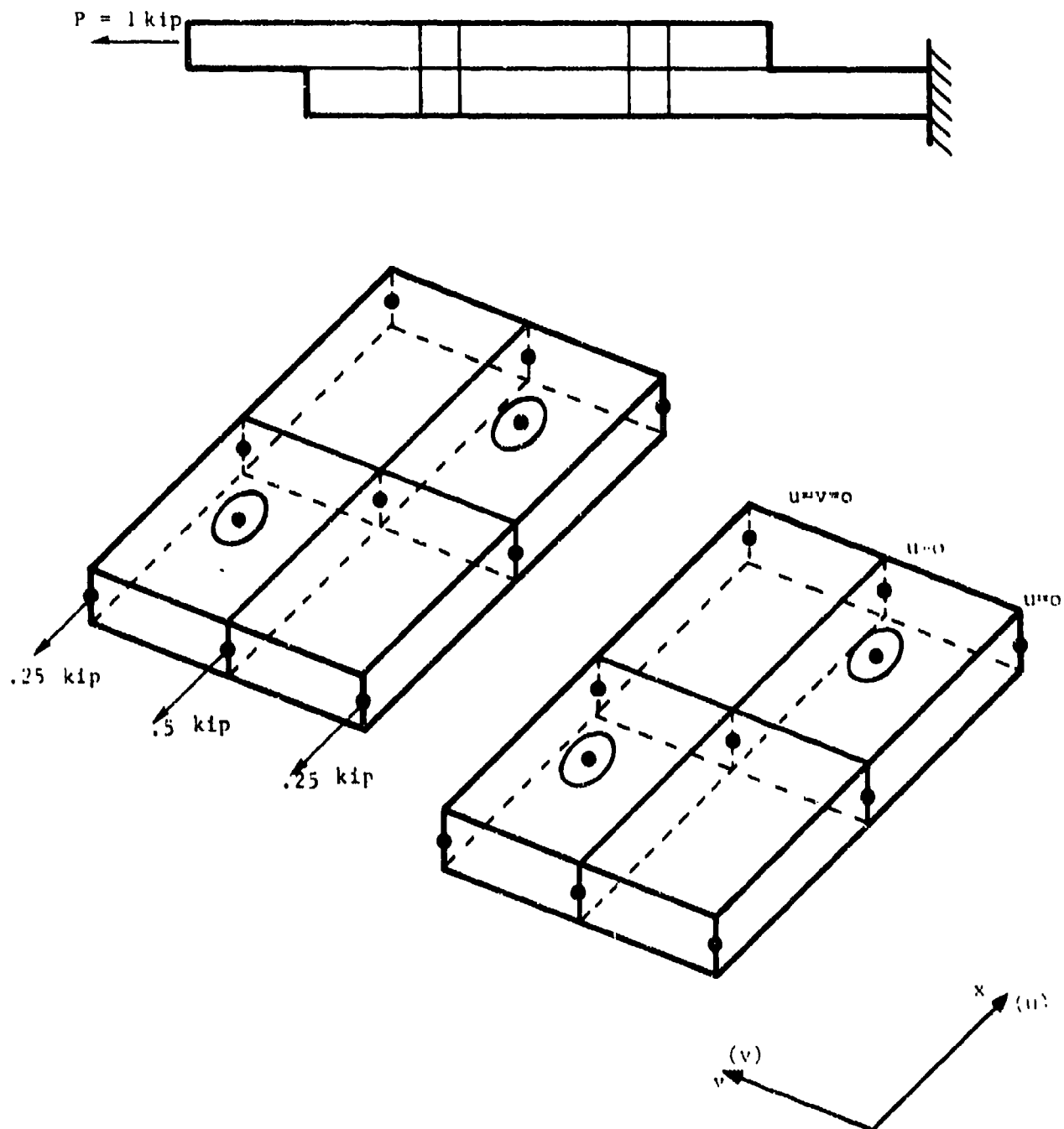


Figure 3. Application of Load and Displacement Boundary Conditions in the SANCJ Code

in the fiber direction of the lamina. The ratios of the averaged stresses to the corresponding plain laminate strengths, at selected locations around each fastener and cut-out boundary, are compared to predict the failure mode, the critical fastener or cut-out location and the joint failure load. SAMCJ predicts net section, shear-out and bearing modes of failure at the laminate level. In Reference 1, similar failure predictions for single-fastener joints in composites were made at the lamina level using the SASCJ computer code. Consequently, the failure parameters (characteristic distances for the three failure modes) used with SAMCJ are different from those used with SASCJ.

The incorporation of the transverse effective fastener stiffness values provides SAMCJ the capability to account for fastener flexibility, torque, and load eccentricity (single versus double shear load transfer). The FDFA code, developed in this program (Reference 1), is used to compute the effective fastener transverse stiffnesses, along and perpendicular to the load direction. The effect of the laminate stacking sequence is also accounted for in this analysis. SAMCJ executes FDFA twice to account for the layup variation (by 90 degrees) from the loading direction to the perpendicular direction.

SAMCJ accounts for stress concentration interaction effects introduced by neighboring cut-outs, free edges and proximate fastener locations. This is made possible by the use of the FIGEOM stress analysis, developed in this program (Reference 1), to generate element stiffness matrices. FIGEOM accounts for finite planform plate dimensions through a boundary collocation solution procedure.

SAMCJ computes the magnitude and the orientation of the load at each fastener location. It is a two-dimensional load distribution analysis that does not rely on an experimental measurement of "joint stiffness" required by other analyses prior to the initiation of this program. In a design situation, many

fastener arrangements can be analytically and economically evaluated by SAMCJ to arrive at the best fastener pattern for the assumed loading conditions.

When the bolted plates are tapered, the SAMCJ user can input equivalent uniform thickness elements to approximate the tapering effect. Adjacent elements in the tapered plate will have different thickness values. This feature is essential in the analysis of most practical joints.

SAMCJ has been developed for the strength prediction of bolted laminated structural parts. It currently assumes that the selected fasteners preclude fastener failure. Also, it applies the same failure procedure to both the bolted plates, accounting for net section, shear-out and bearing failures via the average stress failure criteria. The composite-to-metal joints tested in this program (References 2 and 3) were designed to preclude metallic failures. Therefore, validated failure parameters were not generated for the metallic plates. However, available test results in the open literature may be used to generate these failure parameters, if needed.

2.2 Development of Special Finite Elements

A bolted joint region in a structural part presents many difficulties in performing an accurate analysis. The local three-dimensional effects and the implicit indeterminacy in the fastener load distribution add to the complexity of the analysis. An approximate solution procedure is therefore mandatory in developing a strength analysis for multifastener bolted joints. A finite element approach was adopted in the development of the SAMCJ computer code. Special finite elements were developed to adequately represent the complex stress state in the neighborhood of fasteners and cut-outs, and to account for the effective transverse fastener stiffnesses. The following sub-sections describe the development of the special finite elements.

2.2.1 The Effective Fastener Element

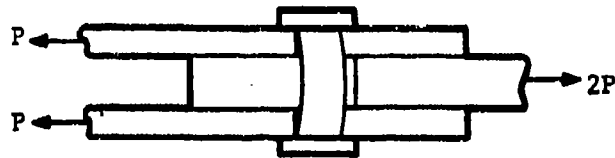
The effective fastener element represents the response of a fastener constrained by its surrounding medium. Its displacement is a function of many joint variables which include the fastener size, modulus and torque, the bolted plate material properties and the layup of laminated plates, the load eccentricity (single versus double shear), and the geometry of the joint. In Reference 1, a finite difference fastener analysis (the FDFA computer code) was developed to account for the effects of these joint parameters on the fastener deflection. This was accomplished by modeling an isolated fastener as a Timoshenko beam resting on an elastic foundation. A brief synopsis of the salient features of this analysis is presented here for completeness.

Figures 4 to 6 illustrate the qualitative influence of joint configuration (single versus double shear), fastener geometry and properties, and fastener end constraints. These effects are accounted for in the mathematical representation shown in Figure 7, and by the incorporation of appropriate boundary conditions (Figures 8 and 9). The elastic foundation moduli for the bolted plates are plywise uniform in a laminate, and are computed based on a stress analysis that accounts for the finite plate dimensions (FIGEOM computer code). The transverse fastener displacement is governed by a fourth order ordinary differential equation, and is computed by solving a central difference formulation of the equation. The fastener length is divided into many nodes, each node representing a ply (or a fraction thereof) in a laminate (see Figures 10 and 11).

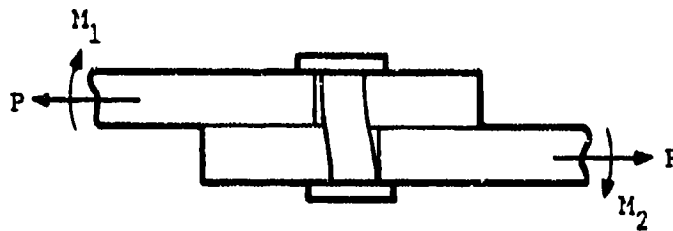
The relative displacement between the bolted plates is computed to obtain the effective fastener stiffness value as follows

$$K_x = P / (\bar{u}_T - \bar{u}_B)$$

(1)

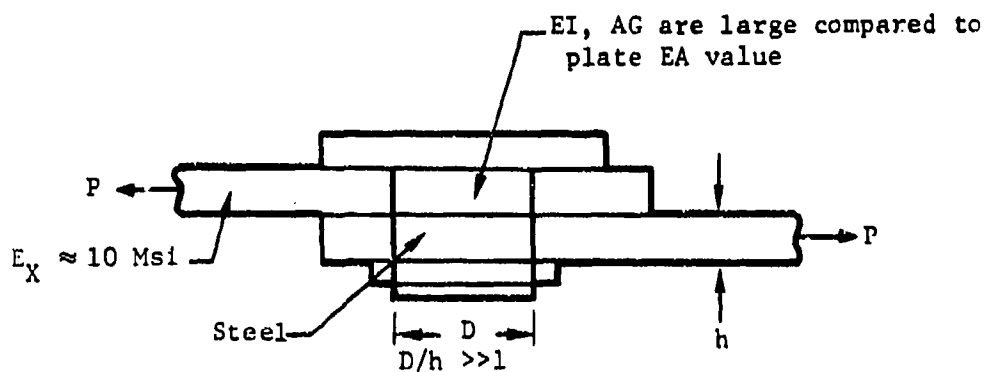


A Double-Lap Configuration.

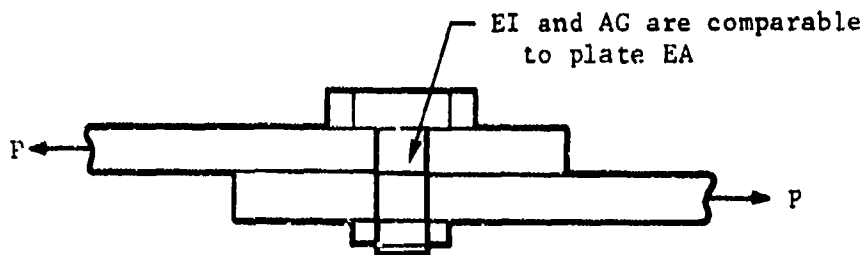


A Single-Lap Configuration.

Figure 4. Effect of Joint Configuration (Single Versus Double Shear) on Fastener Deflection.



(a) Rigid Fastener -- negligible fastener bending & shear deformation



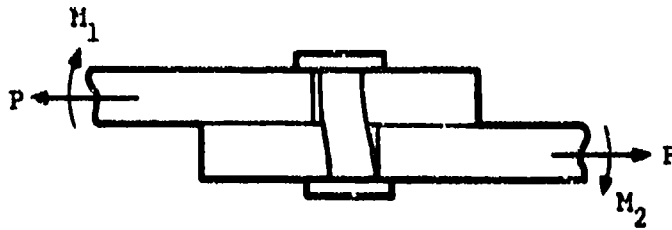
(b) Flexible Fastener -- Measurable fastener bending and shear deformation

EA - plate axial stiffness

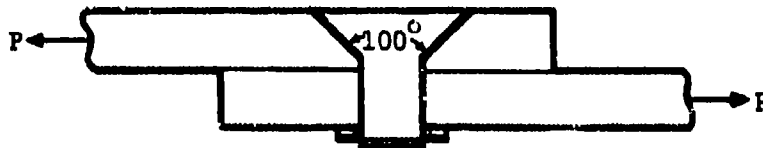
EI - fastener bending stiffness

GA - fastener shear stiffness

Figure 5. Typical Rigid and Flexible Fasteners.



(a) Fixed - Fixed Conditions (Protruding head fastener -- high torque-up)

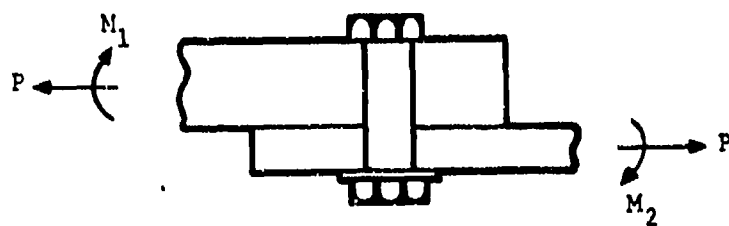


(b) Fixed - Free conditions (countersunk fastener, -- high torque-up)

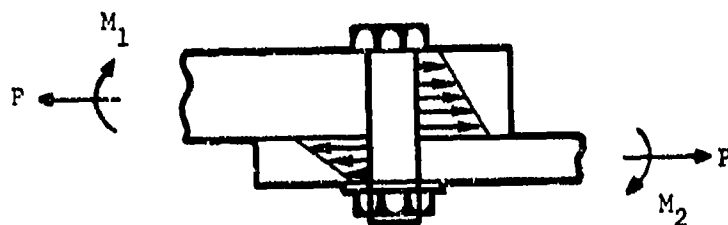


(c) Free-Free Conditions (pin)

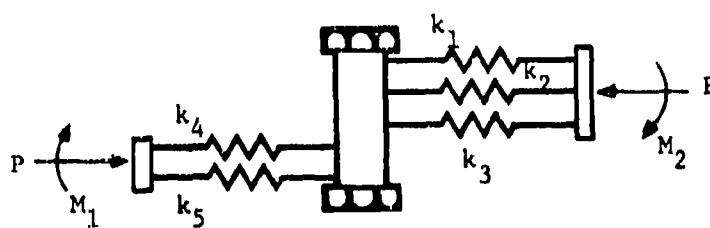
Figure 6. A Single-Lap Configuration with Various End Constraints on the Fastener.



(a) Single Lap Bolted Joint



(b) Typical Fastener/Plate Displacement Variation



(c) Mathematical Representation

Figure 7. Representation of a Single-Lap Configuration by an Equivalent Fastener Problem.

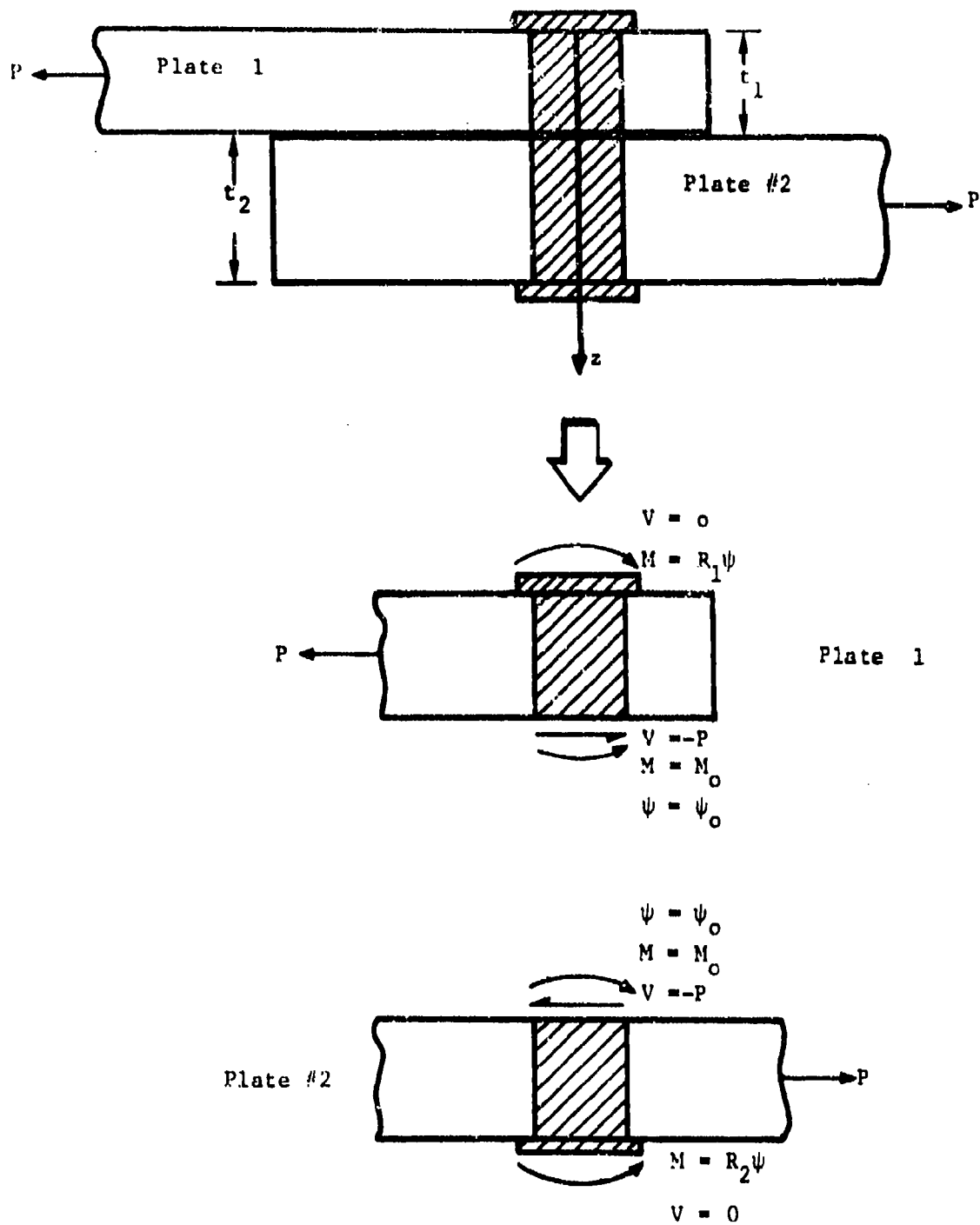


Figure 8. Boundary and Continuity Conditions for a Typical Single-Lap Joint.

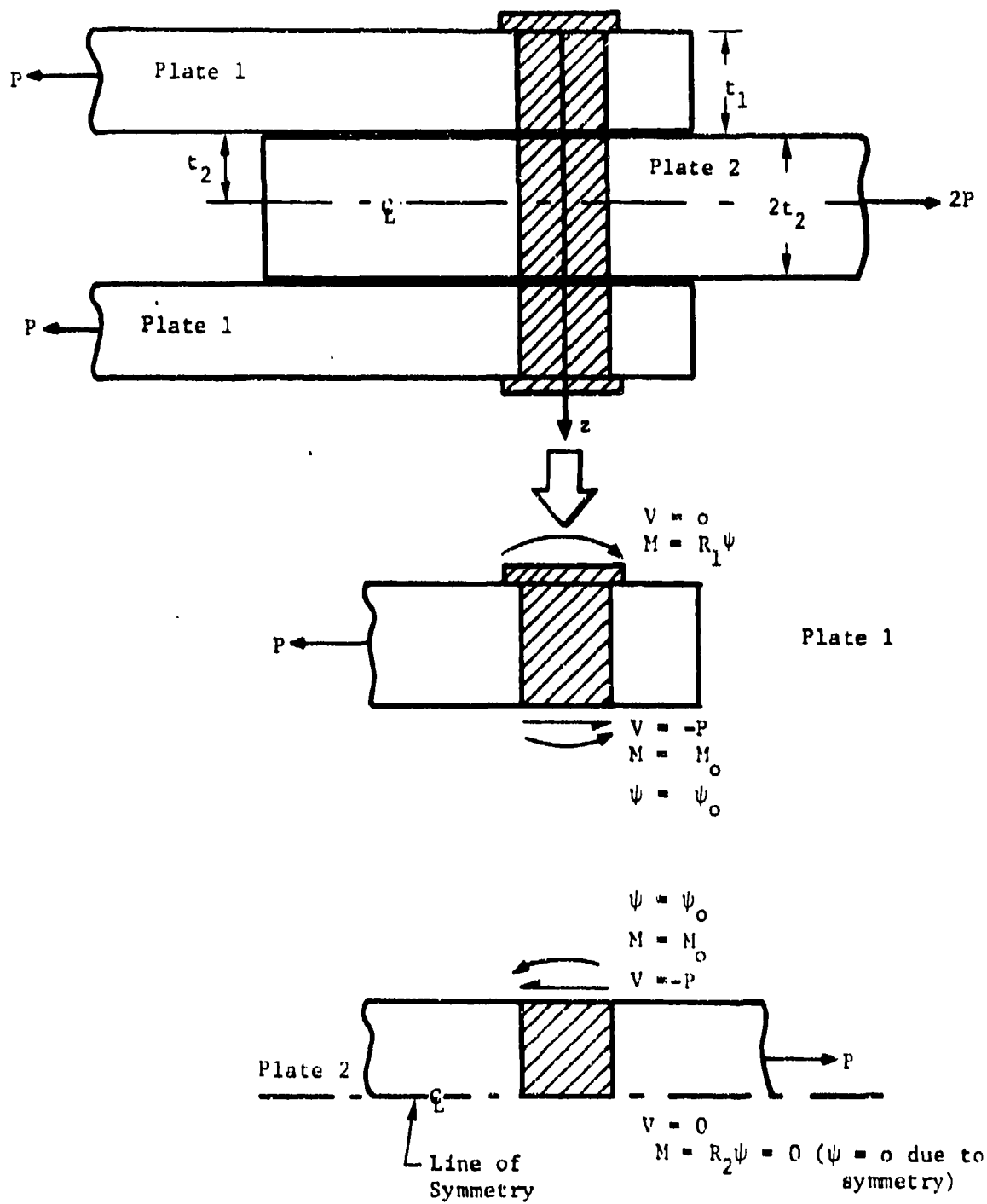


Figure 9. Boundary and Continuity Conditions for a Typical Double-Lap Joint.

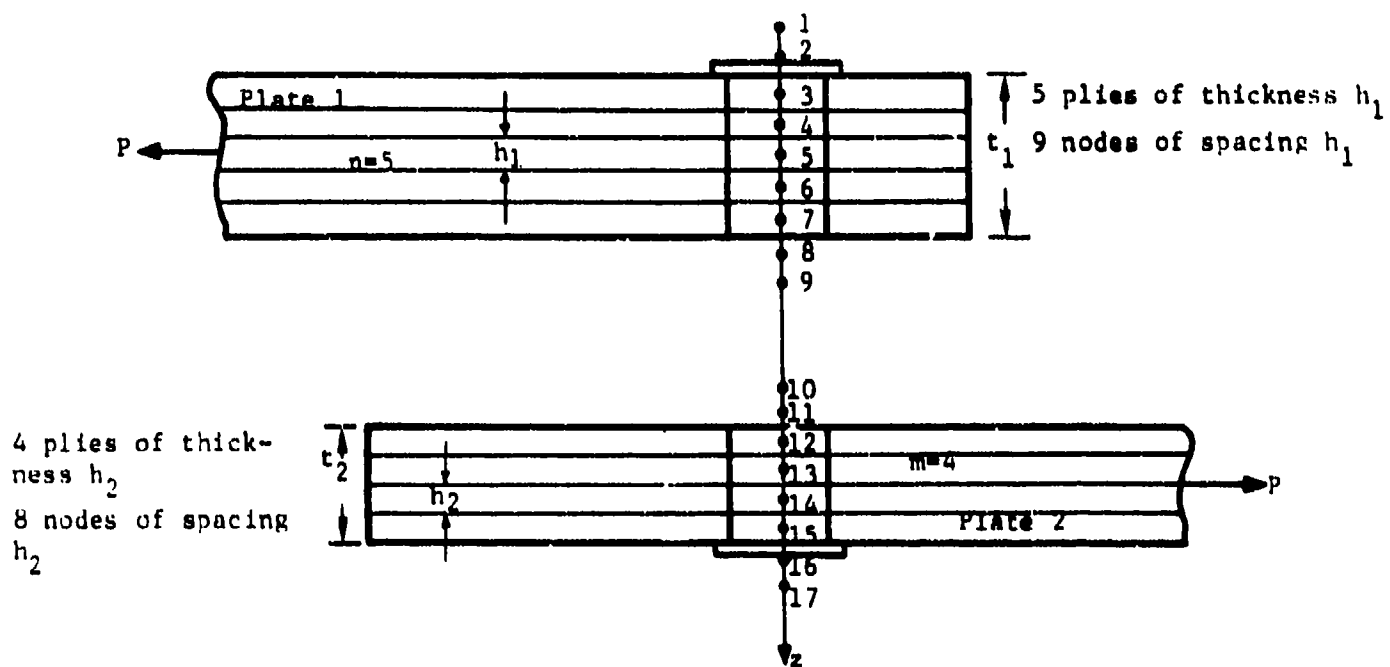


Figure 10. An Example of the Node Layout and Number Scheme in a Single Lap Shear Joint Configuration.

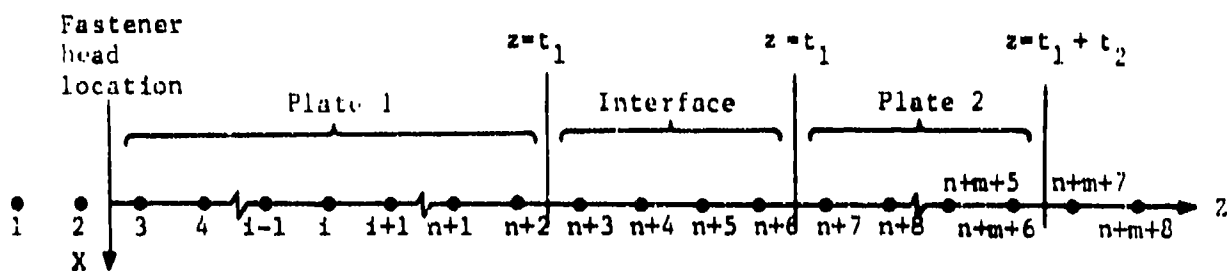


Figure 11. A General Node Arrangement with n Nodes in Plate 1 and m Nodes in Plate 2.

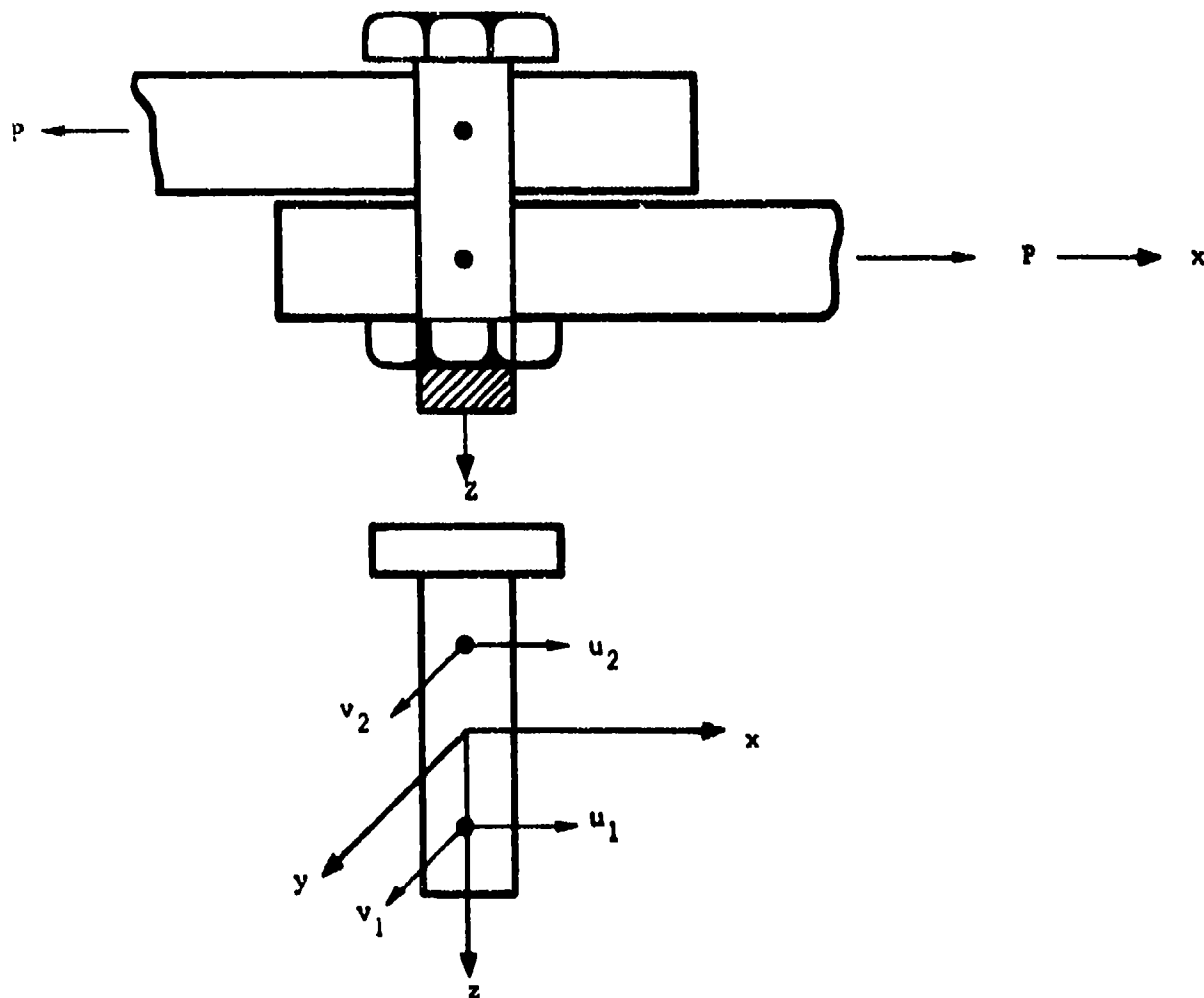
where \bar{u}_T and \bar{u}_B are the average relative displacements between the top and bottom surfaces in the top and bottom plates, respectively. P is the load applied along the x direction in the xy plane of the bolted plates. When both the bolted plates are isotropic, the effective transverse fastener stiffnesses in the x and y directions are identical; i.e., $k_y = k_x$. If either plate is a laminated composite, this analysis is performed twice for each fastener. The layup used to compute k_x is rotated by 90 degrees to obtain k_y .

As shown in Figure 12, the two-node effective fastener element allows two degrees of freedom (DOF) at each node, perpendicular to the axis of the element. Through the FDFA computation of k_x and k_y , a 4×4 effective fastener stiffness matrix is generated. Until now, these stiffnesses, referred to as joint stiffnesses, and were only obtained as experimentally measured quantities.

2.2.2 Element Stiffness Matrix For a Plate With a Loaded Hole

In a general multiply-fastened panel, significant moments and out-of-plane forces can be generated by the applied loading, particularly in a single-shear load transfer configuration. The present analysis assumes that the loaded hole, unloaded hole and plain elements behave essentially as membranes under plane stress conditions.

The characteristic feature of the loaded and unloaded hole elements is the presence of a stress concentrator (the hole) which complicates the process of determining stiffness coefficients. The FIGEOM code, developed and described in Reference 1, is capable of computing the state of stress within a doubly-connected region of



$$\begin{matrix}
 & u_1 & v_1 & u_2 & v_2 \\
 \begin{matrix} u_1 \\ v_1 \\ u_2 \\ v_2 \end{matrix} & \begin{bmatrix} k_x & 0 & -k_x & 0 \\ 0 & k_y & 0 & -k_y \\ -k_x & 0 & k_x & 0 \\ 0 & -k_y & 0 & k_y \end{bmatrix}
 \end{matrix}$$

Figure 12. Effective Fastener Representation and Stiffness Matrix

finite dimensions, under arbitrary inplane biaxial loading. The successful development of FIGEOM motivated the adoption of a flexibility approach to computing the element stiffness matrix. The natural mode method, originally proposed by Argyris, is employed for this purpose (Reference 4).

The natural mode method was originally developed as a simpler alternative to the sometimes tedious matrix displacement method of determining element stiffness relationships. The natural mode method recognizes that the total number of kinematic degrees of freedom in an element can be separated into straining and rigid body modes. Only the straining modes give rise to stiffnesses that are referred to as natural or invariant stiffnesses. The natural stiffness matrix is of a lower order than the global stiffness matrix. The natural mode technique proceeds from a flexibility standpoint in which natural load cases are initially imposed to compute the natural flexibilities. The natural flexibility matrix is subsequently inverted to yield the natural stiffness matrix. The natural stiffness matrix is then expanded to yield the global stiffness matrix using relationships between the natural modes and the nodal displacements.

The natural flexibility coefficients are computed based on the principle of virtual work. When stresses are varied while strains are held constant, a calculus of variations definition of the virtual work is:

$$\delta W_c = \iiint_V \{\epsilon\}^T \delta \{\sigma\} dV \quad (2)$$

where v is the volume of the domain of interest. The stresses and strains introduced by the natural loads are defined as:

$$\{\sigma\} = [\sigma_x \sigma_y \tau_{xy}]^T = [\bar{\sigma}] \{P_N\} \quad (3)$$

$$\{\epsilon\} = [\epsilon_x \epsilon_y \gamma_{xy}]^T = h[A]^{-1} [\bar{\sigma}] \{P_N\} \quad (4)$$

where $\{\sigma\}$ and $\{\epsilon\}$ are the states of stress and strain at a point in the plate of thickness h , $\{P_N\}$ is a vector of natural or generalized loads, $h[A]$ is the inplane flexibility matrix for a laminated or metallic plate, and $\{\bar{\sigma}\}$ contains the contribution of each natural load case to the total stress state in the plate. Equation 2 may then be written as:

$$\delta W_c = \{P_N\}^T \left\{ \iiint_V [\bar{\sigma}]^T h[A]^{-1} [\bar{\sigma}] dV \right\} \delta \{P_N\} \quad (5)$$

The natural flexibility matrix may then be defined as:

$$[F_N] = \iiint_V [\bar{\sigma}]^T h[A]^{-1} [\bar{\sigma}] dV \quad (6)$$

Integrating in the thickness direction,

$$[F_N] = h^2 \iint_S [\bar{\sigma}]^T [A]^{-1} [\bar{\sigma}] dS \quad (7)$$

where S is the area of the domain of interest. If $\{\rho_N\}$ is the natural displacement vector, the flexibility relationship is expressed as:

$$\{\rho_N\} = [F_N] \{P_N\} \quad (8)$$

or

$$\{P_N\} = [F_N]^{-1} \{\rho_N\} = [K_N] \{\rho_N\} \quad (9)$$

where $[K_N]$ is the natural stiffness matrix.

To relate the displacements in the natural and global coordinate systems, the global displacement vector can be represented as a combination of elastic and rigid body components. Assuming n nodes in the plate element, and two degrees of freedom (u and v in the x and y directions, respectively) at each node,

$$\{\rho\} = [u_1 \ v_1 \ u_2 \ v_2 \ \dots \ u_n \ v_n]^T = \{\rho_e\} + \{\rho_o\} \quad (10)$$

The elastic global displacements at the n nodes are related to the

natural loads as follows:

$$\{p_e\} = [A_N] \{P_N\} \quad (11)$$

where $[A_N]$ is a transformation matrix. Substituting Equation 9 into Equation 11, one obtains:

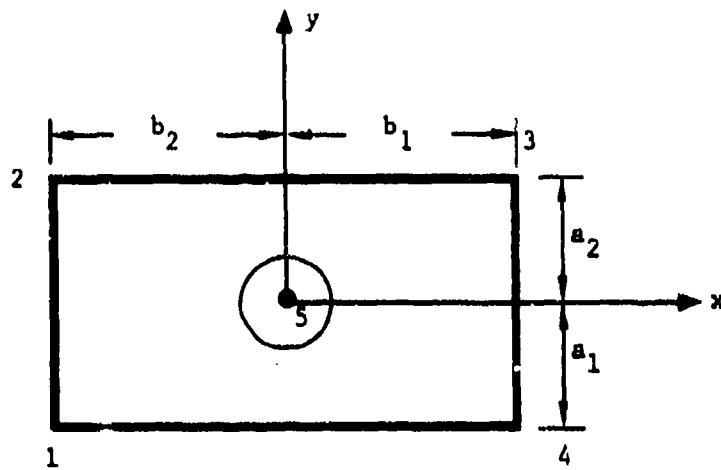
$$\{p_e\} = [A_N] [K_N] \{p_N\} \quad (12)$$

The rigid body components of the global displacements are expressed as:

$$\{p_o\} = [A_o] \{p_o'\} \quad (13)$$

where $\{p_o'\}$ contains the rigid body translations in the x and y directions (u , v), and the rigid body rotation about the z direction (θ_z). The $[A_o]$ matrix is solely dependent on the element geometry, and an example for a five-node element is presented in Figure 13.

The relationships in Equations 12 and 13 are adjoined to yield the following expression for the global displacements (see Equation 10):



$$A_0 = \begin{bmatrix} 1 & 0 & a_1 \\ 0 & 1 & -b_2 \\ 1 & 0 & -a_2 \\ 0 & 1 & -b_2 \\ 1 & 0 & -a_2 \\ 0 & 1 & b_1 \\ 1 & 0 & a_1 \\ 0 & 1 & b_1 \\ 1 & 0 & 0 \\ 0 & 1 & 0 \end{bmatrix}$$

Figure 13. A_0 Matrix for the five-Node Element Containing Element Rigid Body Modes.

$$\{ \rho \} = \left[\begin{array}{cc} [A_N] & [K_N] : [A_o] \end{array} \right] \begin{bmatrix} \rho_N & \rho_o' \end{bmatrix}^T \quad (14)$$

The inverse of Equation 14 yields a relationship between the displacements in the natural and global coordinate systems:

$$\begin{aligned} [\rho_N : \rho_o']^T &= \left[\begin{array}{cc} [A_N] & [K_N] : [A_o] \end{array} \right]^{-1} \{ \rho \} \\ &= \left[\begin{array}{cc} [a_e] & : [a_o] \end{array} \right]^T \{ \rho \} \end{aligned} \quad (15)$$

$$\text{Or, } \{ \rho_N \} = [a_e]^T \{ \rho \} \quad (16)$$

Incorporating Equation 16 into the principle of virtual work, the following relationship between the nodal (global) loads and the natural loads is obtained:

$$\{ P \} = [a_e]^T \{ P_N \} \quad (17)$$

The global stiffness matrix is then related to the natural stiffness matrix $[K_N]$ through the transformation matrix $[a_e]$, as follows:

$$[K_g] = [a_e]^T [K_N] [a_e] \quad (18)$$

The order of the natural flexibility matrix is less than the total number of degrees of freedom (DOF) in the element by three. The 5-node, 10-DOF loaded hole element, (See Figure 14) therefore, requires seven natural load cases that form an uncoupled, orthogonal set. These load cases fully interrogate nodal interactions, and represent the basic element deformation modes, including membrane stretching, shear and bending (see Figure 15). In computing the natural flexibility matrix, Equation 7 is evaluated numerically using a standard Gaussian integration scheme to approximate the surface integral:

$$\begin{aligned}
 [F_N] &= h^2 \iint_S \begin{Bmatrix} \bar{\sigma}_x(x, y) \\ \bar{\sigma}_y(x, y) \\ \bar{T}_{xy}(x, y) \end{Bmatrix}^T [A]^{-1} \begin{Bmatrix} \sigma_x(x, y) \\ \sigma_y(x, y) \\ T_{xy}(x, y) \end{Bmatrix} dx dy \\
 &= h^2 \sum_{i=1}^N \sum_{j=1}^N \begin{Bmatrix} \sigma_x(x_i, y_i) \\ \sigma_y(x_i, y_i) \\ T_{xy}(x_i, y_i) \end{Bmatrix} [A]^{-1} \begin{Bmatrix} \sigma_x(x_i, y_i) \\ \sigma_y(x_i, y_i) \\ T_{xy}(x_i, y_i) \end{Bmatrix} w_i w_j
 \end{aligned} \quad (19)$$

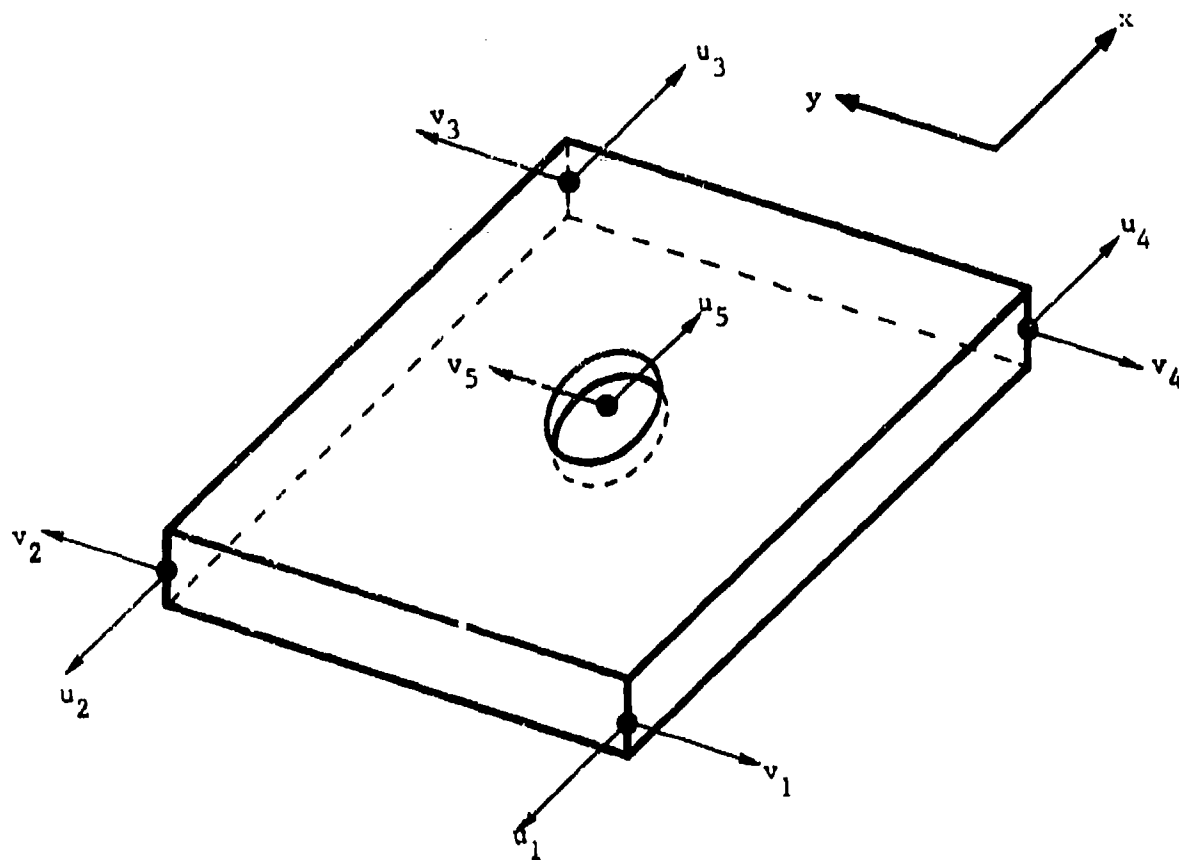


Figure 14. Five-Node Loaded Hole Element With Depicted Nodal Degrees of Freedom

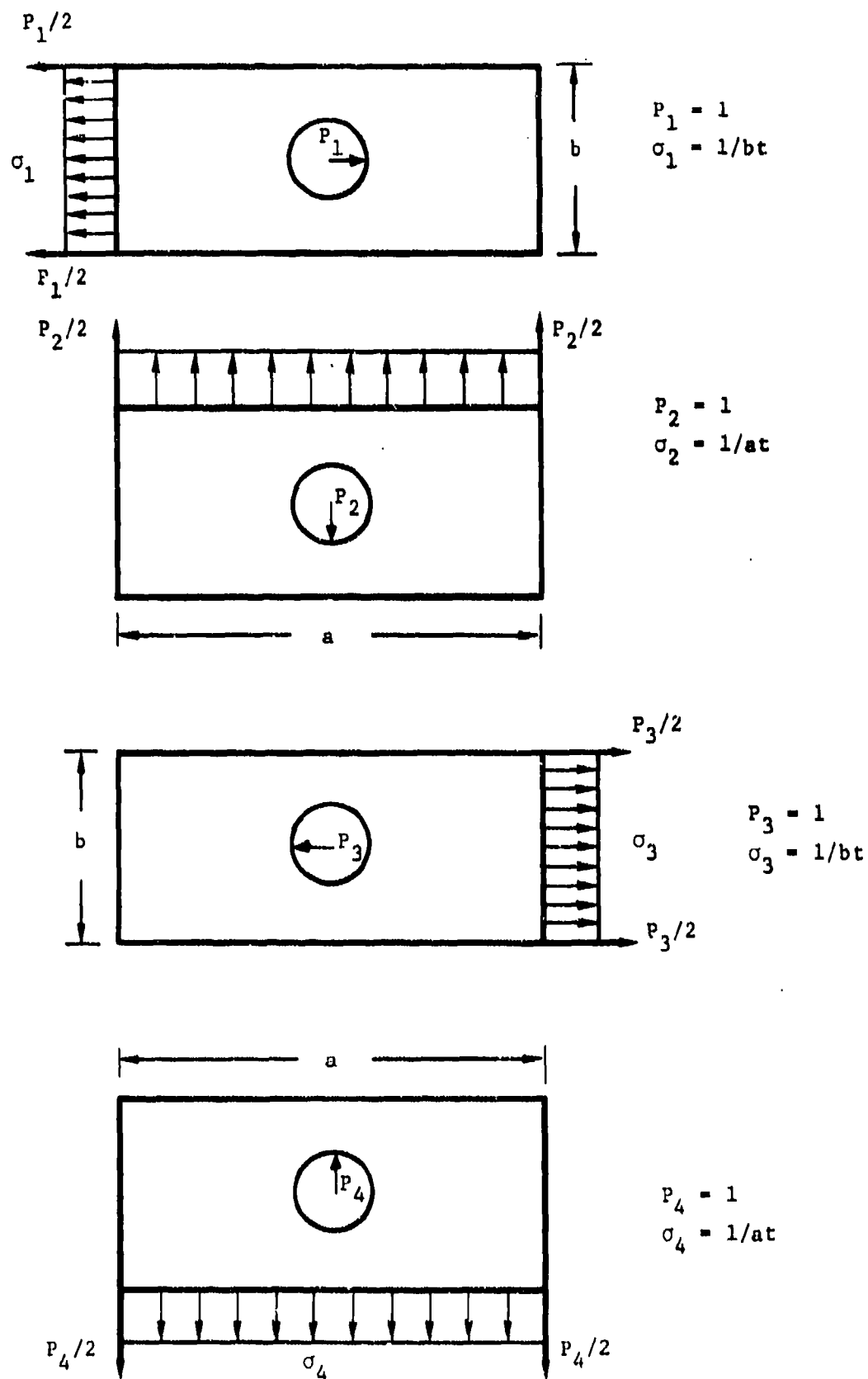
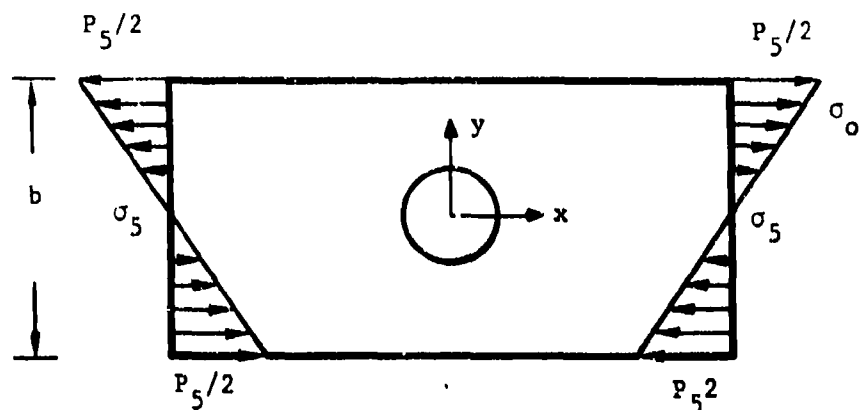


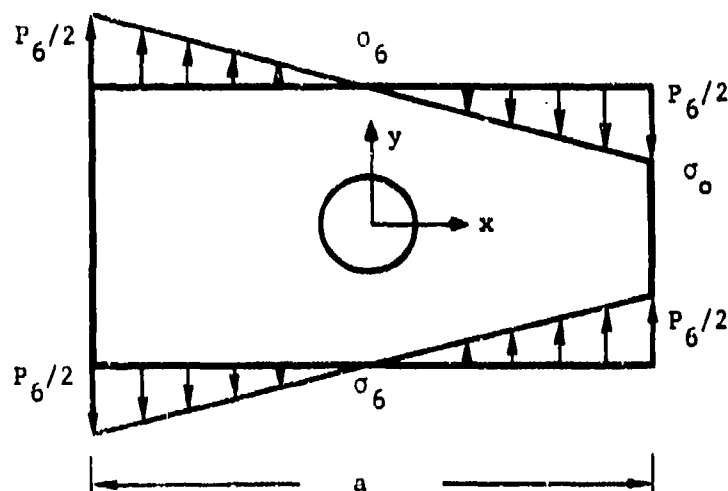
Figure 15. The Seven Natural Load Cases for the Loaded Hole Element.



$$P_5 = 1$$

$$\sigma_0 = (1/bt)^3$$

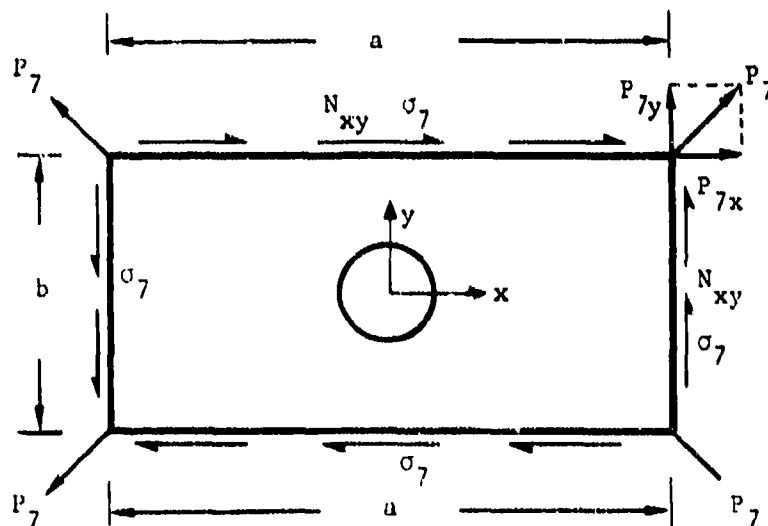
$$\sigma_5 = \frac{2\sigma_0}{b}$$



$$P_6 = 1$$

$$\sigma_0 = (1/at)^3$$

$$\sigma_6 = \frac{2\sigma_0}{a} x$$



$$P_{7x} = aN_{xy}$$

$$P_{7y} = bN_{xy}$$

$$P_7 = 1$$

$$\sigma_7 = \frac{2}{t(a^2 + b^2)}$$

Figure 15. The Seven Natural Load Cases for the Loaded Hole Element.
(Concluded).

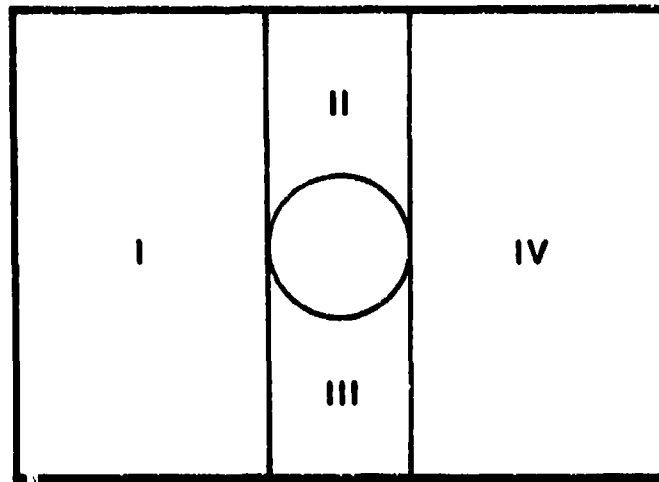
where W_i and W_j are weighting functions at (x, y) locations.

The integration (summation) in Equation 19 is performed by dividing the element into four regions. The stresses for each load case are computed in each region, at locations that correspond to fifth order Gaussian quadrature points, scaled to the geometry of the element. The computed stresses are summed and weighted in accordance with Equation 19 to yield the natural flexibility coefficients. A typical arrangement of Gaussian quadrature points in an element is shown in Figure 16.

In the loaded hole element, the first four load cases, in which the externally applied load is reacted at the boundary, cause a significant non-uniform distortion of the element edges. An exaggerated displacement profile for one of these load cases is shown in Figure 17. These straining modes are not adequately represented by storing only the nodal displacements in the $[A_N]$ matrix. To correct this problem, the average edge normal displacements are assigned to the nodes (see Figure 17).

2.2.3 Stiffness Matrices For a Plate With an Unloaded (Open) Hole and For Plain (Unnotched) Elements

The generation of global stiffness matrices for the open hole and plain elements follows the procedure outlined in Section 2.2.2. These elements contain only four nodes (8 DOF) each (see Figure 18). Therefore, only five natural load cases are required to generate their natural flexibility matrices (Figure 19). The transformation of the 5×5 natural flexibility matrices to the 8×8



GAUSSIAN POINTS

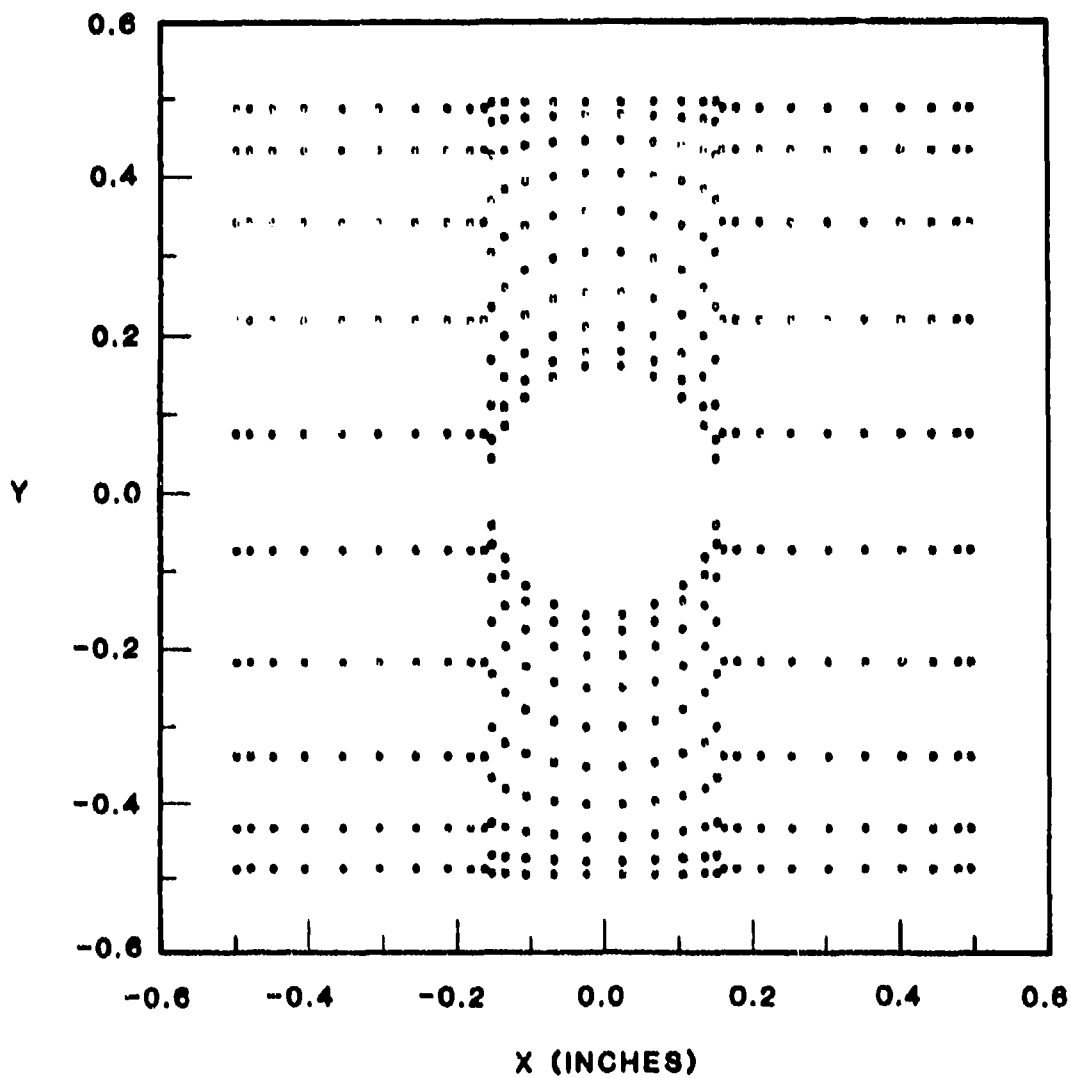
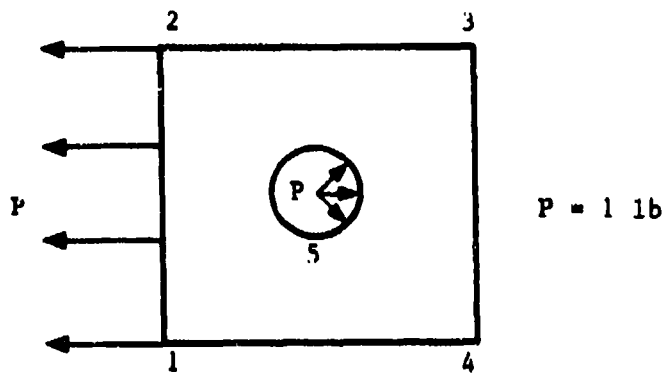
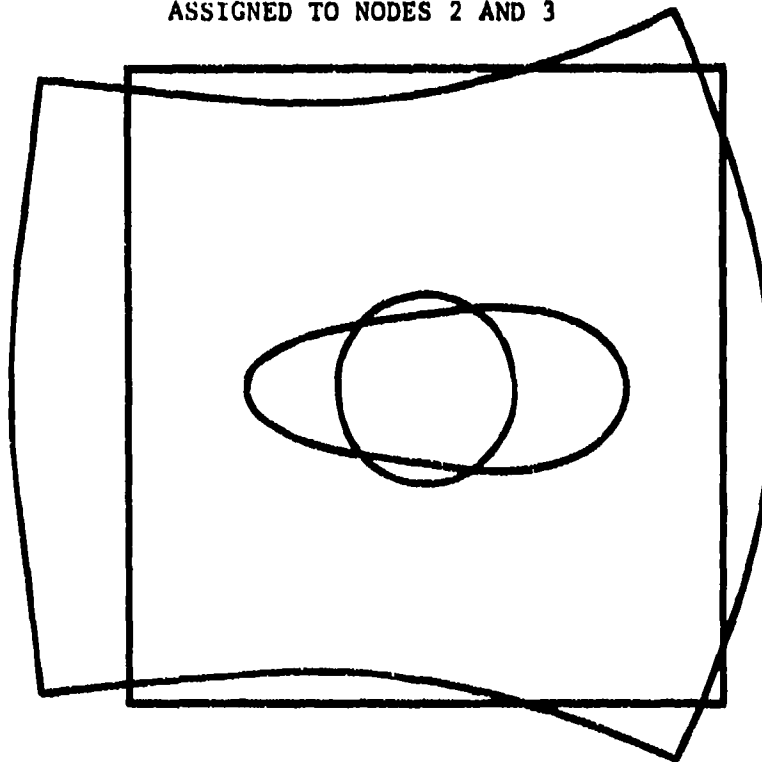


Figure 16. Typical Distribution of Gaussian Quadrature Points in Loaded and Unloaded Hole Elements



THE AVERAGE "V" DISPLACEMENT IS
ASSIGNED TO NODES 2 AND 3



DEFORMED SHAPE AT
A MAGNIFICATION OF
 10^6 ($P=1000 \text{ kips}$)

THE AVERAGE "U"
DISPLACEMENT IS
ASSIGNED TO NODES
3 AND 4

Figure 17. Exaggerated Deformation Profile For a Natural Load Case.

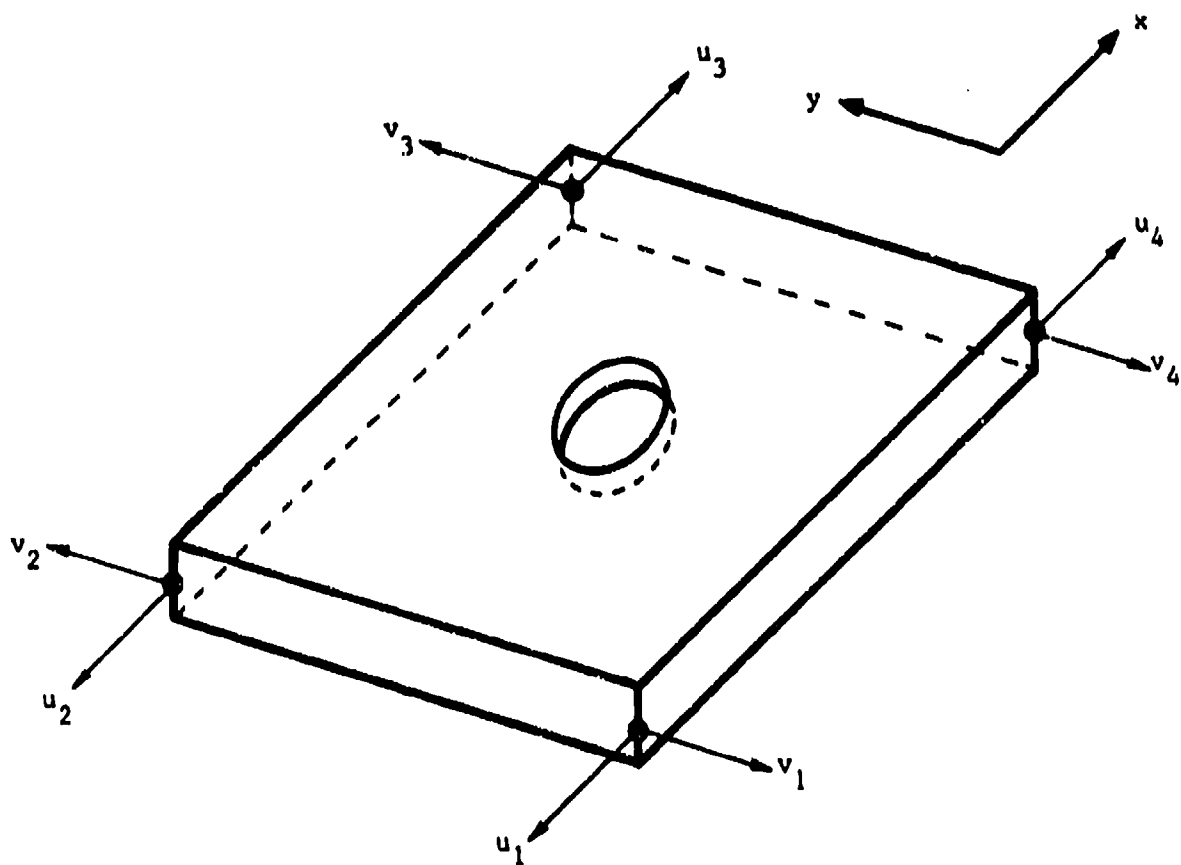


Figure 18. The Four-Node Open Hole Element With Depicted Nodal Degrees of Freedom

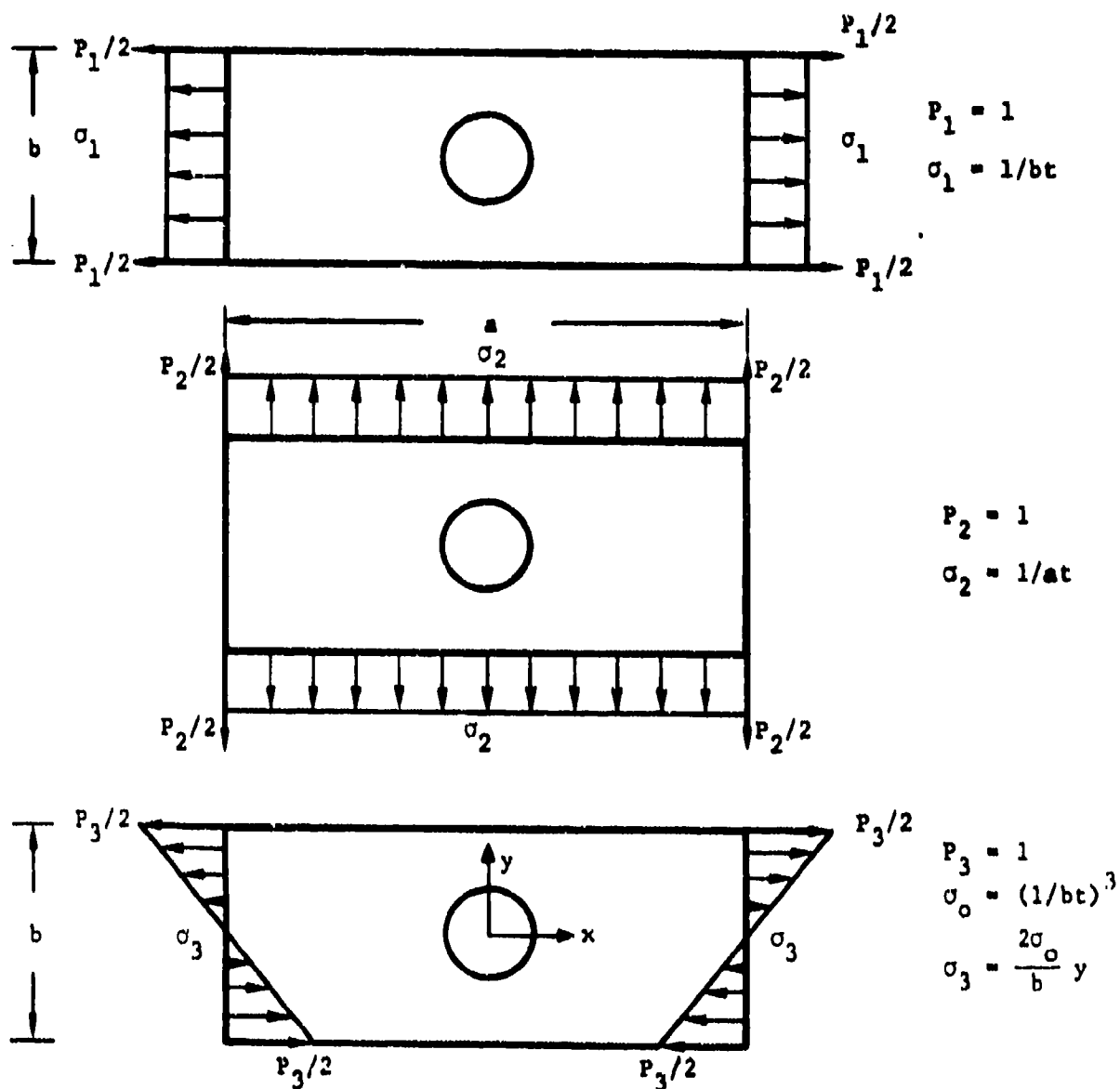
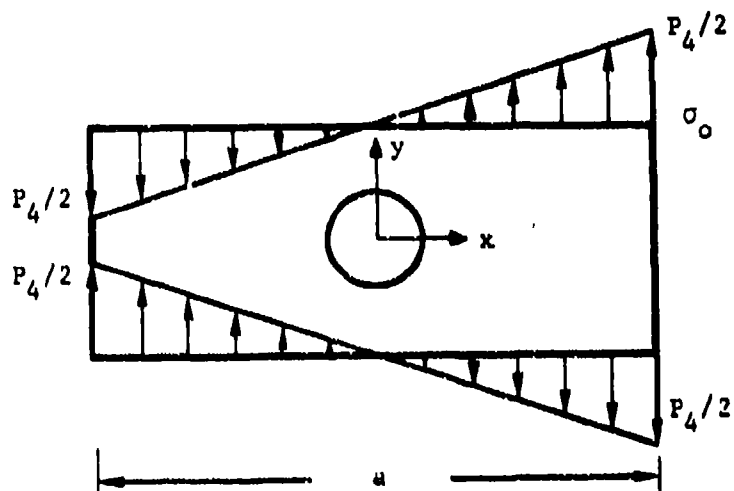


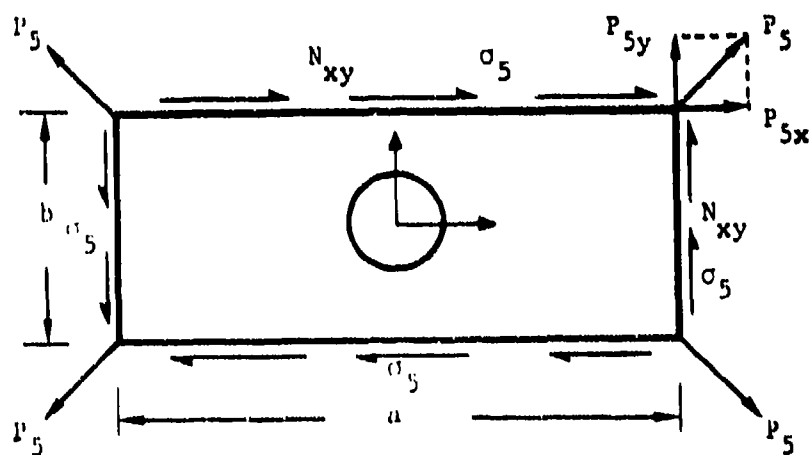
Figure 19. The Five Natural Load Cases for the Overload Hole and Plain Elements.



$$P_4 = 1$$

$$\sigma_o = (1/at)^3$$

$$\sigma_4 = \frac{2\sigma_o}{a} x$$



$$P_{5x} = a N_{xy}$$

$$P_{5y} = b N_{xy}$$

$$P_5 = 1$$

$$\sigma_5 = \frac{2}{t(a^2 + b^2)}$$

Figure 19. The Five Natural Load Cases for the Unloaded hole and Plain Elements. (Concluded)

global stiffness matrices for the two elements follows Equations 9 to 18. Since FIGEOM was developed to analyze doubly-connected planform regions, the plain element stiffnesses are obtained using the open hole element algorithm, setting the hole radius to a minimum value. This also provides the added benefit of using the same set of subroutines to generate the stiffness matrices for all the plate elements (loaded hole, unloaded hole and plain elements).

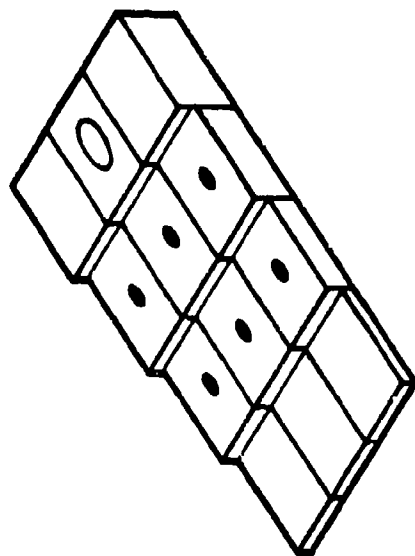
2.3 Load Distribution Among Fasteners

Figure 20 shows a typical bolted joint and its finite element representation. The stiffnesses of each element are initially computed and stored (see Section 2.2). The global joint stiffness matrix is then formed by assembling the individual stiffness matrices for the loaded hole, unloaded hole, plain and effective fastener elements. As described in Section 3.1, the SAMCJ user only defines the type, geometry and properties of the individual elements. SAMCJ internally processes this information to generate the global joint stiffness matrix.

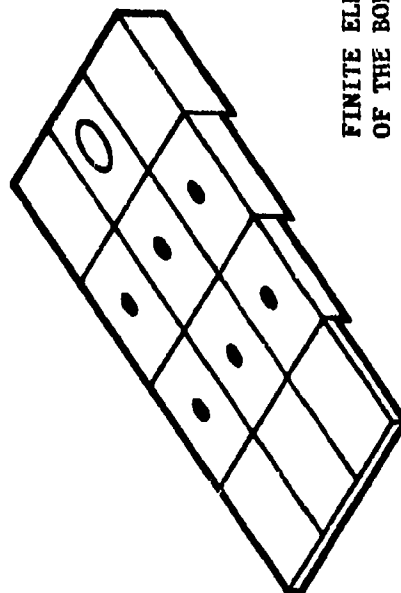
Figure 3 shows the load introduction and boundary constraint locations assumed by SAMCJ. Currently, SAMCJ assumes that a uniaxial 1-kip load is applied along the x (longitudinal) direction on the left edge of the top plate (see Figure 3). Therefore, the u displacement is constrained along the right edge of the bottom plate. A corner node along this edge is also constrained in the y direction to prevent a rigid body translation in that direction (see Figure 3). The user specifies the applied load to be tensile or compressive.

The assembled, global joint stiffness matrix is related to the nodal displacements and loads as follows:

$$\{P\} = [K_g] \{p\} \quad (20)$$



SAMPLE TAPERED JOINT



FINITE ELEMENT MODEL
OF THE BOLTED PLATES

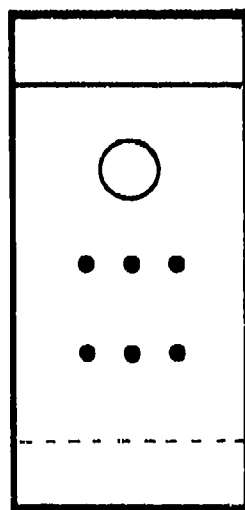


Figure 20. Finite Element Model of a Sample Tapered Bolted Joint

Each bolted plate contains M nodes, which include the fastener nodes. Each node has two degrees of freedom (u and v displacements). Therefore, the global joint stiffness matrix is 4M x 4M in size. The imposed boundary constraints reduce the size of the stiffness matrix that is eventually used to compute the nodal displacements and boundary constraint forces. Incorporation of the nodal displacements into element equilibrium equations yield the nodal forces in the individual elements. The loads at node 5 in each loaded hole element provide the x and y components of the fastener load in that element.

2.4 Stress State at Any Location in a Bolted Plate

The stress state at any internal point in an element is computed using a procedure similar to the computation of the natural flexibility matrix. During the generation of element natural flexibility matrices, the stress states at locations within the element are computed and stored for unit values of every natural load case. Desired stress recovery locations are pre-selected for this purpose. The relationship between the stress states at these pre-selected n points and the natural force system is:

$$\{\sigma\} = [S_N] \{P_N\} \quad (21)$$

where $\{\sigma\}$ contains σ_x , σ_y and σ_{xy} at the selected S locations, and $[S_N]$ contains the stresses per unit natural load at the same locations. As discussed in Section 2.2.2, the natural load vector is related to the natural nodal displacement vector as follows:

$$\{P_N\} = [K_N] \{\rho_N\} \quad (22)$$

And, the natural displacements are related to the global (nodal) displacement as follows:

$$\{\rho_N\} = [a_e]^T \{\rho\} \quad (23)$$

where (24)

$$\{\rho\} = \{u_1 \ v_1 \ u_2 \ v_2 \ \dots \ u_{10} \ v_{10}\}$$

Substituting Equations 21 and 22 into Equation 20, one obtains:

$$\{\sigma\} = \left[[S_N] [K_N] [a_e]^T \right] \{\rho\} = [S] \{\rho\} \quad (25)$$

where $[S]$ is a $3N \times 10$ matrix for a loaded hole element (10 DOF), and a $3N \times 8$ matrix for an open hole element (8 DOF).

Terms in the $[S]$ matrix are computed at the same time the element flexibility and stiffness matrices are calculated. Hence, after the global joint equations are solved for the nodal displace-

ments, the stresses in any element are recovered at these preselected points using Equation 24.

2.5 Strength and Failure Mode Prediction for a Bolted Plate

SAMCJ predicts the strength of a bolted plate using average stress failure criteria at the laminate level (see Figure 21). In Reference 1, the same criteria were applied at the lamina level to predict progressive ply failures in a singly-fastened laminate (the SASCJ computer code). The characteristic distances over which the stresses are averaged in SAMCJ are different from those used in SASCJ. Also, failure is assumed to be a one-step (catastrophic) process. The strength of a bolted plate corresponds to the initial failure at a fastener or cut-out location, in the bearing, shear-out or net section failure mode.

Appropriate failure sites are identified by SAMCJ in every element. These sites vary with the applied loading (see Figure 22). The characteristic distances for the net section, shear-out and bearing modes of failure are divided into many regions. Following the procedure outlined in Section 2.4, the appropriate stress components corresponding to a 1-kip joint load are computed at these points, and their average values over the respective characteristic distances are stored. The ratios of these average stresses to the corresponding unnotched strengths are subsequently computed and relatively evaluated to predict the strength of the bolted plate, the failure site and the failure mode. Under tensile loading, the average σ_x value over a^{ns} is divided by the unnotched tensile strength to predict net section tensile failure. Under compressive loading, the average σ_x value over a^{ns} is divided by the unnotched compressive strength to predict net section compressive failure. The average σ_x value over a^{brg} is divided by the unnotched compressive strength to predict bearing failure. The average τ_{xy} value over a^{so} is divided by the unnotched shear strength to predict shear-out failure.

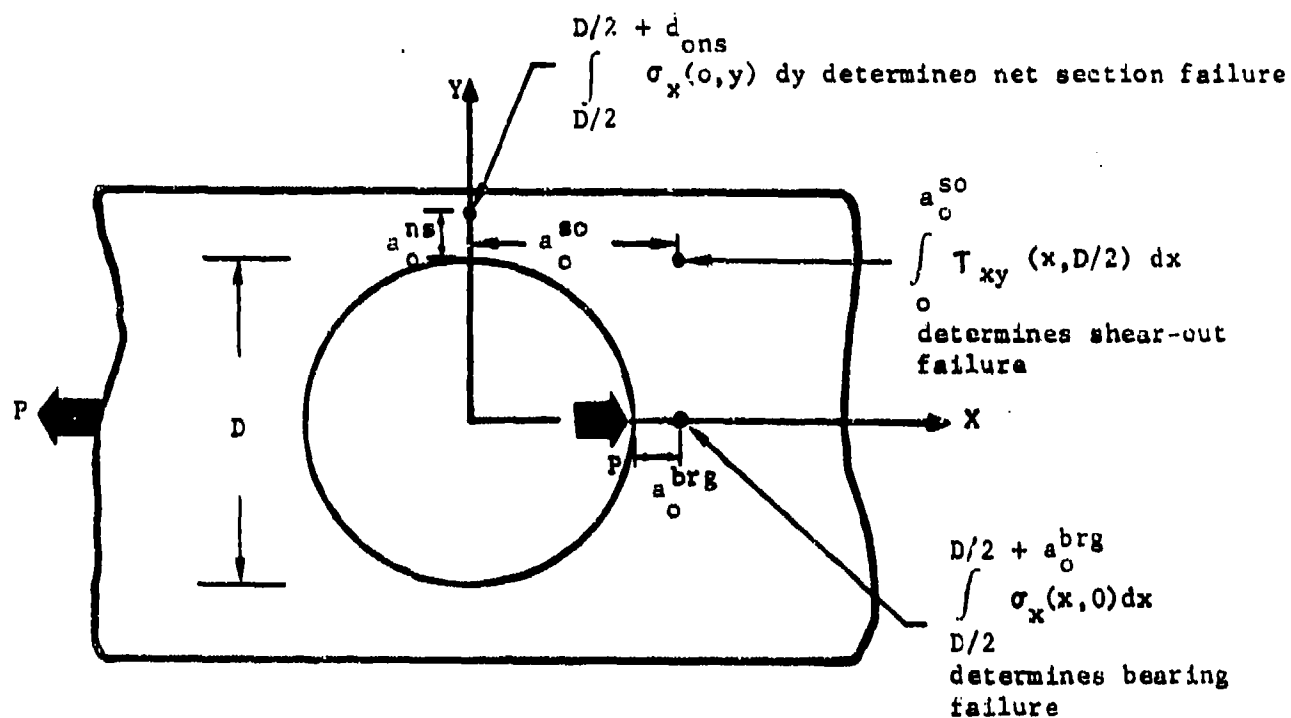


Figure 21. The Characteristic Distances Used in the Average Stress Failure Criteria.

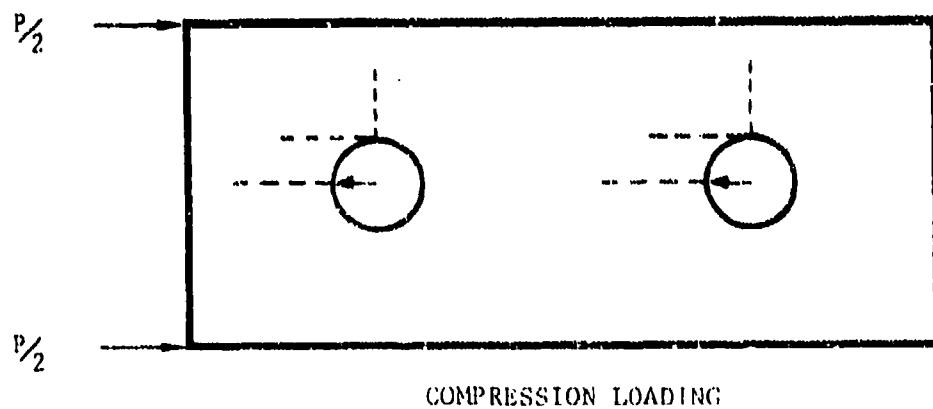
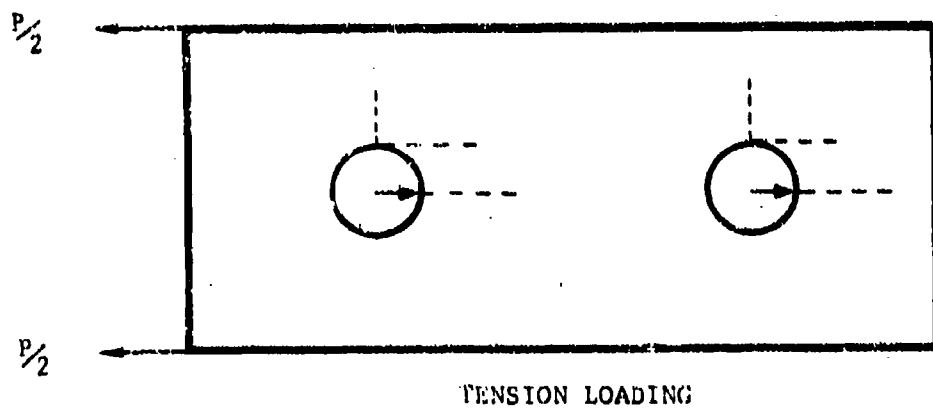


Figure 22. Locations Where Average Stresses are Obtained Under Tension and Compression Loading to Predict Net Section, Bearing, and Shearout Modes of Failure

The unnotched laminate strengths, under tension and under compression, are computed by SAMCJ based on input fiber-directional failure strain values (tensile and compressive). Laminate strengths under N_x and N_{xy} loadings (inplane normal and shear stress resultants, respectively) are assumed to correspond to first fiber failure in a ply. This simplistic strength prediction procedure introduces inaccuracies that have been acknowledged and discussed in the literature. Nevertheless, SAMCJ adopts this procedure for lack of a validated alternative.

SAMCJ assumes that a net section, shear-out or bearing failure of any element results in joint failure. This assumption results in a one-step strength, failure site and failure mode prediction for a multiply-fastened plate. A 1-kip tensile or compressive load is applied, and fastener loads and normalized averaged stresses corresponding to net section, shear-out and bearing failure modes are computed. The failure value of the applied load corresponds to a unit value of the maximum normalized average stress. An identification of the maximum normalized average stress, and its location, provides the joint failure mode and the critical fastener or cut-out location.

2.6 Current SAMCJ Limitations

SAMCJ is a versatile code that predicts the strength of bolted laminates and the corresponding failure mode. However, there are segments of the analysis that can be improved through additional efforts that are beyond the scope of this program. These limitations are discussed below.

The representation of a loaded hole by a five-node element (with ten DOF) is discussed in Section 2.2.2. Let a and b be the planform dimensions of the element in the x and y directions, respectively, and D , the hole diameter. When a/D and b/D are small (less than 2), and the element aspect ratio (a/b) is less than

unity, the highly distorted element shape cannot be appropriately accounted for even with averaged displacements assigned to the nodes (see Figure 17).

Fastener load distributions were predicted for two test cases using three forms of the $[A_0]$ matrix. In one form, the actual nodal displacements were used as the A terms. In the second form, the midside displacement value for the highly deformed edge was assumed to be the nodal values on that side in the $[A_0]$ matrix. In the third form, the average displacement of the deformed edge was used as the nodal values in the $[A_0]$ matrix. The considered test cases are from Reference 2. One contains two fasteners in the load direction, and the other contains five fasteners in the load direction. Figures 23 and 24 present the fastener load distributions predicted by the three forms of the $[A_0]$ matrix, along with experimentally measured fastener loads for the two test cases (Reference 2). The best correlation between analytical predictions and test measurements is obtained when the nodal displacements are assumed to be the average value along the deformed edge. SAMCJ, therefore, generates the $[A_0]$ matrix for the loaded hole element following this procedure.

In dividing a bolted plate into many elements (loaded or unloaded hole elements, as well as plain elements), it is advisable to maintain element geometries that do not render the generated stiffness matrices inaccurate. Figure 25 presents results from a study conducted on a singly fastened metallic plate. P is the recovered load that is obtained by integrating the stress along a line transverse to the load direction as shown in Figure 25. P is the applied load, or the sum of the nodal loads (especially in the interior elements in a general multifastened plate). The recovered load (P) approaches the applied load value (P) when the plate aspect ratio (a/b) increases beyond unity. Also, a/D and b/D must have a minimum value of approximately 3. In predicting failure in the net section, bearing and shear-out modes, the computed average stress values are multiplied by P/P_r , to remove

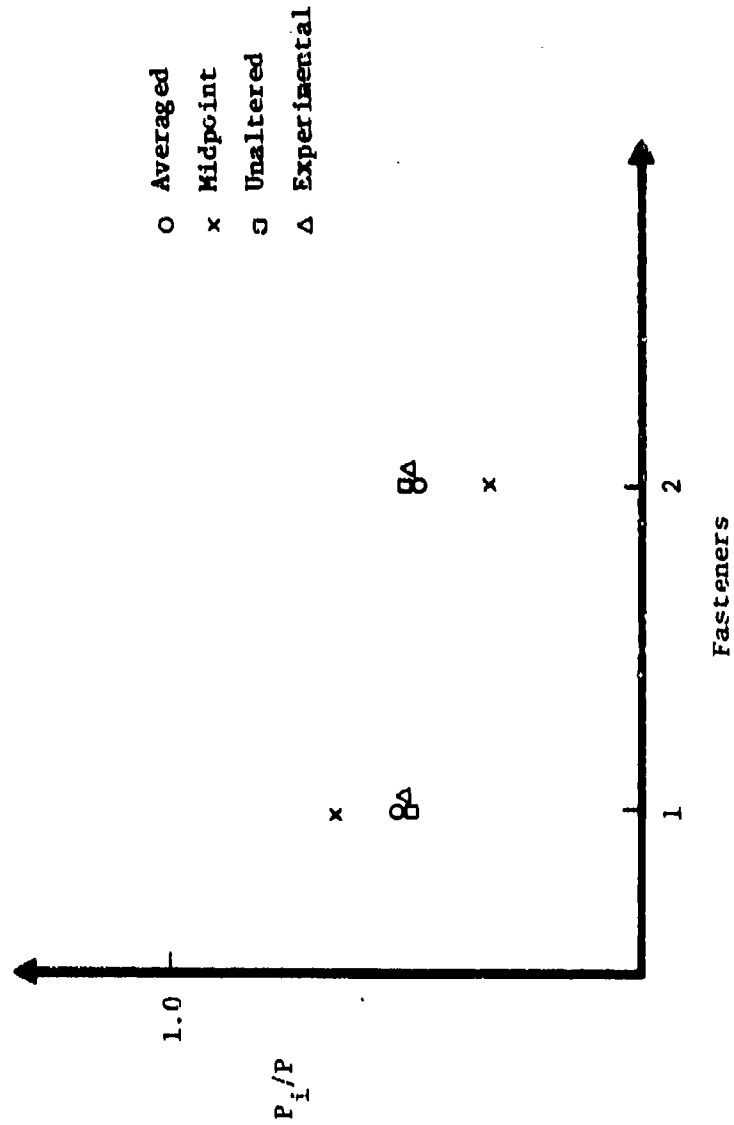
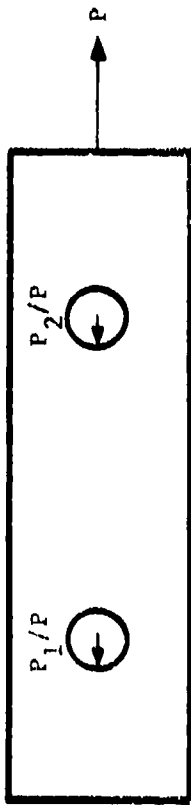
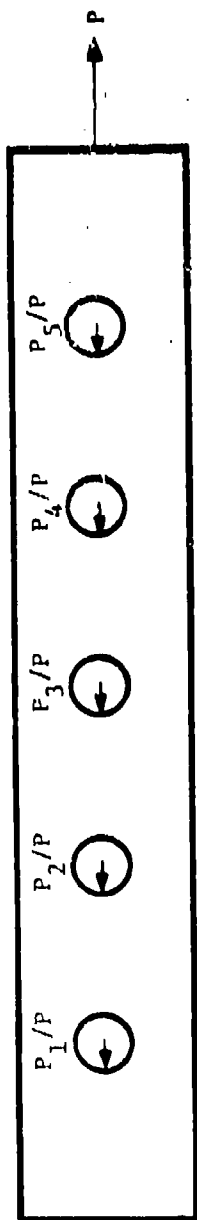


Figure 23. Comparison of Experimental Data with the Analytical Predictions Using Three Forms of (A_n) Matrices (Two Rows of Fasteners).



O Averaged
 x Midpoint
 □ Unaltered
 Δ Experimental

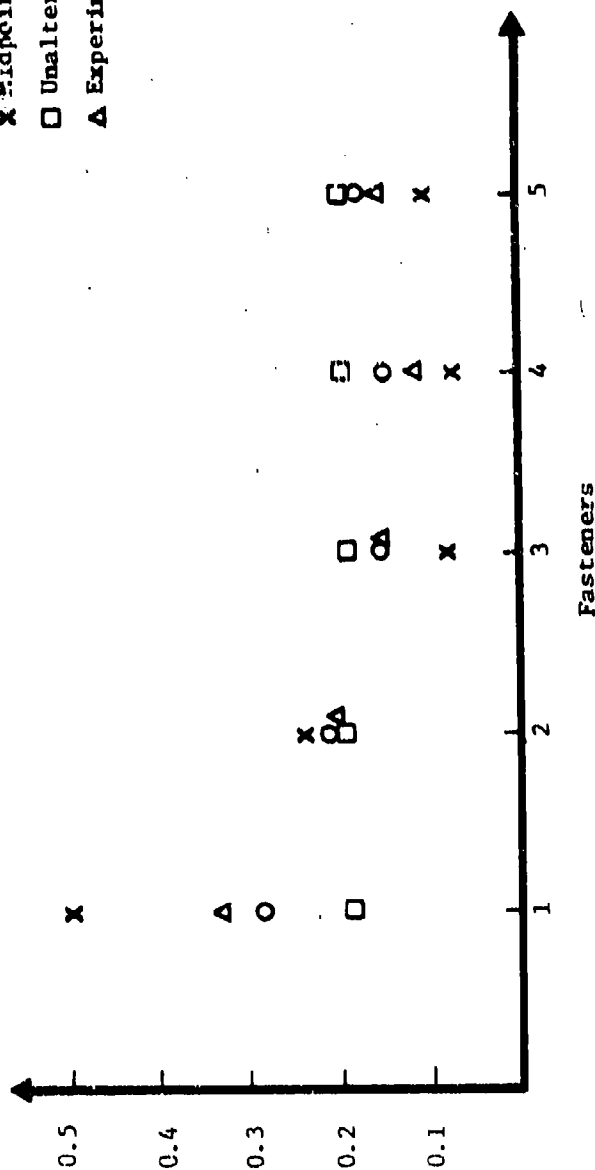
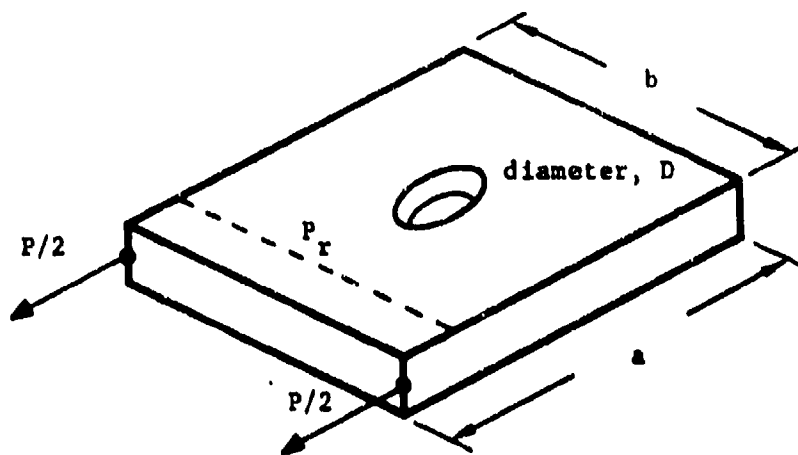


Figure 24. Comparison of Experimental Data with the Analytical Predictions Using Three Forms of (A_n) Matrices (Fives Rows of Fasteners).



$D = 0.3125 \text{ inch}$

a/D	b/D	P_r/P
1.6	1.6	5.38
3.2	1.6	2.27
6.4	1.6	1.57
16.0	1.6	1.29
1.6	3.2	1.24
3.2	3.2	1.76
6.4	3.2	1.37
16.0	3.2	1.16
1.6	6.4	-0.0995
3.2	6.4	0.989
6.4	6.4	1.23
16.0	6.4	1.16
3.2	16.0	-0.46
6.4	16.0	0.029
16.0	16.0	1.23

Figure 25. Element Load Recovery for Various a/D and b/D Ratios.

geometry (modeling) effects from the computed stresses.

The generation of a higher order loaded hole element may eliminate the approximation introduced by the five node element, and result in a P_r/P value that is approximately unity for any element geometry. A nine node element, including midside nodes, is recommended for future investigation. Other factors that will improve SAMCJ predictions are more accurate computations of the unnotched strengths, and a modified fastener analysis that can account for countersunk fastener geometry.

2.7 Design Application

The design of a bolted joint in composite structures involves the selection of the fastener type, size and arrangement (spacing between adjacent fasteners), and geometry changes in the bolted plates (layup change and change in the planform dimensions). SAMCJ can quickly interrogate the effects of all these parameters on the joint strength, to provide a near optimum value for each. In doing so, SAMCJ is independent of test measurements like "joint stiffnesses," and is, therefore, a rapidly usable analytical design tool. If the bolted laminate is to be fabricated using a new material, only the basic lamina properties and the characteristic distances for the average stress failure criteria have to be determined, prior to performing the analysis. When a characterized material is used in the bolted structural part, SAMCJ predicts its strength without requiring complementary test results. The fastener size and spacing, and the bolted plate geometry and properties, are varied systematically to analytically predict their effect on the joint strength and efficiency (weight, durability, etc.). These parametric studies provide guidance in the selection of the most efficient bolted joint configuration for the assumed loading.

2.8 Test Requirements

As mentioned in Section 2.7, SAMCJ predicts the strengths

of bolted laminates without requiring complementary test results when the laminate is fabricated using a characterized material. A material is said to be characterized when the basic lamina properties (stiffnesses, strengths, failure strains and other physiochemomechanical properties) and relevant structural properties (characteristic distances for the prediction of net section, bearing and shear-out modes of failure in notched laminates, etc.) are available. If a new material is used in a bolted laminate, its basic lamina properties and failure parameters have to be obtained prior to using SAMCJ for strength predictions.

SECTION 3

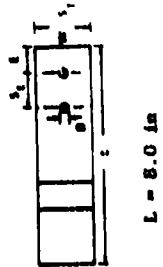
ANALYTICAL PREDICTIONS

In the experimental part of Task 2 in this Northrop/AFWAL program, over 160 composite-to-aluminum multifastener joints were tested under static loading (see Table 1 and Figure 26). Reference 2 contains results from these tests, including fastener load distribution measurements using strain-gaged bolts, failure loads, failure locations and failure modes. Sample test cases from Reference 2 are analyzed below using the SAMCJ computer code. Analytical predictions are compared with test results to establish the validity of the developed analysis.

Bolted laminates were fabricated using AS1/3501-6 graphite/epoxy unidirectional prepreg material containing approximately 35% resin by weight. These included 20- and 40-ply laminates with 50/40/10, 70/20/10, 30/60/10 and 25/60/15 (percentages of 0, +45 and 90 plies, respectively) layups. The 20-ply 50/40/10, 70/20/10 and 30/60/10 layups had [45/0/-45/0]2/0/90], [45/0/-45/03/90/03]s and [45/0/-45/0/45/90/-45/0/+45]s stacking sequences, respectively. The 40-ply 50/40/10 and 70/20/10 layups had [45/0/-45/0]2/0/90]2s and [45/0/-45/03/90/03]2s stacking sequences, respectively. The 40-ply 25/60/15 laminate had a [45/0/-45/0/45/90/-45/0/+45]2s stacking sequence, with the twelfth 0 ply replaced by a 90 ply.

The tested fastener arrangements included: two fasteners in tandem, two at an angle to the load direction, three fasteners in tandem, three fasteners in each of two columns with an adjacent cut-out, and four fasteners in each of two columns with a cut-out either between or adjacent to the rows. Rows and columns of fasteners are along and perpendicular to the load direction, respectively. The fastener spacing in the load and transverse directions (S_L and S_T , respectively), specimen width and edge distance (W and E ,

TABLE 1. TASK 11 TESTS ON MULTIFASTER JOINTS.

TEST CASE	SPECIMEN	# OF 0° ±45° AND 90° FIBERS	S _L D	S _T D	W D	E D	FASTER	LOADING	COMPOSITE/ METAL GEOMETRY	COMMENTS*	SCHEMATIC
201	1A29, 1A44, 1A59, 1A36, 1A51, 1A37, 1A52, 1A17	50/40/10 ↓	4	6	6	3	518464-5 ↓ 515335 ↓ 518464-5	ST ↓ SC ↓ ST ↓ SC ↓ ST	1 ↓ 2 ↓ 2 ↓ 1 ↓ 3 ↓ 4 ↓ 4	CSK CSK DL DL, ETW ETW ETW T=0 T=200	
202	2.6, 2.8, 2.10	70/20/10									
203	3.6, 3.8, 3.10	30/60/10									
204	1A30, 1A45, 1A60	50/40/10									
205	1A31, 1A46, 1A61										
206	1A32, 1A47, 1A15										
207	1A33, 1A48, 1A63										
208	1A34, 1A49, 1A64										
209	1A35, 1A50, 1A65										
210	1A66, 1A40, 1A55,										
211	1A67, 1A81, 1A56, 1A20										
212	1A38, 1A53, 1A68										
213	1A39, 1A54, 1A69										
214	2.7, 2.9, 2.11	30/20/10	3								
215	3.7, 3.9, 3.11	30/60/10	2	6	6	3	518464-5	ST	5		
216	1B19, 1B21, 1B23	50/40/10	2	2	8	3	518464-5	ST	5		
217	1B25, 1B27, 1B29								6		
218	1B30, 1B39, 1B41								↓		
219	1B28, 1B35, 1B38								SC		
220	1D4, 1D5, 1D6		3	3	9				ST		
221	1D1, 1D2, 1D3		4	4	10	3			↓		

*For all test cases Diameter = 7/16 inch (PH); Torque = 100 in-lb; Test Environment is STD; and Joint Type is Single-Lap (SL) unless otherwise noted.

ST = Static Tension

PH = Protruding Head

SL = Single-Lap

STD = Room Temperature Dry

SC = Static Compression

CSK = 100° Countersink

DL = Double-Lap

ETW = Elevated Temperature Wet

Tension Head

TABLE 1. TASK 11 TESTS ON MULTIFASTER JOINTS. (CONTINUED)

TEST CASE	SPECIMEN	2 OF 6° -45° AND 90° FIBERS	$S \frac{L}{D}$	$S \frac{T}{D}$	$M \frac{D}{D}$	$E \frac{D}{D}$	FASTER	LOADING	COMPOSITE/ METAL GEOMETRY	COMMENTS*	SCHEMATIC
222	1B32, 1B34, 1B40	50/40/10	2	2	8	3	51B335	ST	5	CSK	
223	2.12, 2.13, 2.14	70/20/10	1	1	1	1	51B464-5	1	6	DL	
224	3.12, 3.13, 3.14	30/60/10	1	1	1	1	51B464-5	1	1	DL	
225	1B1, 1B3, 1B5	50/40/10	4	4	10	3	51B464-5	ST	9	DL	
226	1B2, 1B4, 1B6	1	1	1	1	1	51B335	1	10	DL, ETU	
227	1B7, 1B9, 1B11	70/20/10	1	1	1	1	51B464-5	1	9	CSK	
228	1B8, 1B13, 1B12	30/60/10	1	1	1	1	51B335	1	11	DL	
229	2.1, 2.2, 2.3	50/40/10	3	3	9	3	51B335	ST	9	CSK	
230	3.1, 3.2, 3.3	50/40/10	4	4	10	3	51B335	SC	9	CSK	
231	1C2, 1C4, 1C6	50/40/10	3	3	9	3	51B335	ST	12	DL	
232	1B13, 1B15, 1B17	50/40/10	4	4	10	3	51B335	SC	13	DL	
233	1C8, 1C10, 1C11	50/40/10	4	4	10	3	51B464-5	ST	12	DL	
234	1C13, 1C15, 1C17	1	1	1	1	1	51B335	1	13	DL, ETU	
235	1C19, 1C21, 1C23	70/20/10	1	1	1	1	51B464-5	1	12	CSK	
236	1C20, 1C22, 1C24	30/60/10	1	1	1	1	51B335	SC	13	DL	
237	1C25, 1C27, 1C29	70/20/10	1	1	1	1	51B464-5	ST	1	DL	
238	2.4, 2.5, 2.15	50/40/10	2	3	9	3	51B464-5	ST	14	DL	
239	3.4, 3.5, 3.15	50/40/10	2	3	9	3	51B464-5	SC	14	DL	
240	1C26, 1C28, 1C30	50/40/10	2	3	9	3	51B464-5	ST	14	DL	
241	1C31, 1C33, 1C35	50/40/10	2	3	9	3	51B464-5	SC	14	DL	

*For all test cases Diameter 5/16 inch (PU); Torque = 100 in-lb; Test Environment is RTD; and Joint Type is Single-Lap (SL) unless otherwise noted.

SL = Static Tension

PH = Protruding Head

SL = Single-Lap

RTD = Room Temperature Dry

SU = Static Compression

CSK = 100° Countersink
Tension Head

DL = Double-Lap

ETU = Elevated Temperature Wet

TABLE I. TASK II TESTS ON MULTIFASTER JOINTS. (CONCLUDED).

TEST CASE	SPECIMEN	OF 0° 45° 90° FIBERS	$\frac{S}{L}$	$\frac{S}{T}$	$\frac{W}{D}$	E	FASTENER	LOADING	COMPOSITE/ METAL GEOMETRY	COMMENTS*	SCHEMATIC
242	10A4, 10B10, 10B12	50/40/10	4	4	14.4	3.2	51B464-5	ST	15	DL HD = 1.0	<p>L = 11.0 in.</p>
243	10B11, 10B15, 10B17						51B335		16	CSK	
244	10B13, 10B14, 10B16						51B464-5	SC	17	DL, L = 9.5	
245	10B1, 10B2, 10B3	70/20/10						ST	16	HD = 1.0	
246	12.1, 12.2, 12.3						51B464-5	ST	16		
247	14.1, 14.2, 14.3	25/60/15	4	4	14.4	3.2			16		
248	10A1, 10A3, 10B4	50/40/10	4	4	16	3.2	51B464-5	ST	18	HD = 1.0	<p>L = 11.0 in.</p>
249	10A5, 10A6, 10A7	50/40/10	-	4	16	3.2	51B335	ST	19	CSK HD = 1.0	<p>L = 13.0 in.</p>
250	10A9, 10B6, 10B3	50/40/10	4	-	4.8	3.2	51B464-5	ST	20	DL T = 250	<p>L = 13.0 in.</p>
251	10A10, 10A13, 10A16						51B335		21	CSK	
252	10A11, 10A14, 10A17								21	CSK	
253	10A12, 10A15, 10A18	50/40/10	4	4	4.8	3.2		ST	21	CSK	

* For all test cases Diameter = 5/16 inch (PH); Torque = 100 in-lb; Test Environment is RTD, and Joint Type is Single-Lap (SL) unless otherwise noted.

ST = Static Tension PH = Protruding Head SL = Single-Lap RTD = Room Temperature Dry
 SC = Static Compression CSK = 100° Countersink DL = Double Lap ETV = Elevated Temperature Wet
 Tension Head

COMPOSITE METAL GEOMETRY*	t_1	t_2	L	a
1	.31	.73	7.5	2.25
2	.26	--	7.5	--
3	.31	.73	6.5	1.52
4	.31	.73	6.5	1.21
5	.31	.73	7.5	2.88
6	.26	--	8.0	--
7	.31	.73	8.0	3.06
8	.31	.73	8.0	2.75
9	.31	.73	8.0	2.75
10	.26	--	8.0	--
11	.31	.73	8.0	3.06
12	.31	.73	8.0	2.75
13	.26	--	8.0	--
14	.26	--	8.0	--
15	.38	--	6.0	--
16	.50	1.25	10.0	4.75
17	.38	--	8.0	--
18	.50	1.25	8.0	2.75
19	.50	1.25	12.0	4.00
20	.38	--	10.0	--
21	.50	1.25	10.5	1.5

All dimensions in inches
*See Table 2-1 for applicable test cases

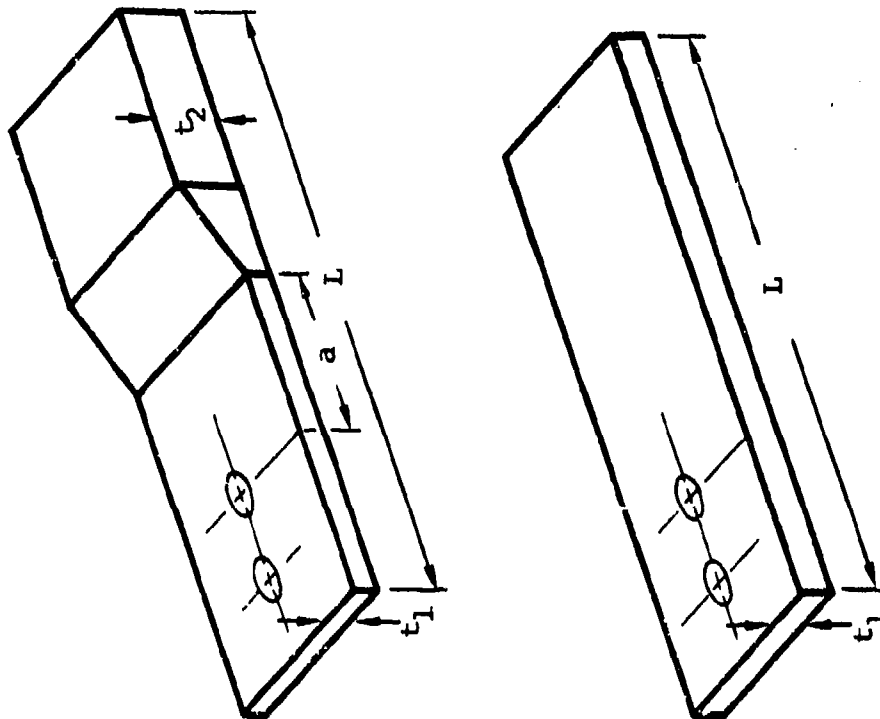


Figure 26. Dimensions of the Metal Plates for the Various Composite-To-Metal Multifastener Joints.

respectively), and cut out diameter (H) and location, for the various test cases, are listed in Table 1.

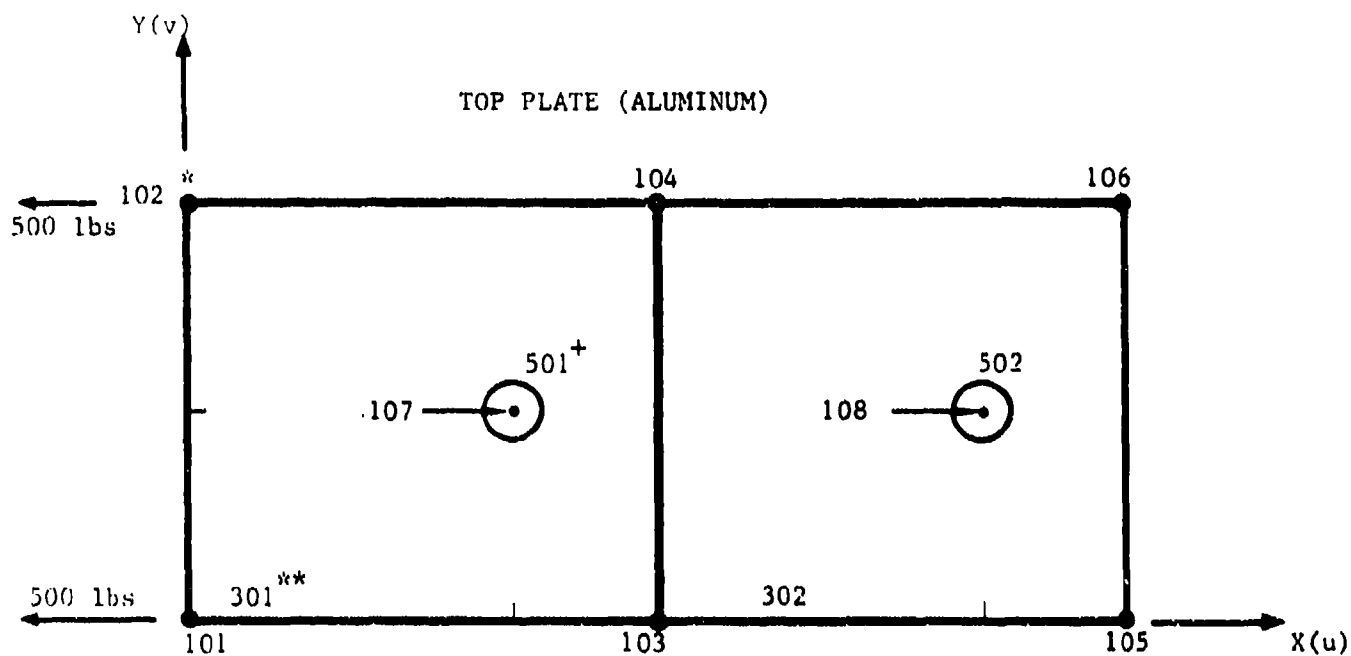
Aluminum plates were bolted to laminates to effect load transfer in single- and double-shear configurations. The metallic plates were machined from 7075-T7 raw stock, and contained fastener hole arrangements that were compatible with those in the laminated specimens. Figure 26 presents the dimensions of the metal plates used in the various tests.

Most of the tests used 5/16-inch diameter, protruding head steel fasteners. Selected tests in a single shear configuration used 5/16-inch diameter, 100 countersunk (tension head) steel fasteners. The fasteners were torqued to 100 in.-lb, prior to testing, unless otherwise specified.

3.1 Composite-to-Metal Joints with Two Fasteners in Tandem

Four test cases (201, 202, 203 and 206 in Table 1), addressing joints with two fasteners in tandem (along the loading direction), were analyzed using the SAMCJ computer code. Test case 201 was modeled as shown in Figure 27. The top plate was modeled to be the 0.31-inch-thick aluminum plate, and the bottom plate was modeled to be the 20-ply, 50/40/10 (percentages of 0 /+45 /90 plies) graphite/epoxy plate. A 1-kip load is applied to the left edge of the top plate, and the right edge of the bottom plate is constrained, as shown in Figure 27. u and v are the nodal displacements in the x and y directions, respectively. The mentioned loading of the top plate and the constraining of the bottom plate are automatically done by SAMCJ. If two or more rows of elements were present in the model, the applied 1-kip load will be distributed among three or more nodes in proportion to the element widths.

The SAMCJ input data, in English units, for test case 201 are listed in Figure 28. The first entry (1) identifies the loading



- * GRID-POINT IDENTIFICATION
- ** LOADED HOLE ELEMENT IDENTIFICATION
- + EFFECTIVE FASTENER ELEMENT IDENTIFICATION

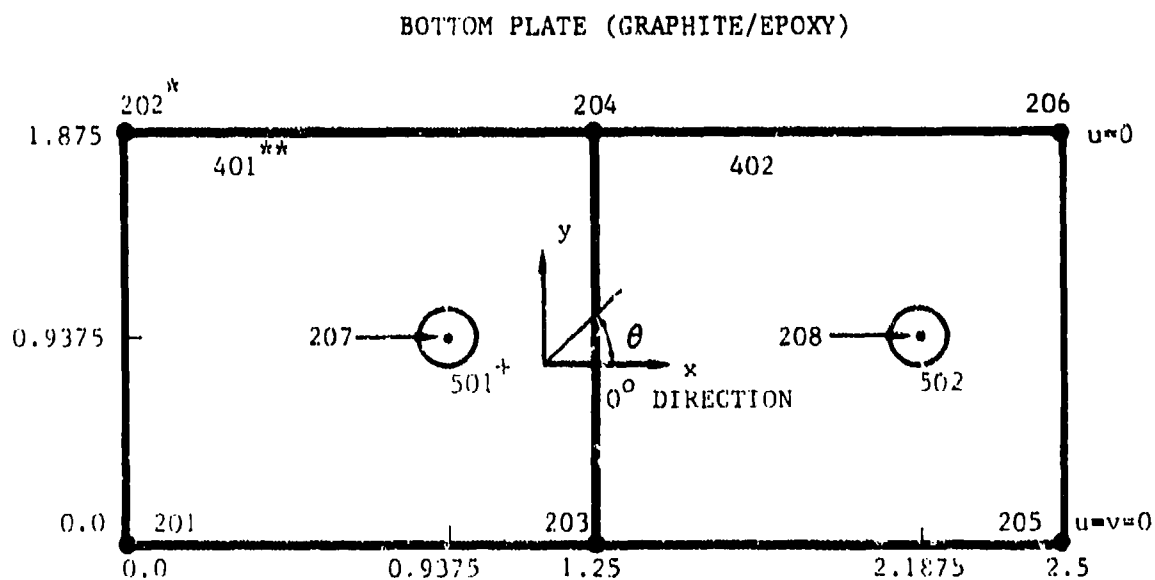


Figure 27. Finite Element Model for Test Case 201

Figure 28. SAMCJ Input for Test Case 201

configuration to be a single-shear configuration. For a double-shear load transfer, this entry would be 2. The second entry (1) identifies the load to be in static tension. For static compressive loading, this entry would be 2. The third entry requests the type of fastener used in the joint. The entry of a 1 specifies the fastener to have a protruding head and a 2 specifies the fastener to have a countersunk head. The next two entries say that the top plate is a metal (M), identified as "Aluminum." The two entries following these say that the bottom plate is a composite laminate (C), identified as "50/40/10 AS1/3501-6...". Subsequently, the Young's modulus (10.0D6) and Poisson's ratio (0.3) for aluminum, and the fiber-directional, transverse and shear moduli and Poisson's ratio (18.5D6, 1.9D6, 0.85D6 and 0.3, respectively) for the composite lamina are input. The next five entries specify that four (4) different fiber orientations are present in the laminate (0, 45, -45 and 90 degrees with respect to the loading direction). The following three entries say that the elements in the bottom plate contain 1 layup of 20 plies, of 0.565-inch thickness each. The stacking sequence for this layup is input next, where 1, 2, 3 and 4 refer to 0, 45, -45 and 90-degree fiber orientations, respectively. Subsequently, the fastener is identified as "Steel," and its Young's modulus, Poisson's ratio and diameter (30.0D6, 0.3, 0.3125) are input.

Eight grid-points each are specified in the top and bottom plates (101 to 108 and 201 to 208, respectively), along with their x and y coordinates (see Figure 27). Following this, two elements are specified in each plate, along with their nodal connectivity and element type information. Nodal connectivity is specified starting from the bottom left node, going clockwise around the element boundary, and ending at the fastener (internal) node. Element 301 in the top plate, for example, has 101, 102, 104 and 103 as its corner nodes, and 107 as its fastener node. The fifth node will be entered as 0 for plain and unloaded hole elements. The element type information follows the fifth node identification. It is 1, 2 and 3 for plain, loaded hole and unloaded hole elements,

respectively. Following this, additional element data are specified for the two plates. These include the element thicknesses or layup identification number for plain and loaded hole elements, and additional information (x and y coordinates of the hole center and the hole radius) for unloaded hole elements. For test case 201, elements 301 and 302 in the top plate (metal) are specified to be 0.31-inch thick. Elements 401 and 402 in the bottom plate (composite) are specified to contain the stacking sequence identified as one (1). The element definitions are succeeded by the definition of two effective fasteners (501 and 502). These are identified as fasteners that connect nodes 107 and 108 in the top plate to nodes 207 and 208 in the bottom plate, respectively.

The one (1) following this states that groups of identical elements will be specified in the two plates. If two (2) is entered here, all elements will be assumed to be different from one another, resulting in larger computational costs. The entry " 1 1 0 0" refers to the number of groups of effective fasteners, loaded hole, unloaded hole and plain elements, respectively, in the top plate. A zero (0) specifies the absence of an element type. The number of elements in each group, and the corresponding element numbers, are input subsequently. In Figure 27, two identical loaded hole elements (301 and 302) are identified in the top plate. Following this, the number of groups of loaded hole, unloaded hole and plain elements in the bottom plate (1, 0 and 0, respectively) is entered. In figure 27, 2 identical loaded hole elements (401 and 402) are identified in the bottom plate.

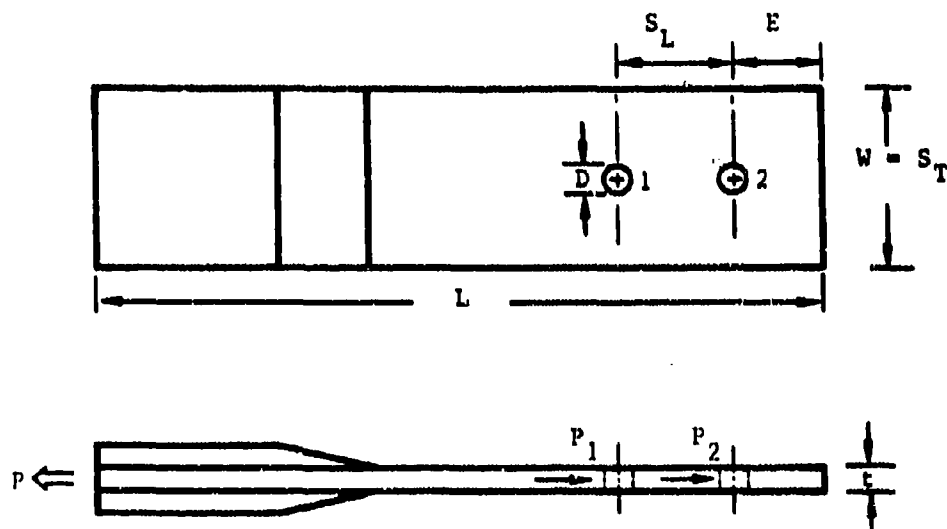
The last four lines of input introduce the failure parameters for the materials in the two plates. For metallic plates, the tensile, compressive and shear strengths (250.0D3 each in Figure 27), and the averaging distances for net section, bearing and shear-out modes of failure (0.5 each in Figure 28) are input. Since the joints were designed to fail the laminated plates, and SAMCJ was developed primarily for the prediction of the strength of

bolted laminates, the failure parameters for the metallic plates were input to be arbitrarily high. This information is followed by the failure parameters for the bottom (composite) plate. The first line specifies the fiber directional failure strains for the material under tension (0.012), compression (0.0175) and shear (0.012). These values are used by SAMCJ to compute the plain laminate tensile, compressive and shear strengths, based on laminated plate theory and the assumption of laminate failure corresponding to first fiber failure in any of its plies. The last line in Figure 28 specifies the distances over which the longitudinal (0.10 and 0.25) and shear (0.25) stress components are averaged, to predict net section, bearing and shear-out modes of failure, respectively (see Figure 21).

SAMCJ predictions for test case 201 are compared with test results from Reference 2 in Figure 29. The two fasteners are predicted to carry nearly equal loads, in agreement with the values measured using strain-gaged bolts (Reference 2). The assumed failure parameters (a_{ons} , a_{obrg} and a_{oso} of 0.10, 0.25 and 0.25 inch, respectively) and the average stress failure criteria predict the observed shear-out mode of failure at the inner fastener location(1). The predicted failure load (9.48 kips) agrees very well with the average measured value (9.51 kips). Note that a bearing mode of failure at the same fastener location is predicted to occur at only a slightly larger load level (9.71 kips). This indicates the possibility of either failure mode, within the scatter region of the measured failure load. Observations in Reference 2 also indicated the dual failure mode possibility for specimens in test case 201.

SAMCJ predictions for test case 202 are compared with test results in Figure 30. In this case, the model in Figure 27 is used along with a 70/20/10 layup for the bottom plate. The input data in Figure 28 can be easily modified to account for this change. SAMCJ predicts a nearly equal load distribution between the two fasteners, and a shear-out mode of failure in the highly fiber-dominated layup.

Test Case 201; Static Tension, Single-Shear 20-Ply, 50/40/10
 Laminate, $t=0.113$ in, $t_{A1}=0.31$ in, $D=5/16$ in, $S_L/D=4$, $E/D=3$,
 $W/D=6$, a_{ons} , a_{obrg} , a_{oso} = 0.10, 0.25, 0.25 inch, respectively.

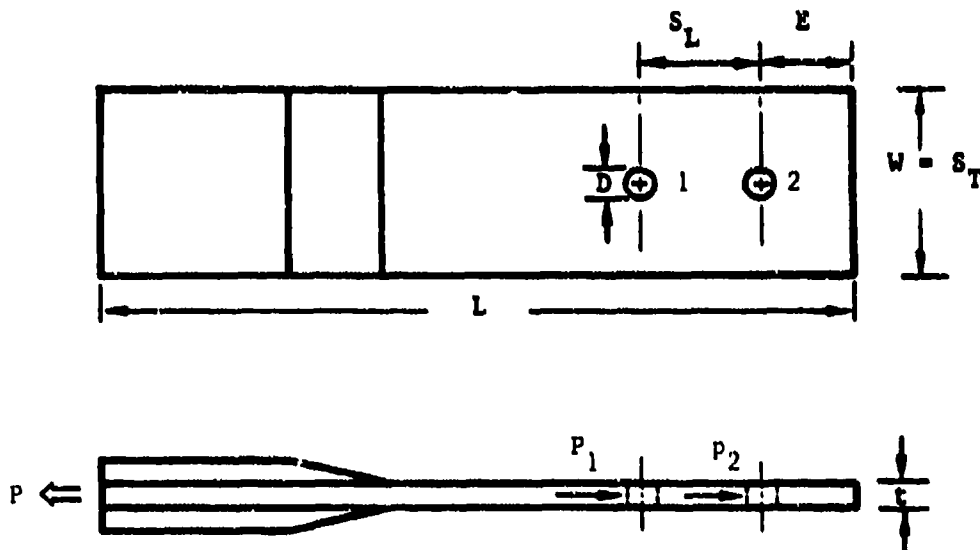


	SAMCJ PREDICTION	TEST RESULTS (Ref. 2)
P_1/P	0.51	0.49
P_2/P	0.49	0.51
$P_{failure}$ (kips)	9.48 (9.71)*	9.51
FAILURE LOCATION	1 (1)	1, 2
FAILURE MODE(S)	SHEAR-OUT (BEARING)	SHEAR-OUT, BEARING, DELAMINATION

* Possible failure mode and location at a slightly higher load level

Figure 29. SAMCJ Predictions and Test Results for Test Case 201

Test Case 202; Static Tension, Single-Shear 20-Ply, 70/20/10 laminate, $t=0.108$ in, $t_{A1}=0.31$ in, $D=5/16$ in, $S_L/D=4$, $W/D=6$, $E/D=3$, a_{ons} , a_{ohrg} , a_{oso} $A1=0.10$, 0.25 , 0.25 inch, respectively.



	SAMCJ PREDICTION	TEST RESULTS (Ref. 2)
P_1/P	0.51	-
P_2/P	0.49	-
$P_{failure}$ (kips)	6.90	7.92
FAILURE LOCATION	1	1, 2
FAILURE MODE(S)	SHEAR-OUT	SHEAR-OUT

Figure 30. SAMCJ Predictions and Test Results for Test Case 202

As in test case 201, and in every other test case discussed in this section, the failure parameters were assumed to be invariant (a values of 0.10, 0.25 and 0.25 inch for net section, bearing and shear-out modes of failure, respectively). The predicted failure load (6.90 kips) is 13% lower than the average measured value (7.92 kips).

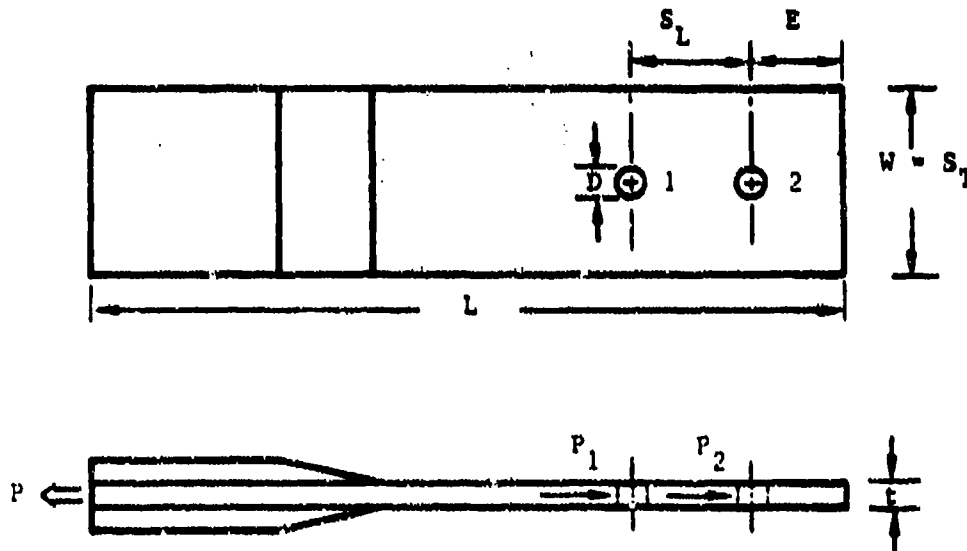
Figure 31 presents SAMCJ predictions for test case 203, where the laminate layup is changed to a 30/60/10 layup. The input data for this case are identical to those for the previous two cases, with the exception of the laminate layup definition and its cured ply thickness. In this case, a bearing mode of failure is predicted at the inner fastener location. This agrees with the observation in Reference 2. The predicted failure load for this case (7.18 kips) is 20% lower than the average measured value (8.92 kips).

The composite-to-metal joint in test case 206 is tested in a double shear configuration, instead of the single-shear configuration in test case 201. Test results from Reference 2 are compared with SAMCJ predictions for this case in Figure 32. Again, the measured nearly equal load distribution is predicted by SAMCJ, along with the observed shearout mode of failure at the inner fastener location. The predicted failure load (9.57 kips) is in excellent agreement with the measured average value (9.60 kips).

3.2 Composite-to-Metal Joints with Two Fasteners at an Angle to the Load Direction

The bolted plates in test cases 216 to 224 (see Table 1) contain two fasteners each at an angle to the load direction. When the fastener spacings in the load direction (S) and the transverse direction (S_T) are reduced, the modeling of each bolted plate results in inaccurate SAMCJ computations. Refer to Figure 33 for three different models of each bolted plate in test case 221 ($S/D = S_T/D = 4$). The off-center fastener location in the four element

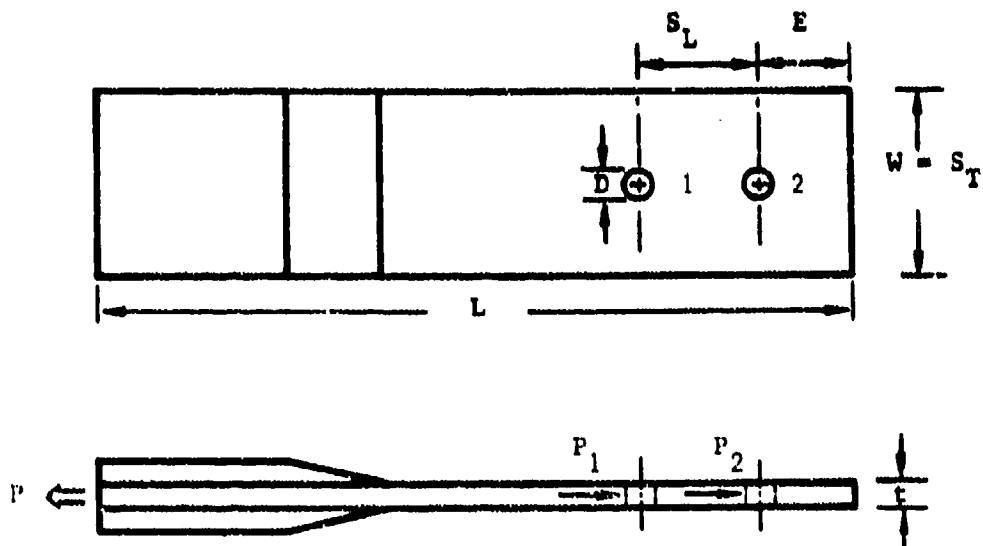
Test Case 203; Static Tension, Single-Shear 20-Ply, 30/60/10 Laminate, $t=0.106$ in, $t_{A1}=0.31$ in, $D=5/16$ in, $S_L/D=4$, $W/D=6$, $E/D=3$, a values=0.10, 0.25 and 0.25 in for net section, bearing and shear-out, respectively.



	SAMCJ PREDICTION	TEST RESULTS (Ref. 2)
P_1/P	0.53	0.47
P_2/P	0.47	0.53
$P_{failure}$ (kips)	7.18	8.92
FAILURE LOCATION	1	1
FAILURE MODE(S)	BEARING	BEARING

Figure 31. SAMCJ Predictions and Test Results for Test Case 203

Test Case 206; Static Tension, Double-Shear 20-Ply,
50/40/10 Laminate, $t=0.114$ in, $t_{AL}=0.26$ in, $D=5/16$ in,
 $S_L/D=4$, $W/D=6$, $E/D=3$, a_{ons} , a_{obrg} , $a_{oso}=0.10$, 0.25 ,
 0.25 inch, respectively.



	SAMCJ PREDICTION	TEST RESULTS (Ref. 2)
P_1/P	0.52	0.49
P_2/P	0.48	0.51
$P_{failure}$ (kips)	9.57 (9.80)*	9.60
FAILURE LOCATION	1 (1)	1
FAILURE MODE(S)	SHEAR-OUT (BEARING)	SHEAR-OUT, NET SECTION, DELAMINATION

* Possible failure mode and location at a slightly higher load level

Figure 32. SAMCJ Predictions and Test Results for Test Case 206

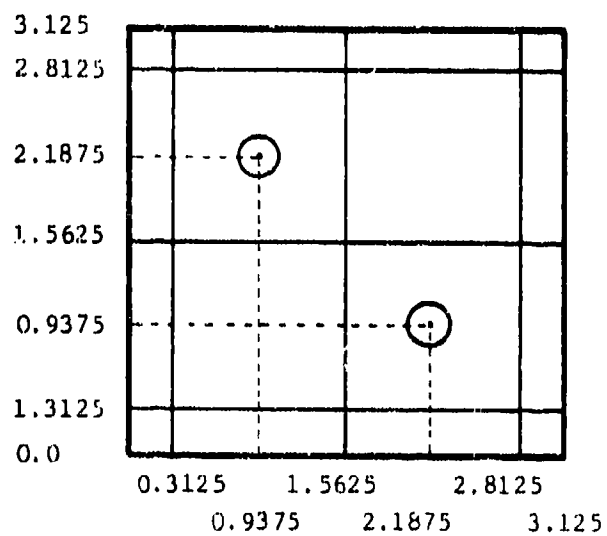
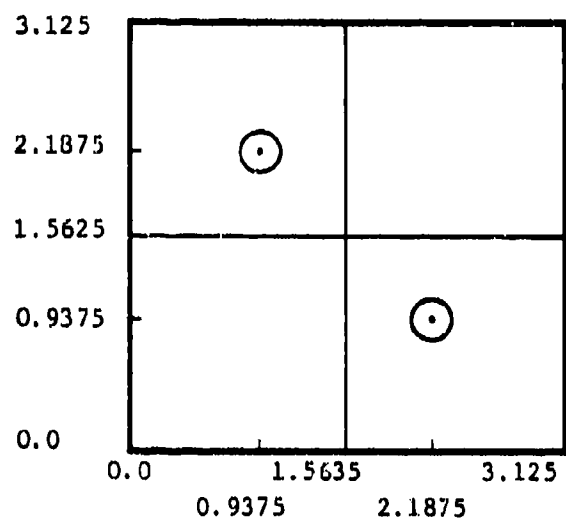
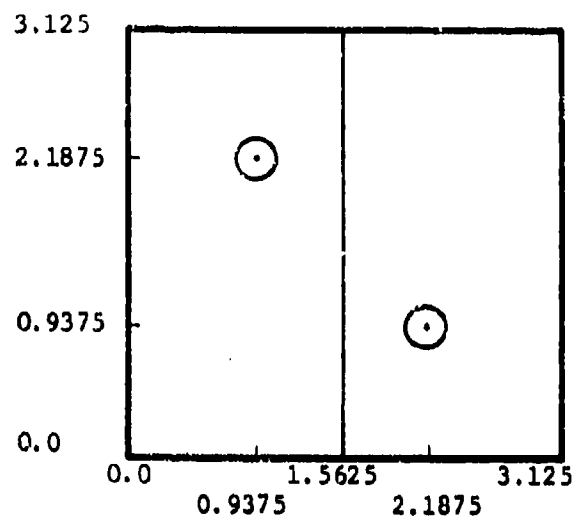


Figure 33. Two-, Four- and Sixteen-Element Models of the Bolted Plates in Test Case 221.

models of the bolted plate causes two of the element boundaries to be very close to the fastener hole boundary. These distances are reduced even further in other test cases (216 to 220, and 222 to 224 in Table 1). Consequently, the computed average stresses at the fastener locations are influenced by the proximity of the element boundaries.

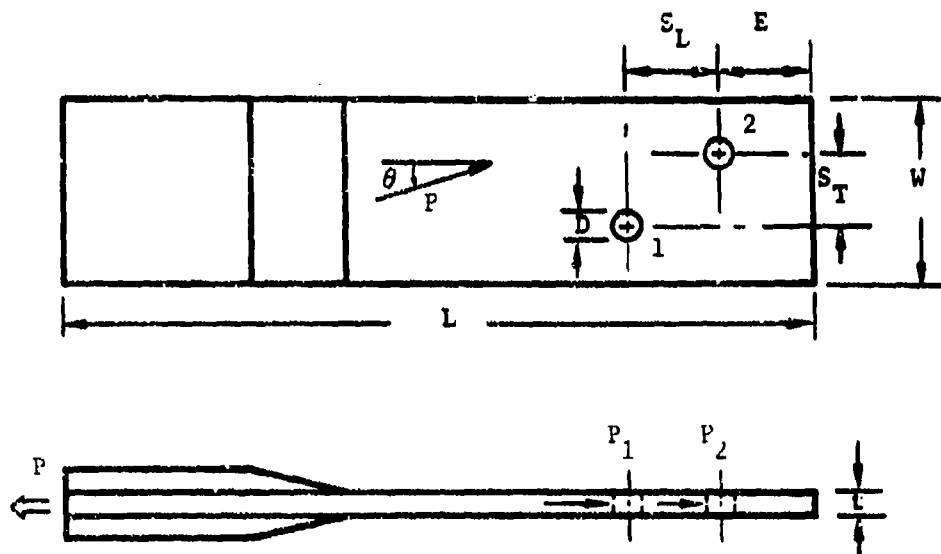
Two-, four- and sixteen-element models of each bolted plate in test case 221 result in SAMCJ predictions that are shown in Figure 34. In agreement with the strain-gaged bolt measurements in Reference 2, the two fasteners are predicted to carry equal loads that are aligned along the load direction. While the equal load distribution is to be expected, the lack of a significant transverse (y) component of the fastener load defeats intuition. SAMCJ predictions and the test results from Reference 2 indicate nearly zero values for F_{y1} and F_{y2} , pointing to the absence of significant y components of the fastener loads.

SAMCJ predicts the failure location (inner fastener) and the failure mode (shearout) recorded during the test in Reference 2. However, the predicted failure load is nonconservative, and is dependent on the modeling of the bolted plates. For the two-element models in Figure 33, SAMCJ predicts a failure load of 12.5 kips, which is 29% larger than the measured average value (9.7 kips). For the four- and sixteen element models, the SAMCJ predictions (15.2 and 16.6 kips) are 57% and 71% larger than the measured average value, respectively.

When the fasteners are very close to one another, as in test case 216 to 224, SAMCJ is unable to conservatively predict the measured failure loads. A higher order element, proposed for future development in Section 2, is expected to yield better analytical predictions for such test cases.

3.3 Composite-to-Metal Joints with Four Fasteners in a Rectangular Pattern

Test Case 221, Static Tension, Single-Shear
 20-Ply, 50/40/10 Laminate, $t=0.113$ in., $t_{AL}=0.31$ in.
 $D=5/16$ in., $S_L/D=4$, $S_T/D=4$, $W/D=10$, $E/D=3$



	SAMCJ PREDICTION	TEST RESULTS (Ref. 2)
P_1/P	0.50	0.53
θ_1 (degrees)	-0.2	0.7
P_2/P	0.50	0.47
θ_2 (degrees)	0.2	2.4
$P_{failure}$ (kips)	12.5 (15.2, 16.6)*	9.70
FAILURE LOCATION	1	1, 2
FAILURE MODE(S)	SHEAR-OUT	SHEAR-OUT

* The values within parenthesis correspond to the 4 and 16 element models, respectively, of each plate

Figure 34. SAMCJ Predictions and Test Results for Test Case 221

Test cases 225, 229 and 230 in Table 1 consider composite-to-metal joints in a single-shear configuration, with four fasteners in a rectangular pattern. The finite element model for each of the bolted plates in test cases 225, 229 and 230 is shown in Figure 35. The laminates in the three test cases contained 20 plies each in 50/40/10, 70/20/10 and 30/60/10 layups.

Figure 36 compares SAMCJ predictions with the test results from Reference 2 for test case 225. The predicted fastener load distribution is nearly equal, with the inner fasteners carrying a slightly larger fraction of the load (8%). This agrees with the test results in Reference 2. SAMCJ predicts a shearout failure at the inner fastener location. The predicted shearout load levels corresponding to the two inner fasteners were 18.1 and 18.9 kips. In Reference 2, the same failure location (inner fasteners) and failure mode were observed in two out of three replicates. In the remaining replicate, though, a net section failure occurred across the inner fasteners. The shearout failures in two specimens were accompanied by delaminations in the laminate. The failure load predicted by SAMCJ (18.1 kips) is only 6% larger than the measured average value (17.1 kips).

SAMCJ predictions for the bolted 70/20/10 laminate in test case 229 are presented in Figure 37. The fastener load distribution is identical to that predicted for the 50/40/10 laminate, and agrees with the test results from Reference 2. The predicted failure location (inner fasteners) and failure mode (shearout) correlate well with the observations in Reference 2. As before, shearout is accompanied by delaminations in the failed laminate. The failure load predicted by SAMCJ (11.8 kips) is 21% lower than the measured average value (14.9 kips).

SAMCJ predictions for the bolted 30/60/10 laminate in test case 230 are presented in Figure 38. In this case, the predicted loads in the inner fasteners (3,4) are 17% larger than those in the

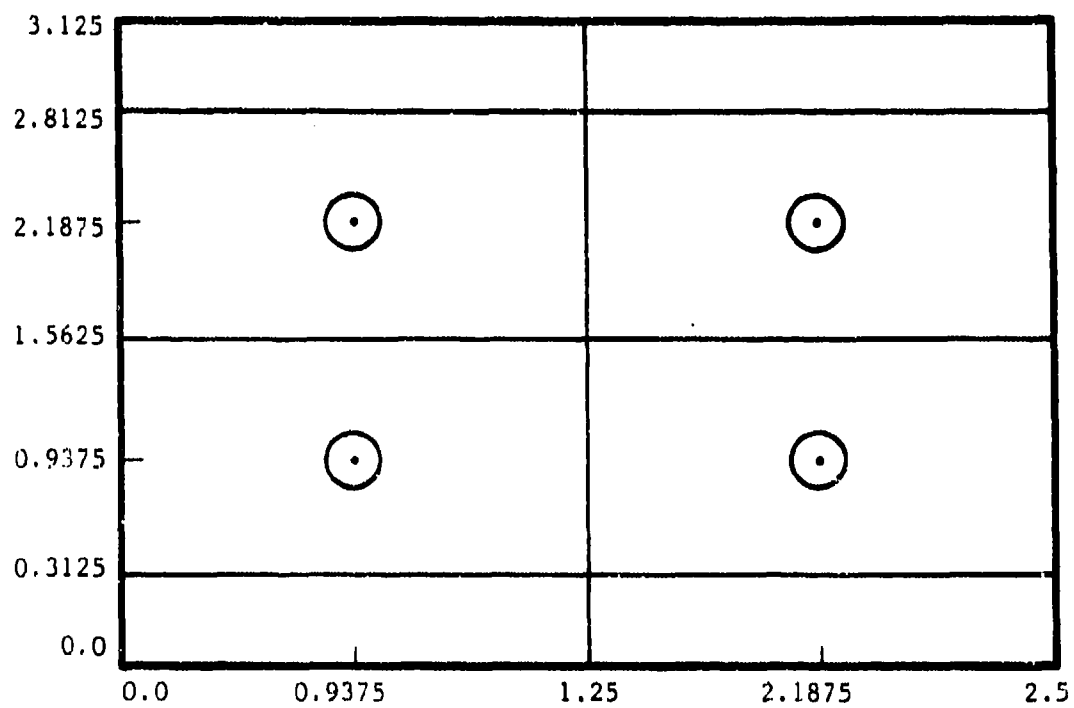
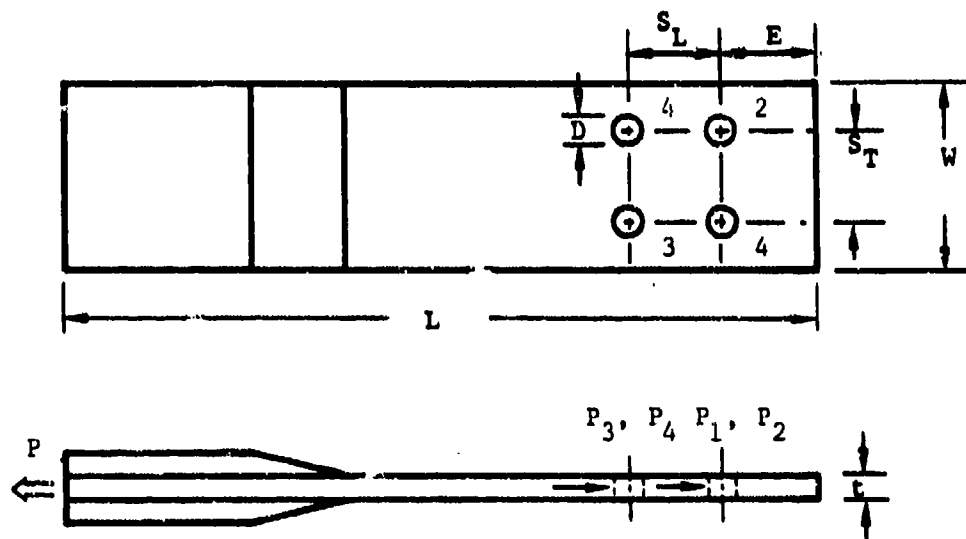


Figure 35. Eight-Element Model of Each Bolted Plate in Test Cases 225, 229 and 230

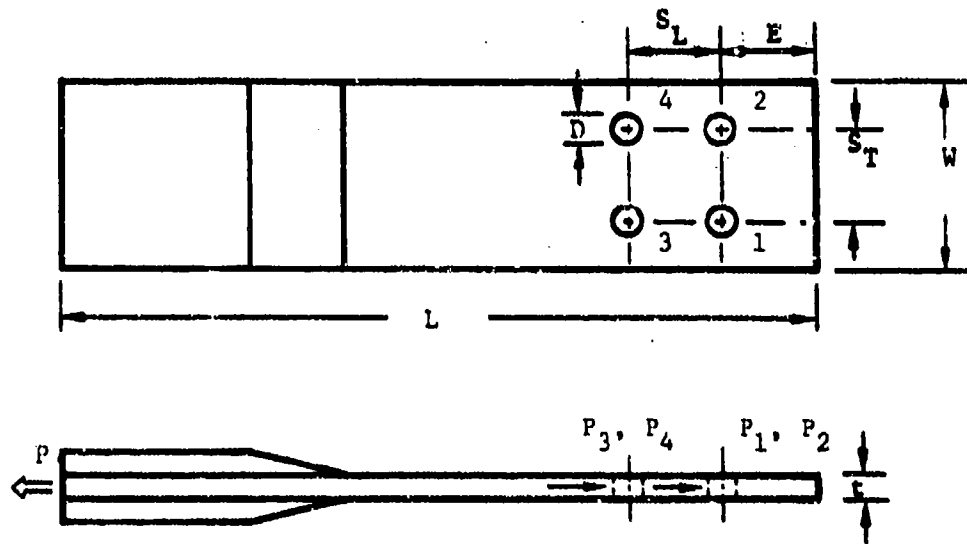
Test Case 225, Static Tension, Single-Shear
 20-Ply, 50/40/10 Laminate
 $D=5/16$ in. $t=0.117$ in., $t_{AL}=0.31$
 $S_L/D=S_T/D=4$, $W/D=10$, $E/D=3$



	SAMCJ PREDICTION	TEST RESULTS (Ref. 2)
P_1/P	0.24	0.25
P_2/P	0.24	0.25
P_3/P	0.26	0.29
P_4/P	0.26	0.21
$P_{failure}$ (klps)	18.1 (18.9)	17.1
FAILURE LOCATION	4 (3)	3, 4
FAILURE MODE(S)	SHEAR-OUT	SHEAR-OUT, NET SECTION, DELAMINATION

Figure 36. SAMCJ Predictions and Test Results for Test Case 225.

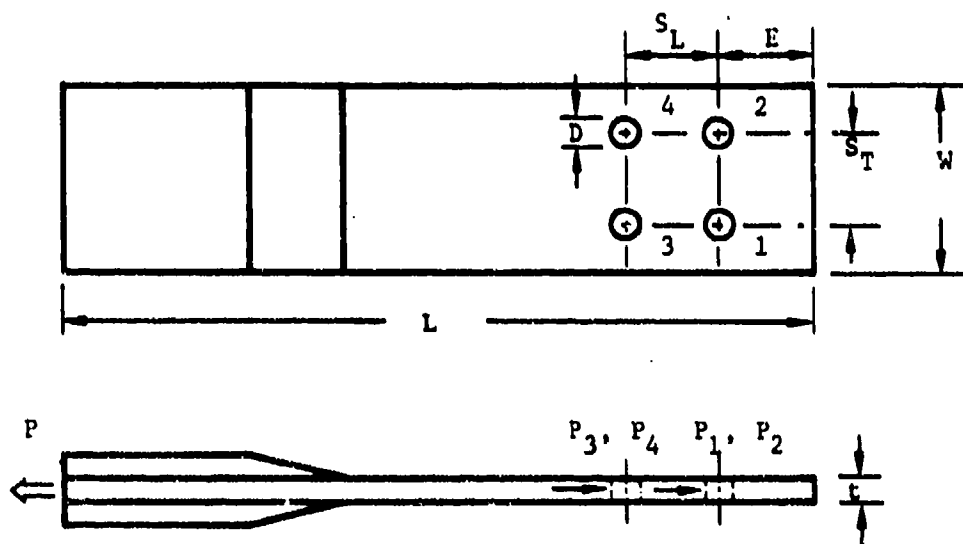
Test Case 229, Static Tension, Single-Shear
 20-Ply, 70/20/10 Laminate
 $D=5/16$ in., $t=0.105$ in., $t_{AI}=0.31$ in.
 $S_L/D=S_T/D=4$, $W/D=10$, $E/D=3$



	SAMCJ PREDICTION	TEST RESULTS (Ref. 2)
P_1/P	0.24	0.25
P_2/P	0.24	0.24
P_3/P	0.26	0.29
P_4/P	0.26	0.22
$P_{failure}$ (kips)	11.8 (12.3)	14.9
FAILURE LOCATION	4 (3)	4, 3, 2, 1
FAILURE MODE(S)	SHEAR-OUT	SHEAR-OUT, DELAMINATION

Figure 37. SAMCJ Predictions and Test Results for Test Case 229.

Test Case 230, Static Tension, Single-Shear
 20-Ply, 30/60/10 Laminate, $t=0.106$ in., $t_{AL}=0.31$ in.
 $D=5/16$ in., $S_L/D=S_T=4$, $W/D=10$, $E/D=3$



	SAMCJ PREDICTION	TEST RESULTS (Ref. 2)
P_1/F	0.23	0.24
P_2/P	0.23	0.26
P_3/P	0.27	0.26
P_4/P	0.27	0.24
$P_{failure}$ (kips)	12.4 (12.8)	16.4
FAILURE LOCATION	4 (3)	3, 4
FAILURE MODE(S)	NET SECTION	NET SECTION, DELAMINATION

Figure 38. SAMCJ Predictions and Test Results for Test Case 320.

outer fasteners (1,2). SAMCJ predicts a net section failure across the inner fastener holes (3,4) at a load level of 12.4 kips. In Reference 2, the predicted net section failure was observed at the predicted site, accompanied by delaminations. The failure load predicted by SAMCJ (12.4 kips) is 24% lower than the measured average value (16.4 kips).

3.4 Composite-to-Metal Joints with Three Fasteners in a Triangular Pattern

Test cases 233 to 241 in Table 1 address double-shear load transfer joints that contain three fasteners in a triangular pattern. In predicting the effect of these fastener patterns, SAMCJ encountered the same difficulties described in Section 3.2. Figure 39 presents a four-element model of the bolted plates in test cases 234, 238 and 239. SAMCJ used this model to make the predictions discussed below.

A 50/40/10 laminate is considered in test case 234. The fastener loads and their orientations to the load direction, predicted by SAMCJ, are presented in Figure 40. SAMCJ predictions correlate well with the strain-gaged bolt measurements in Reference 2. Test observations indicated a combination of shearout and net section failures at the innermost fastener location. SAMCJ predicts a shearout failure at the same location. The failure load predicted by SAMCJ (17.0 kips) is 38% larger than the measured average values (12.3 kips). As in the case of two fasteners at an angle to the load direction, a nonconservative failure load prediction is made.

In test case 238, a 70/20/10 laminate layup is considered. The fastener loads predicted by SAMCJ correlate well with the measured values in Reference 2. The predicted load orientations at fastener locations 1 and 2 (see Figure 41) are in fair agreement with strain-gaged bolt measurements. However, the measurement at the third location is suspect, and does not correlate with SAMCJ prediction. SAMCJ predicts failure at 11.4 kips, in a shearout mode

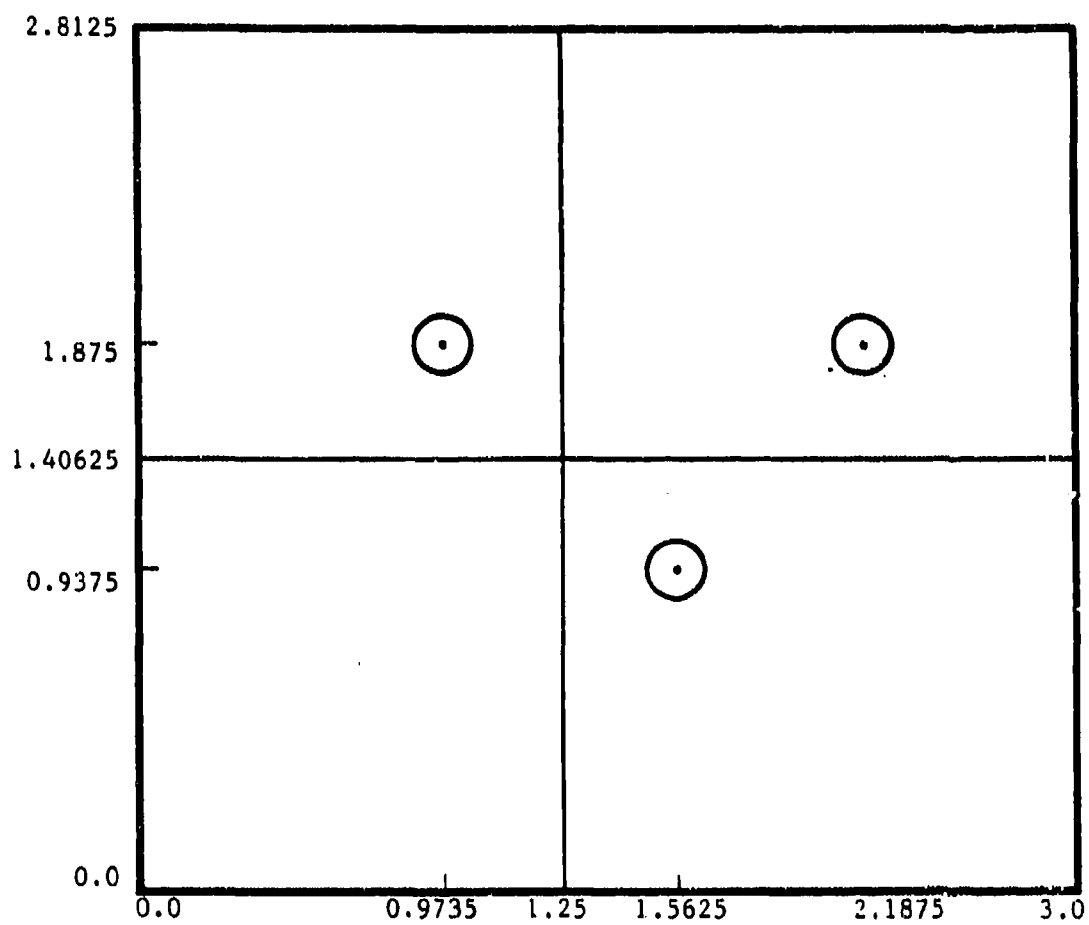
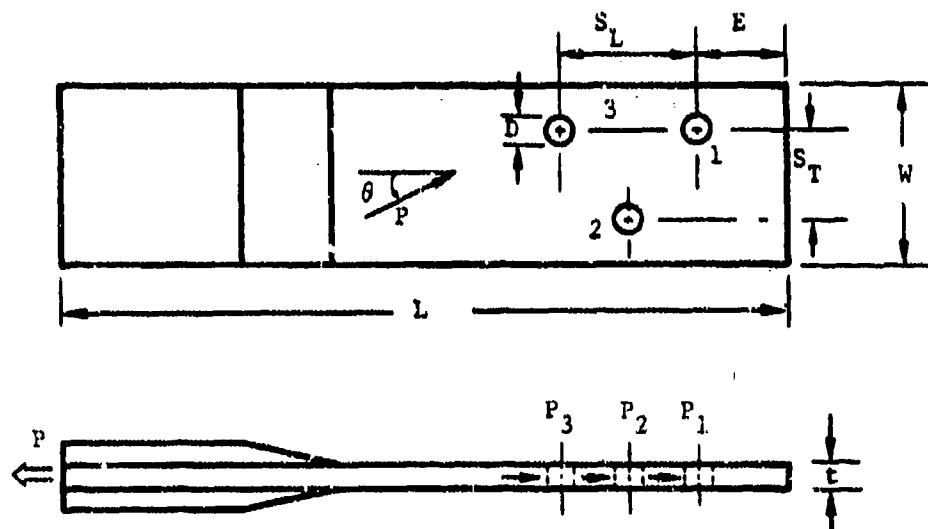


Figure 39. Four-Element Model of the Bolted Plates in Test Cases 234, 238 and 239

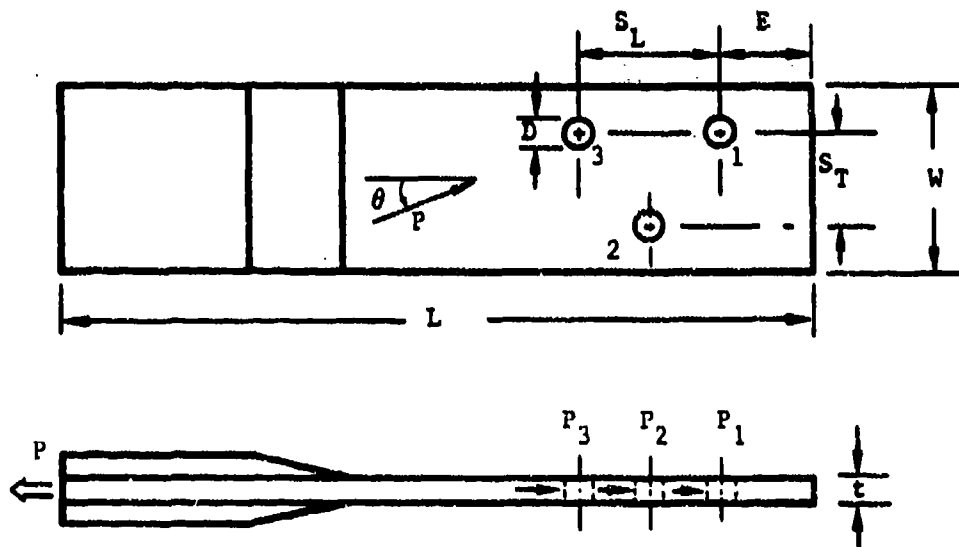
Test Case 234, Static Tension, Double-Shear
 20-Ply, 50/40/10 Laminate, $t=0.117$ in., $t_{AL}=0.26$ in.
 $D=5/16$ in., $S_L/D=4$, $W/D=9$, $S_T/D=E/D=3$



	SAMCJ PREDICTION	TEST RESULTS (Ref. 2)
P_1/P	0.26	0.25
P_2/P	0.43	0.46
P_3/P	0.32	0.30
θ_1 (degrees)	11.4	16.7
θ_2 (degrees)	0.7	-4.7
θ_3 (degrees)	-10.2	-9.6
$P_{failure}$ (kips)	17.0	12.3
FAILURE LOCATION	3	3, 2
FAILURE MODE(S)	SHEAR-OUT	SHEAR-OUT, NET SECTION

Figure 40. SAMCJ Predictions and Test Results for Test Case 234.

Test Case 238, Static Tension, Double-Shear
 20-Ply, 70/20/10 Laminate, $t=0.107$ in., $t_{AL}=0.26$ in
 $D=5/16$ in., $S_L/D=4$, $W/D=9$, $S_T/D=E/D=3$.



	SAMCJ PREDICTION	TEST RESULTS (Ref. 2)
P_1/P	0.26	0.28
P_2/P	0.44	0.39
P_3/P	0.30	0.33
θ_1 (degrees)	9.3	4.5
θ_2 (degrees)	0.6	-1.5
θ_3 (degrees)	-8.6	-0.7
$P_{failure}$ (kips)	11.4	12.9
FAILURE LOCATION	3	3, 1, 2
FAILURE MODE(S)	SHEAR-OUT	SHEAR-OUT, DELAMINATION

Figure 41. SAMCJ Predictions and Test Results for Test Case 238.

at the innermost fastener location. Delaminations accompanied the predicted shearout failures in the test specimens (Reference 2). The predicted failure load (11.4 kips) is 12% lower than the average measured value (12.9 kips).

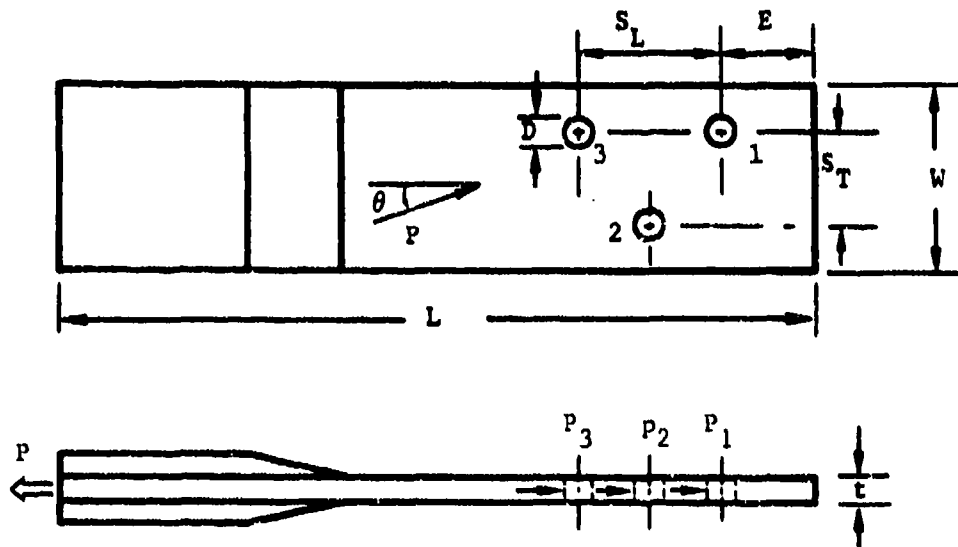
SAMCJ predictions for the 30/60/10 laminate (test case 239) are presented in Figure 42. The fastener loads predicted correlate well with the measured values in Reference 2. The predicted load orientations at fastener locations 1 and 2 are in fair agreements. Again, the measurement at the third location is suspect, and does not correlate with SAMCJ predictions. SAMCJ predicted failure at 11.7 kips, with a net section failure mode at fastener location 3. Net section failures occurred at both locations number 3 and 2 in the test specimens (Reference 2). The predicted failure load (11.7 kips) is 11% lower than the average measured value (13.2 kips).

3.5 Composite-to-Metal Joints with Six Fasteners and an Adjacent Circular Cut-Out in the Laminate

Test cases 243, 246 and 247 address a single-shear load transfer between 0.5-inch-thick aluminum plates (without a cutout) and 40-ply laminates of 50/40/10, 70/20/10 and 25/60/15 layups, with a one inch diameter circular cut-out adjacent to the fasteners. The bolted laminates with the circular cutout were modeled as shown in Figure 43, for the three test cases.

SAMCJ predictions for the 40-ply 50/40/10 laminate (test case 243) are presented in Figure 44. SAMCJ predicts the applied load to be divided nearly equally among the six fasteners, with fasteners at locations 2 and 5 carrying the largest fraction. This correlates fairly well with the strain-gaged bolt measurements in Reference 2. SAMCJ predicts failure to occur in a net section mode, across the 1-inch-diameter circular cutout. Two out of three test replicates failed in the predicted manner. One replicate, however, failed in a net section mode, across the inner fasteners (4,5,6).

Test Case 239, Static Tension, Double-Shear
 20-Ply, 30/60/10 laminate, $t=0.107$ in., $t_{AL}=0.26$ in
 $D=5/16$ in., $S_L/D=4$, $W/D=9$, $S_T/D=E/L=3$



	SAMCJ PREDICTION	TEST RESULTS (Ref. 2)
P_1/P	0.26	0.27
P_2/P	0.41	0.39
P_3/P	0.33	0.34
θ_1 (degrees)	14.0	9.2
θ_2 (degrees)	0.8	-3.6
θ_3 (degrees)	-12.0	2.4
$P_{failure}$ (kips)	11.7	13.2
FAILURE LOCATION	3	3, 2
FAILURE MODE(S)	NET SECTION	NET SECTION

Figure 42. SAMCJ Predictions and Test Results for Test Case 239.

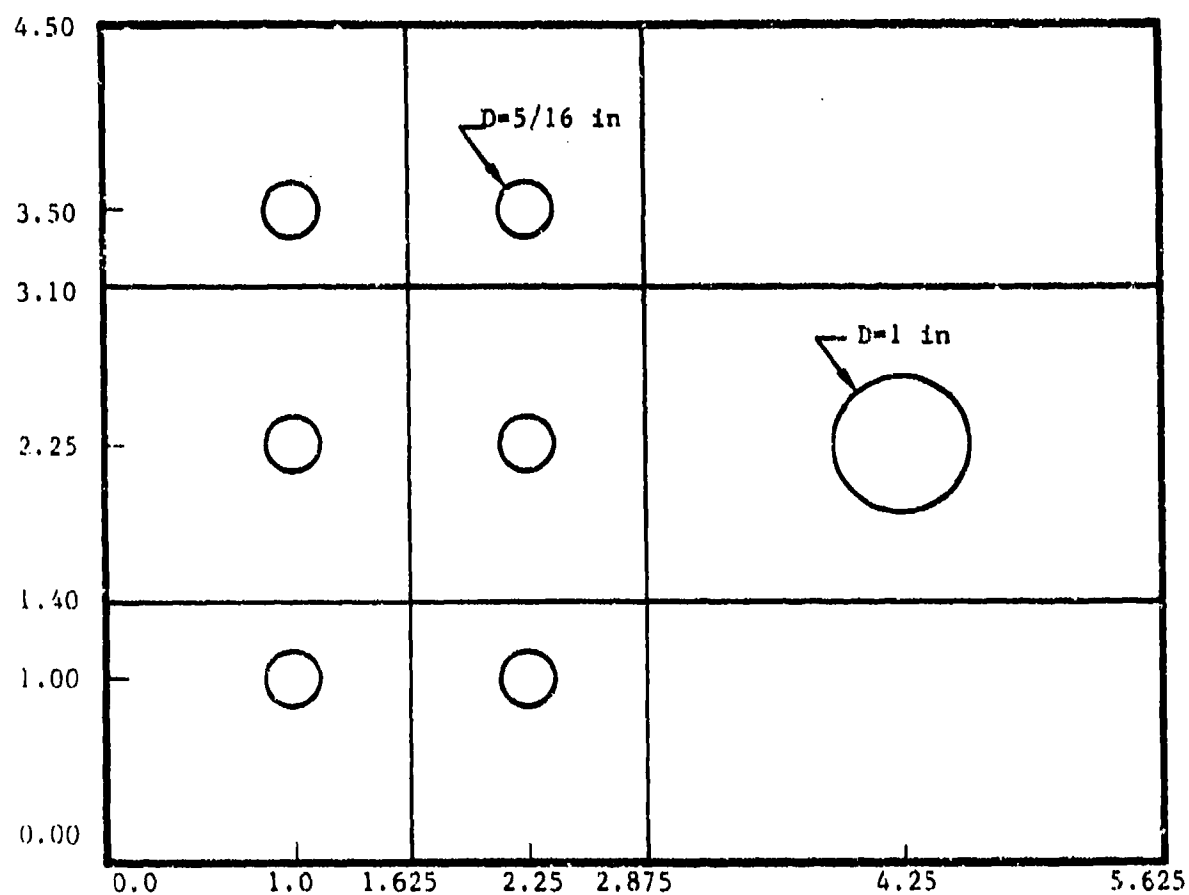
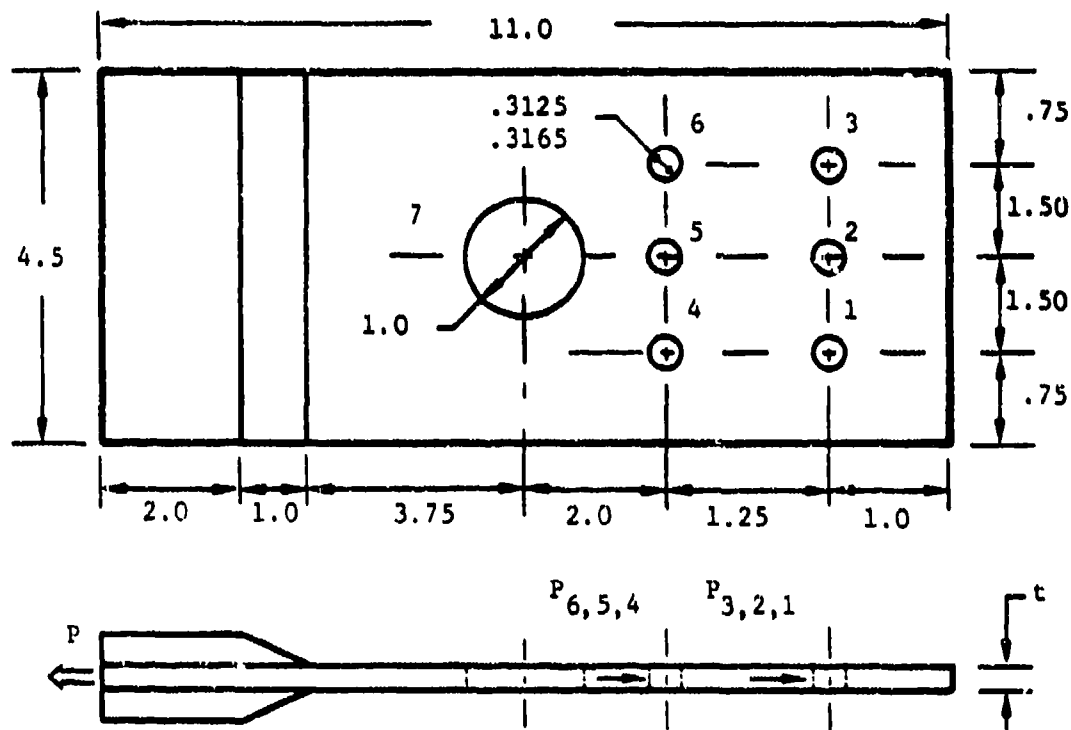


Figure 43. Nine-Element Model of the Bolted Plates in Test Cases 243, 246 and 247

Test Case 243, Static Tension, Single-Lap
 40-Ply, 50/40/10 Laminate, $t=0.247$ in., $t_{AL}=0.50$ in.
 $D=5/16$ in., $H_D=1$ in., $S_L/D=S_T/D=4$, $W/D=14.4$, $E/D=3.2$



	SAMCJ PREDICTION	TEST RESULTS (Ref. 2)
P_1 / P	0.164	0.162
P_2 / P	0.181	0.150
P_3 / P	0.163	0.188
P_4 / P	0.158	0.177
P_5 / P	0.176	0.161
P_6 / P	0.157	0.165
$P_{failure}$ (kips)	38.3 (53.7)*	42.0
FAILURE LOCATION	7 (5)	7 and 4, 5, 6
FAILURE MODE(S)	NET SECTION (NET SECTION)	NET SECTION

* Next possible failure mode and location at a higher load level

Figure 44. SAMCJ Predictions and Test Results for Test Case 243.

**THIS REPORT HAS BEEN DELIMITED
AND CLEARED FOR PUBLIC RELEASE
UNDER DOD DIRECTIVE 5200.20 AND
NO RESTRICTIONS ARE IMPOSED UPON
ITS USE AND DISCLOSURE.**

DISTRIBUTION STATEMENT A

**APPROVED FOR PUBLIC RELEASE;
DISTRIBUTION UNLIMITED.**

The failure load predicted by SAMCJ (38.3 kips) is 9% lower than the measured average value (42.0 kips). SAMCJ predicts a higher load level (53.7 kips) for a net section failure across the inner fastener holes, observed in one out of three test replicates.

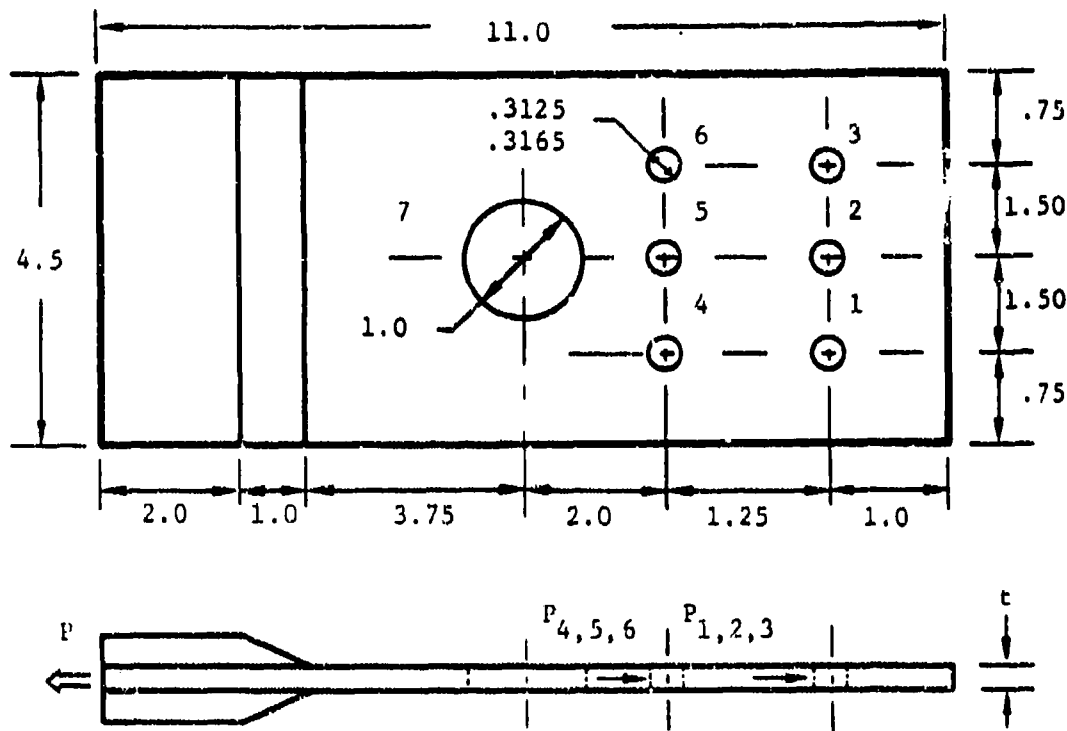
SAMCJ predictions for the 40-ply, 70/20/10 laminate (test case 246) are presented in Figure 45. Predicted load distribution among the six fasteners is similar to that predicted for the 50/40/10 laminate, and is in fair agreement with test measurements. SAMCJ predicts a shearout mode of failure at an inner fastener location(5), while tests resulted in shearout failures at all the fastener locations (1 to 6), accompanied by delaminations. The failure load predicted by SAMCJ (37.9 kips) is 12% lower than the measured average value (42.9 kips). It is also noted that SAMCJ predicts a net section failure across the 1-inch-diameter circular cut-out at a slightly higher load level (38.8 kips).

SAMCJ predictions for the 40-ply, 25/60/15 laminate with a 1-inch-diameter circular cut-out (test case 247) are presented in Figure 46. A more even load distribution among the six fasteners is predicted in this case, and is in agreement with strain-gaged bolt measurements. SAMCJ predicts failure to occur at 30.6 kips, in a net section mode across the circular cutout (7). Two out of three test replicates in Reference 2 failed in the predicted mode. However, the third replicate failed in a net section mode across the inner fastener holes (4,5,6). SAMCJ predicts this to be the second probable failure at a higher load level (36.0 kips). The predicted failure load (30.6 kips) is 18% lower than the measured average value (37.2 kips).

3.6 Composite-to-Metal Joints with Five Fasteners in a Row

Test cases 250 and 251 consider load transfer between an aluminum plate and a 40-ply, 50/40/10 laminate, in double- and single-shear configurations, respectively. Figure 47 presents the six-element model of the bolted plates used by SAMCJ for both test

Test Case 246, Static Tension, Single-Lap
 40-Ply, 70/20/10 Laminate, $t=0.236$ in., $t_{AL}=0.50$ in.
 $D=5/16$ in., $H_D=1$ in., $S_L/D=S_T/D=4$, $W/D=14.4$, $E/D=3.2$

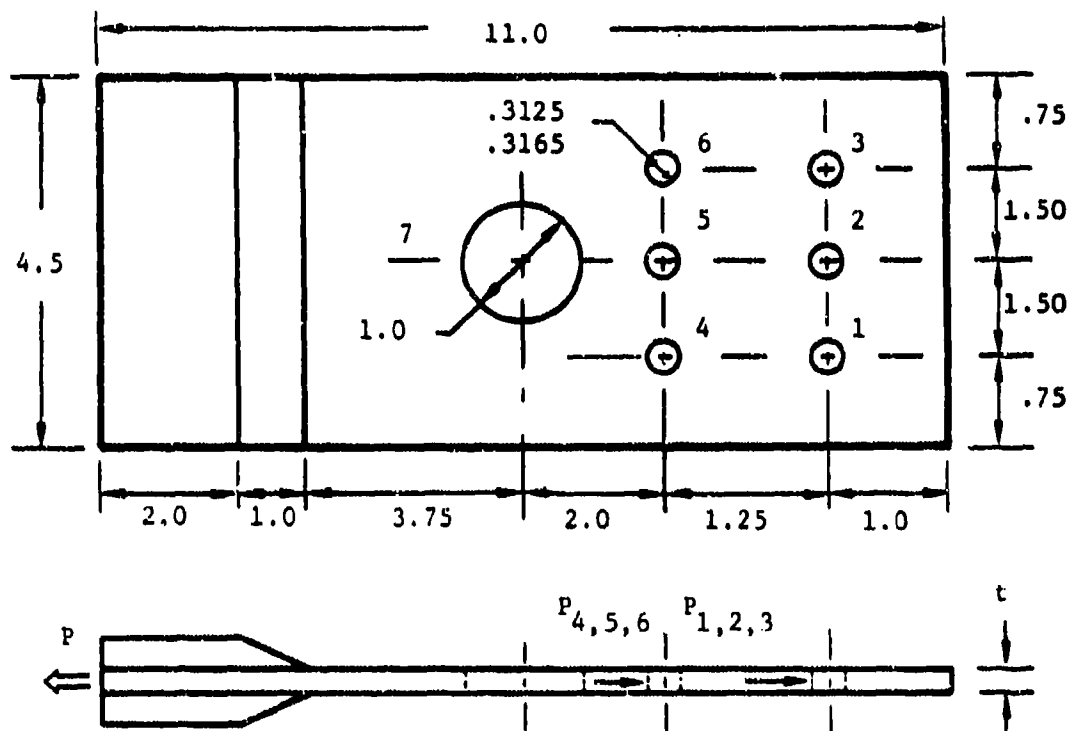


	SAMCJ PREDICTION	TEST RESULTS (Ref. 2)
P_1/P	0.164	0.158
P_2/P	0.188	0.165
P_3/P	0.163	0.199
P_4/P	0.156	0.172
P_5/P	0.177	0.166
P_6/P	0.154	0.140
$P_{failure}$ (kips)	37.8 (38.8)*	42.9
FAILURE LOCATION	5 (7)	1 to 6
FAILURE MODE(S)	SHEAR-OUT (NET SECTION)	SHEAR-OUT, DELAMINATION

*Next possible failure mode and location at a higher load level

Figure 45. SAMCJ Predictions and Test Results for Test Case 246.

Test Case 247, Static Tension, Single-Lap
 40-Ply, 25/60/15 Laminate, $t=0.233$ in., $t_{AL}=0.50$ in.
 $D=5/16$ in., $H_D=1$ in., $S_L/D=S_T/D=4$, $W/D=14.4$, $E/D=3.2$



	SAMCJ PREDICTION	TEST RESULTS (Ref. 2)
P_1 / P	0.161	0.161
P_2 / P	0.178	0.155
P_3 / P	0.160	0.182
P_4 / P	0.163	0.177
P_5 / P	0.177	0.171
P_6 / P	0.162	0.156
$P_{failure}$ (klps)	30.6 (36.0)*	37.1
FAILURE LOCATION	7 (5)	7 and 4, 5, 6
FAILURE MODE(S)	NET SECTION (NET SECTION)	NET SECTION

* Next possible failure mode and location at a higher load level

Figure 46. SAMCJ Predictions and Test Results for Test Case 247.

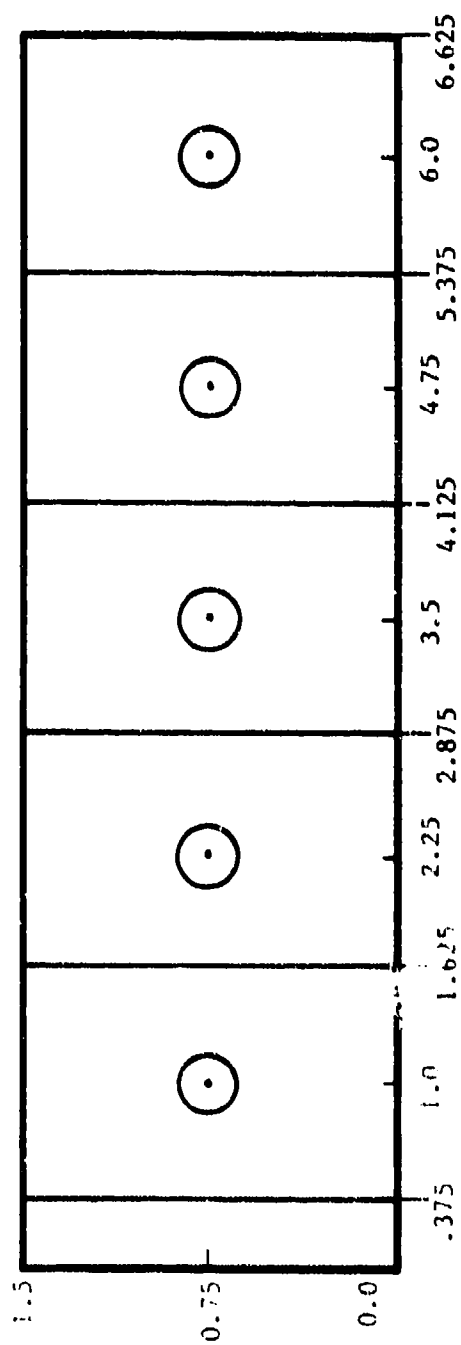


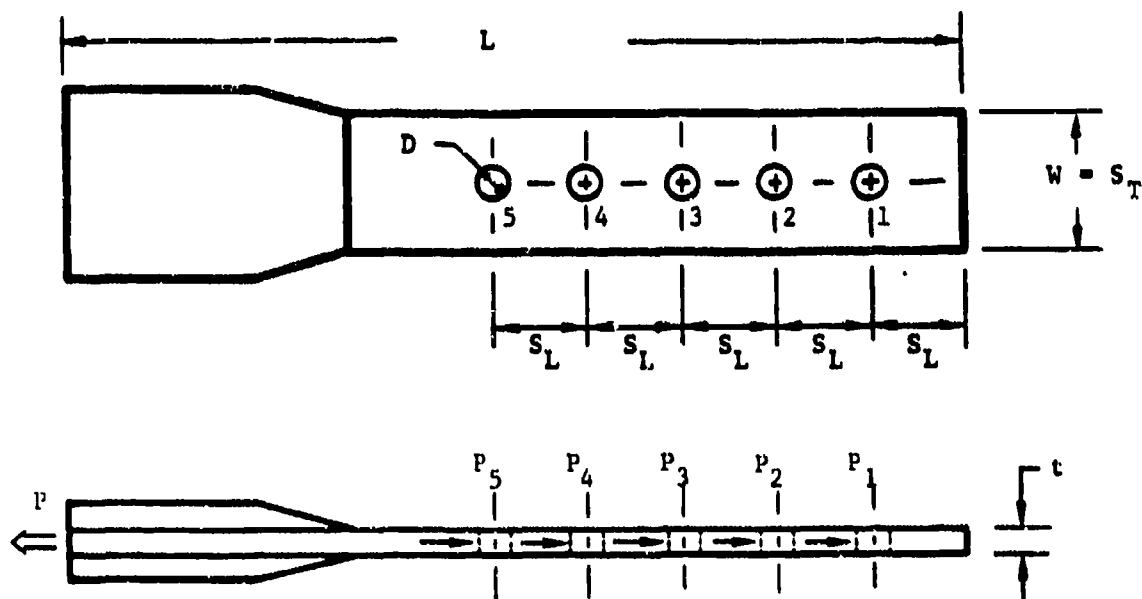
Figure 47. Six-Element Model of the Bolted Plates in Test Cases 250 and 251

cases.

SAMCJ predictions for test case 250 are presented in Figure 48. The predicted load distribution among the fasteners qualitatively follows the trend indicated by the strain-gaged bolt measurements in Reference 2. The predicted peak fastener load fraction (0.293), however, is lower than the measured value (0.345). The innermost fastener (5) is predicted to carry this peak fractional load, in agreement with test results. SAMCJ predicts the laminate to fail in a net section mode across the innermost fastener hole (5). This prediction is also in agreement with the observations in Reference 2. The analytically predicted failure load (13.4 kips) is 24% lower than the measured average value (17.7 kips).

In a single-shear load transfer situation (test case 251), a more even load distribution among the five fasteners is predicted by SAMCJ (see Figure 49). This agrees well with the strain-gaged bolt measurements in Reference 2. The analytically predicted and experimentally observed failure is a net section failure across the innermost fastener hole (5). The failure load predicted by SAMCJ (12.4 kips) is 25% lower than the measured average value (16.6 kips).

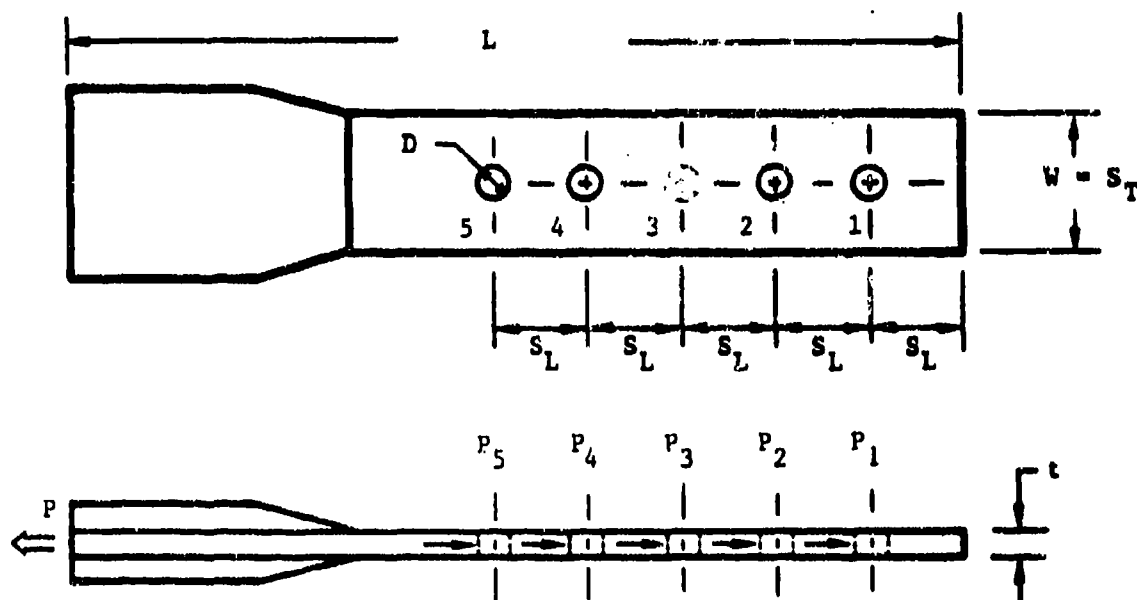
Test Case 250, Static Tension, Double-Shear
 40-Ply, 50/40/10 Laminate $t=0.241$ in., $t_{AL}=0.38$ in.,
 $D=5/16$ in., $S_L/D=4$, $W/D=4.8$, $E/D=3.2$



	SAMCJ PREDICTION	TEST RESULTS (Ref. 2)
P_1 / P	0.172	0.164
P_2 / P	0.156	0.124
P_3 / P	0.167	0.161
P_4 / P	0.211	0.207
P_5 / P	0.293	0.345
$P_{failure}$ (kips)	13.4	17.7
FAILURE LOCATION	5	5
FAILURE MODE(S)	NET SECTION	NET SECTION

Figure 48. SAMCJ Predictions and Test Results for Test Case 250.

Test Case 251, Static Tension, Single-Shear
 40-Ply, 50/40/10 Laminate, $t=0.243$ in., $t_{AL}=0.50$ in.
 $D=5/16$ in., $S_L/D=4$, $W/D=4.8$, $E/D=3.2$



	SAMCJ PREDICTION	TEST RESULTS (Ref. 2)
P_1 / P	0.193	0.204
P_2 / P	0.168	0.177
P_3 / P	0.170	0.171
P_4 / P	0.202	0.178
P_5 / P	0.267	0.270
$P_{failure}$ (kips)	12.4	16.6
FAILURE LOCATION	5	5
FAILURE MODE(S)	NET SECTION	NET SECTION

Figure 49. SAMCJ Predictions and Test Results for Test Case 251.

SECTION 4

CONCLUSIONS

A strength analysis was developed for laminates that are bolted to other laminates or metallic plates by many fasteners. The analysis was programmed to be the SAMCJ computer code. The validity of the developed analysis was established by considering different composite-to-metal joints that were tested in Reference 2. SAMCJ accurately predicted the observed failure location and the failure mode for all the test cases. Predicted fastener load distributions were in agreement with strain-gaged bolt measurements. Predicted failure loads were in reasonable agreement with, and lower than, the measured average values in most of the considered test cases. Nonconservative failure loads (larger than the measured value) were predicted only in a few test cases. In summary, the developed strength analysis adequately predicted the failure load, the failure location and the failure mode for bolted laminates.

The primary limitations of the developed analysis include its inability to account for the effect of countersunk fasteners, its inability to predict the precipitation of delaminations, and the inaccuracies introduced by the five-node representation of a complex problem (a laminate with finite planform dimensions, a fastener hole, and a fastener load distribution around the hole boundary). The fastener analysis segment of SAMCJ can be modified to overcome the first limitation. The failure procedure can be modified to predict delaminations through approximate estimations of interlaminar stresses and an appropriate failure criterion. This task will be similar to that performed in Reference 1. The last limitation (inaccuracies introduced by the five-node element) can be overcome by developing a higher order element (nine node element) following the procedure described in Section 2. The suggested improvements of the developed analysis were beyond the scope of this program, and are recommended as future efforts.

Despite the above limitations, the developed analysis (SAMCJ code) offers the user the following advantages: (1) SAMCJ is a test-independent, one-step analysis that computes the load distribution (magnitude and orientation) among many fasteners, and subsequently predicts the failure load as the lowest value of the computed applied load levels for each of three failure modes at every fastener and cutout location; (2) SAMCJ accounts for stress concentration interaction among fasteners and adjacent cutouts; (3) SAMCJ can approximately account for the effect of tapering of bolted plates; and (4) SAMCJ is a validated analytical tool that can be used in the design of efficient joints in laminated structural parts.

In summary, the strength analysis of bolted laminates (the SAMCJ computer code), developed in this Northrop/AFWAL program, is a significant contribution to the design and analysis of bolted laminated structural parts. Its current limitations do not restrict its immediate applicability to design situations. The analysis is moderately conservative and provides the user with a fairly accurate prediction of the failure location and the overall failure mode. As such, it will be very useful in rapidly and analytically evaluating many bolted joint concepts, to select the most efficient concept for a defined application.

REFERENCES

1. Ramkumar, R. L., et al., "Strength Analysis of Composites and Metallic Plates Bolted Together by a Single Fastener," AFWAL-TR-85-3064, August 1985.
2. Ramkumar, R. L. and Tossavainen, E. W., "Bolted Joints in Composite Structures: Design, Analysis and Verification; Task II Test Results," AFWAL-TR-85-3065.
3. Ramkumar, R. L., and Tossavainen, E. W., "Bolted Joints in Composite Structures: Design, Analysis and Verification; Task I Test Results," AFWAL-TR-84-3047, August 1984.
4. Argyris, J. H. and Scharpf, D. W., "Some General Considerations on the Natural Mode Technique; Part 2, Small Displacements; Part 2, Large Displacements," The Aeronautical Journal of the Royal Aeronautical Society, Vol. 73, April 1969.

SUPPLEMENTARY

INFORMATION



DEPARTMENT OF THE AIR FORCE
AIR FORCE WRIGHT AERONAUTICAL LABORATORIES (AFWAL)
WRIGHT-PATTERSON AIR FORCE BASE, OHIO 45433-6543

REPLY TO: IMST (513/255-7466)
ATTN OF:

1 May 1987

SUBJECT: Correction to AFWAL Technical Reports, AFWAL-TR-86-3034
and 86-3035

TO: ALL ADDRESSES

1. Please delete the second paragraph in the NOTICE page affixed to the inside cover of AFWAL-TR-86-3034, "Strength Analysis of Laminated and Metallic Plates Bolted Together by Many Fasteners" and AFWAL-TR-86-3035, "Design Guide for Bolted Joints in Composite Structures."

2. Please contact the undersigned if you have any questions regarding this letter.

J. Doben

G. DOBEN
Chief, Scientific & Tech Info Gp
Information Services Branch

cc: AFWAL/FIBRA
(V. Venkayya)

UNITED STATES AIR FORCE



SEPTEMBER 18, 1947

AD-B108208